Illinois Water Resources Center
Annual Technical Report
FY 2015

Introduction

In 2015, the Illinois Water Resources Center secured over $2.5 million in base and leveraged funding to work on water resources issues in Illinois. Leveraged funds include an award from US EPA to conduct research and Extension throughout the Great Lakes on projects such as nutrient loss mitigation, community support for sediment remediation projects, Great Lakes monitoring and research integration, and emerging contaminants research and outreach. Other leveraged funding includes assistance to private well owners, small water supply operators, the State of Illinois for its nutrient loss reduction efforts, and several research projects that connect university researchers to USGS scientists.

The Illinois Water Resources Center is part of University of Illinois Extension and we share staff and administrative functions with Illinois-Indiana Sea Grant. Our core USGS funds are used to support about $40,000 in university-based research around the state. We host annual conferences to bring together scientists from around the state to discuss emerging research and policy challenges. Our social media efforts target students and young professionals.

The Illinois Water Resources Center holds the University memberships in organizations like National Institutes for Water Resources, University Council on Water Resources, and Consortium for Advancement of Hydrologic Sciences. We participate on the advisory board for the National Great Rivers Research and Education Center and in the Extension-led North Central Region Water Network.

Research Program Introduction

Illinois' stream mitigation protocol falls short of Clean Water Act requirements

Relevance
A 2008 rule developed under the Clean Water Act Section 404 requires that permitted unavoidable impacts to surface water be offset by the purchase of mitigation credits with the goal of achieving no net loss in ecological function at a national scale. The Army Corps of Engineers St. Louis District is working with regulators and scientists to improve Illinois' stream mitigation protocol to better achieve this goal.

Response
University of Illinois at Urbana-Champaign graduate student Alex Peimer used IWRC funding to conduct a multi-part investigation of the process of compensatory stream mitigation banking in the state and its effectiveness in achieving no net loss.

Results
Using social science and biophysical methodology, this project revealed that permitted impact activities do result in a net loss in functionality, in large part due to the structure and implementation of the Illinois Stream Mitigation Method.

Risks of coal tar sealcoat in sediment may fade with time

Relevance
Americans apply roughly 99 million gallons of coal tar sealcoat to parking lots, driveways, and playgrounds each year to maintain a clean look and protect the asphalt or concrete underneath from water and ice. The abraded sealcoat particles carried into urban waterways by stormwater runoff are rich in polycyclic aromatic hydrocarbons (PAHS) linked to mutations, birth defects, cancer, and death in animals.

Response
With support from the National Competitive Grants Program, Charles Werth and Michael Plewa from the University of Illinois conducted bench scale and field experiments to measure the desorption rate and toxicity of PAHs in Wisconsin's Whitnall Park Pond.

Results
Their findings suggest that PAHs desorb off sealcoat particles and form stronger bonds with charcoal, soot, and other materials found in sediment, decreasing the bioavailability of PAHs associated with coal tar sealcoat.

Low-head dams do not directly hinder reproduction and dispersal of fish communities

Relevance
Decades of research has revealed that in-stream structures like dams alter habitat characteristics, change flow regions and increase siltation upstream of the dam. However, less is known about the impacts of low-head dams, which are more prevalent in Illinois and the country as a whole.

Response
Eastern Illinois University's Robert Colombo and Shannon Smith sampled 12 riverine sites for habitat quality and fish assemblages in the spring and fall of 2015.

Results
While the presence of dams did alter habitat type and quality— which in turn impacts the makeup of fish communities—the study revealed that low-head dams do not obstruct fish dispersal or hinder reproduction to the point of genetic isolation.

Wastewater reuse offers sustainable energy and water management and increased reliability

Relevance
Thermoelectric power plants account for over 85 percent of freshwater withdrawals in Illinois, and fulfilling energy needs is a crucial concern as the region prepares for a changing climate, growing population, and additional demands on water supplies. This concern is heightened by the fact that water reuse for power plants does increase water consumption through increased evaporation.

Response
With seed funding from IWRC, graduate student Zachary Barker modeled wastewater reuse at six thermoelectric power plants in Illinois and estimated the watershed-scale implications and economic value of transitioning plants to a reuse system.

Results
A comparison of existing operations and a reclaimed water system demonstrated that wastewater reuse improves power generation reliability and offers an environmentally and economically sustainable approach to energy and water management both locally and regionally.

Stream restoration alters makeup of fish communities

Relevance
Stream restoration projects are on the rise in Illinois and across the Midwest, but comparatively little effort has been dedicated to monitoring, resulting in ambiguous restoration results, limited project success, and few opportunities to boost future projects with lessons learned.

Response
Using IWRC funds, Eastern Illinois University PhD candidate Anabela Maia conducted field surveys and lab experiments to monitor the restoration of Kickapoo Creek and examine the effects of sedimentation and nutrient loading on fish and macroinvertebrate communities.

Results
The makeup of fish communities shifted significantly in the years following the addition of riffles, boulder substrate, and rip-rap keys in Kickapoo Creek. Results suggest that this shift in ecology may be due to the high energetic costs of navigating complex flows.

Determining the Fate and Toxicity of Polycyclic Aromatic Hydrocarbons Associated with Coal-Tar and Other Carbonaceous Material Particles in Urban Lakes

Basic Information

Title:	Determining the Fate and Toxicity of Polycyclic Aromatic Hydrocarbons Associated with Coal-Tar and Other Carbonaceous Material Particles in Urban Lakes
Project Number:	2011IL239G
USGS Grant Number:	G11AP20211
Start Date:	8/1/2011
End Date:	7/31/2015
Funding Source:	104G
Congressional District:	15 IL
Research Category:	Water Quality
Focus Category:	Non Point Pollution, Sediments, Surface Water
Descriptors:	None
Principal Investigators:	Charles J. Werth, Michael Jacob Plewa

Publications

There are no publications.

IWRC FINAL REPORT SEPTEMBER 2015

USGS-NIWR Project Title:

Determining the Fate and Toxicity of Polycyclic Aromatic Hydrocarbons Associated with Coal-Tar and Other Carbonaceous Material Particles in Urban Lakes

Project PIs and Contact Information:

Dr. Charles J. Werth (PI)
Adjust Professor, Department of Civil & Environ. Eng., University of Illinois at Urbana-Champaign, 205 North Mathews Ave., Urbana, IL 61801, werth@illinois.edu, 217-377-6063
Professor and Bettie Margaret Smith Chair in Environmental Health Engineering, University of Texas at Austin, 301 East Dean Keeton Rd., Austin, TX, 78712, werth@utexas.edu, 512-232-1626

Michael J. Plewa, Professor of Genetics and University Scholar (co-PI)
Department of Crop Sciences, University of Illinois at Urbana-Champaign, 1101 West Peabody Dr., Urbana, IL 61801, mplewa@illinois.edu, 217-333-3614

Problem and Research Objectives:

Particle associated contaminants (PACs) have resulted in the impairment of thousands of streams, lakes, and reservoirs; PACs were responsible for fish-consumption advisories for 39 percent of total river mileage and 43 percent of total lake acreage in the United States in 2008. Results from recent water quality surveys indicate that metal, polychlorinated biphenyl, and DDT concentrations in freshwater sediments have generally decreased since their peak in the mid 1970's, consistent with their use and regulatory histories. However, total concentrations of polycyclic aromatic hydrocarbons (SPAHs) have increased, and generally with increasing urbanization. PAHs are toxic to aquatic life, and many are probable or suspected carcinogens. This is of special concern because many urban surface waters are used for human recreation (e.g., fishing, swimming) and/or drinking water.

Sources of particle-associated PAHs in urban lake sediments are located both within and outside the watershed. They include point (e.g., industrial emissions) and nonpoint (e.g., automobiles) combustion sources, asphalt from roads and parking lots, vulcanized rubber products such as automobile tires, and coal-tar and asphalt based sealcoats on parking lots and driveway pavement and roofs. Results from a number of our recent studies indicate that coal-tar pavement sealcoat is fluvially transported into urban streams and lakes with runoff, and can be the dominant source of PAHs in urban streams and lakes.

The overall goal of this study is to determine the fate and toxicity of PAHs associated with coal-tar particles in urban lake sediments. The specific objectives of this study are listed below.

1) Determine the sorption equilibrium and desorption kinetics of PAHs in coal-tar and other carbonaceous material particles that comprise urban lake sediments. We hypothesize that sorption capacities are low and release rates are high for PAHs in coal-tar and other less condensed carbonaceous materials (CMs) compared to highly condensed CMs like black carbon char and soot.

2) <u>Determine PAH losses and redistribution associated with coal-tar particles in urban lake sediments.</u> We hypothesize that lower molecular weight PAHs are released from coal-tar particles soon after burial (weeks to months) and taken up by more strongly sorbing black carbon, and that higher molecular weight PAHs are only lost to black carbon over much longer time scales (i.e., years) as phenolic and heterocyclic compounds that comprise coal-tar degrade. As a result, we hypothesize that PAHs are largely conserved in lake sediments and are not significantly released to the water column, and that sediment pore-water concentrations of PAHs decrease with aging.

3) <u>Determine the toxicity of PAHs associated with coal-tar and other carbonaceous material particles in urban lake sediments.</u> We hypothesize that toxicity of pore water in sediments decreases with time as PAHs and other organic pollutants redistribute from less strongly sorbing CMs like coal-tar to more strongly sorbing black carbon, and as less recalcitrant pollutants are biologically degraded over time. Such information is important because these lakes are sources of recreation and/or drinking water for large populations, and understanding coal-tar contributions to toxicity is an important step in protecting the environment and public health.

<u>Methodology:</u>

The proposed work combines bench scale laboratory experiments, field experiments, and laboratory analysis of field samples. It is divided into four tasks that cover 1) lake core retrieval, analysis, treatment, and in situ placement, 2) sorption isotherm and desorption kinetic profile measurement, 3) PAH and CM analysis of in situ cores, and 4) toxicity analysis of in situ cores.

Task 1: Lake core retrieval, analysis, treatment, and in situ placement

The deployment and retrieval of all field samples has been completed. The field study was deployed on 5/30/13, and samples were collected 11/2/13, 5/20/14, 10/22/14, and 7/3/15. Details on Task 1 are outlined in previous reports. Briefly, in situ cores were amended with carbonaceous materials (CMs) spiked with deuterated PAHs and placed into the top layer of sediment at Whitnall Park Pond. Images of the in situ cores as well as the four types of CMs are shown below in Figures 1 and 2.

Figure 1: In situ core design and field deployment (credit: Victoria Boyd, UIUC and Peter Van Metre, USGS)

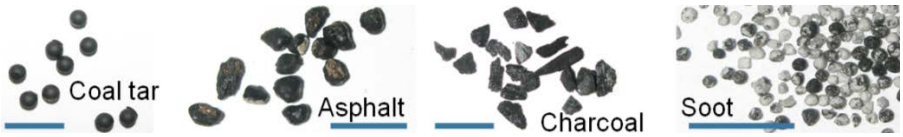

Figure 2: Carbonaceous materials, the scale bar is 1 cm (credit: Victoria Boyd, UIUC)

Each type of CM was spiked with three unique deuterated PAHs in a range of molecular weights. This allows for the transport of PAHs from each CM to be measured. Using a range of molecular weights in the spike makes is possible to determine the effects of PAH molecular weight on transport.

Task 2: Sorption isotherm and desorption kinetic profile measurement
A series of lab experiments will be conducted to supplement the field study using a similar setup. However, the lab experiments will be scaled down and conducted in a controlled, well mixed environment. The purpose of these lab experiments will be to quantify rates of intra-particle exchange, and to extend the field experiments past the two-year sampling period to equilibrium. All CM particles have been prepared and the experiments will begin October 2015.

Task 3: PAH and CM analysis of in situ cores
Retrieval of in situ cores was completed with the help of divers as shown in Figure 3. Analysis of the in situ cores has started. During field deployment the samples were divided into different layers in order to determine if sediment depth had an impact on PAH transport. Mesh screens were added at that time to separate the different layers of sediment. This allowed for the samples to be divided back into the same depths after retrieval. Samples retrieved from the lake were frozen in order to preserve the layering of the sediment and cut open (Figure 4).

Figure 3: Divers retrieved in situ samples (credit: Victoria Boyd, UIUC)

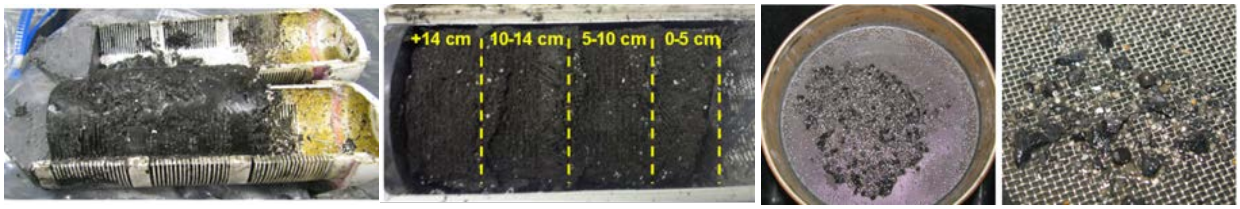

Figure 4: Samples retrieved from the lake were frozen and cut open. Then divided into the original depths, and sieved to separate the particles from the sediment. The particles were separated by hand and analyzed along with the sediment that was sieved away from the particles (credit: Victoria Boyd, UIUC)

The sediment and particles are currently being analyzed for PAHs. Sediment samples and soot and charcoal particles are dried using a Labconco Freeze Dry System prior to analysis.

All samples except coal tar are extracted using EPA method 3534 for pressurized fluid extraction using a Dionex Accelerated Solvent Extractor. Coal tar particles are extracted using a microextraction method in which samples are extracted three consecutive times with 1 mL of 50% acetone and 50% dichloromethane, and sonicated for 3 minutes at 50 °C. The resulting extract is cleaned following EPA method 3630c for silica gel clean up. Finally, sample extracts are analyzed by gas chromatography/mass spectrometry with an Agilent 7890B GC with a DB5-MS capillary column and 5977A inert MSD (EPA method 8270d). All samples will be analyzed for EPA priority 16 PAHs as well as all deuterated PAHs used to spike the particles. Quality assurance will be provided by using three surrogates (fluorene-d10, p-terphenyl-d14, and benzo[a]pyrene-d12) as well as an internal standard (naphthalene-d8). The surrogate standards will be used to correct for PAH losses accrued during extraction and cleanup. The internal standard will be added prior to GC/MS analysis to account for instrument errors.

Task 4: Toxicity analysis of in situ cores

Mutagenicity and cytotoxicity (survivorship) experiments were performed using a single colony isolate of *S. typhimurium* TA100 that was grown overnight in 50 mL LB medium plus 100 µL ampicillin stock solution at 37°C with shaking (200 rpm). The following day, the overnight culture of TA100 was used to evaluate an extract of coal-tar for PAH-induced mutagenicity using a plate incorporation assay. For this assay, overlay tubes were prepared with 2 mL of histidine-biotin, supplemented over agar with 100 µL of overnight bacterial culture and ± 500 µL hepatic microsomal activation (S9) mix. The required volume of the test agent was added to the overlay tube, the tube was flamed sterilized and immediately poured onto a VB minimal plate. The plates were incubated at 37 °C for 36-72 h. Histidine revertant colonies were counted by hand or with a New Brunswick Biotran III automatic colony counter. To confirm the genotype of the TA100 cells, 100 µL of the bacterial cell suspension was added to an LB plate, and spread with a flamed glass rod. Flamed tweezers were used to place a crystal violet disk onto the center of the plate, and the disk was tapped lightly in place. Experiments are planned to evaluate the mutagenicity and cytotoxicity of coal tar extract surrogates containing only PAHs (not other components of the extract), and lake sediment extracts.

Principal Finding and Significance:

Background concentrations in sediment were measured in order to have a baseline to compare the initial conditions of the sediment to the in situ field samples. Sediment samples at time zero are presented in triplicate to show the precision of lab techniques in Figure 5. PAHs are stacked in order of molecular weight, heaviest at the bottom. The PAH concentrations decrease with depth; the PAHs in deeper, older sediment has had more time to degrade and diffuse to the water column.

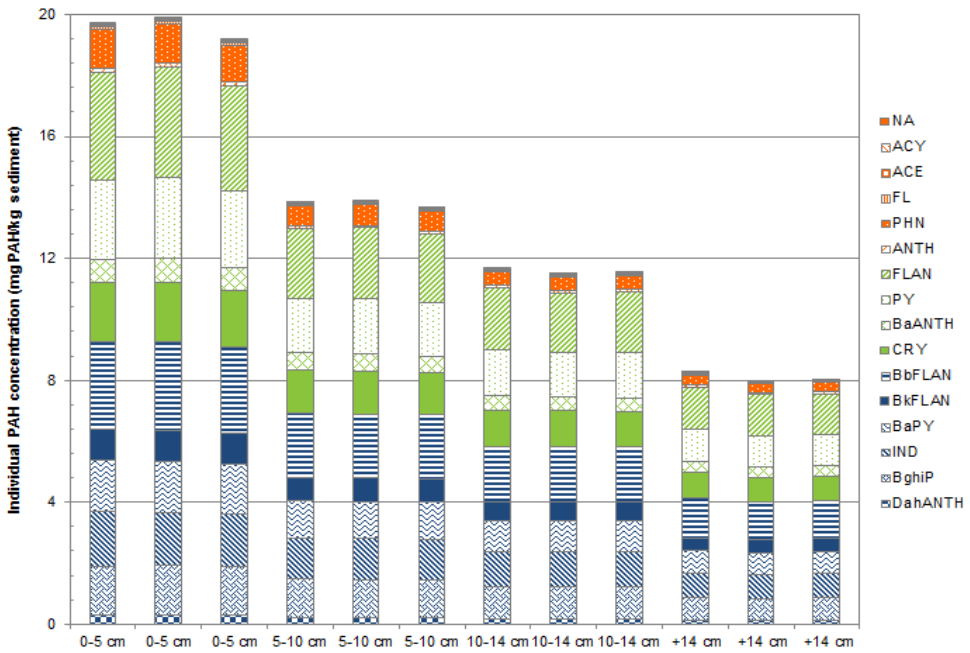

Figure 5: PAH concentrations in original lake sediment (credit: Victoria Boyd, UIUC)

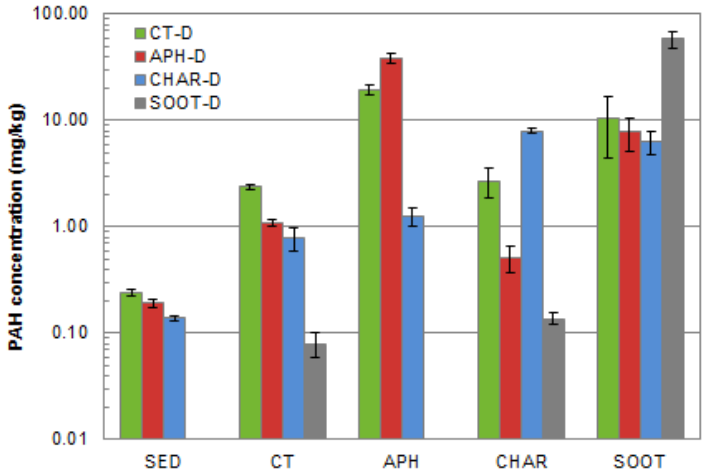

Figure 6: Spiked PAH concentrations in the sample core after 1.5 years in the lake. (credit: Victoria Boyd, UIUC)

The concentrations of the deuterated PAHs on different CMs and sediment in the sample core after 1.5 years in the lake are presented in Figure 6. The graph is divided into the five material groups along the bottom: sediment, coal tar, asphalt, charcoal, and soot. Each color represents the collection of deuterated PAHs initially spiked onto a specific CM. For example, the green bars represent the deuterated PAHs spiked onto coal tar particles (CT-D). All depths have been averaged in this figure. Notice that concentrations of CT-D are seen in all material types. This means the PAHs initially spiked onto coal tar have transported from the coal tar particles to the other materials while in the lake. All spiked PAHs moved from their original source to other materials. The coal tar (green) and asphalt (red) spikes were the most mobile as they were detected in the highest concentrations in all materials, with coal tar spikes having a significantly larger concentrations in sediment and charcoal particles. PAHs spiked to soot (grey) were the least mobile, and were only seen to move to the charcoal and coal tar particles. These results are consistent with our hypothesis that PAHs associated with coal tar would be more mobile than those with charcoal and soot.

A more detailed look at the deuterated PAHs measured in the sediment from the sample core is shown in Figure 7. Triplicate samples from each sampling depth are displayed. The PAHs are divided by the material they were originally loaded onto (same as Figure 6) as well as by molecular weight, the heavier the PAH the darker the color. For example, deuterated PAHs originally spiked onto coal tar particles go from light green (acenaphthene-d at 164 g/mol) to dark green (benzo[b]fluoranthene-d at 264 g/mol). Besides PAHs associated with soot particles, all deuterated PAHs were detected in the sediment, showing transport of a range of molecular weights from each CM. Greater concentrations of heavier PAHs were detected in all samples. This is most likely due to the greater loading of heavier PAHs onto the original CMs due to their lower solubility and greater octanol water partitioning coefficients. Comparison to of the original concentrations of deuterated PAHs on CMs must be completed to determine the extent of transport of spiked PAHs.

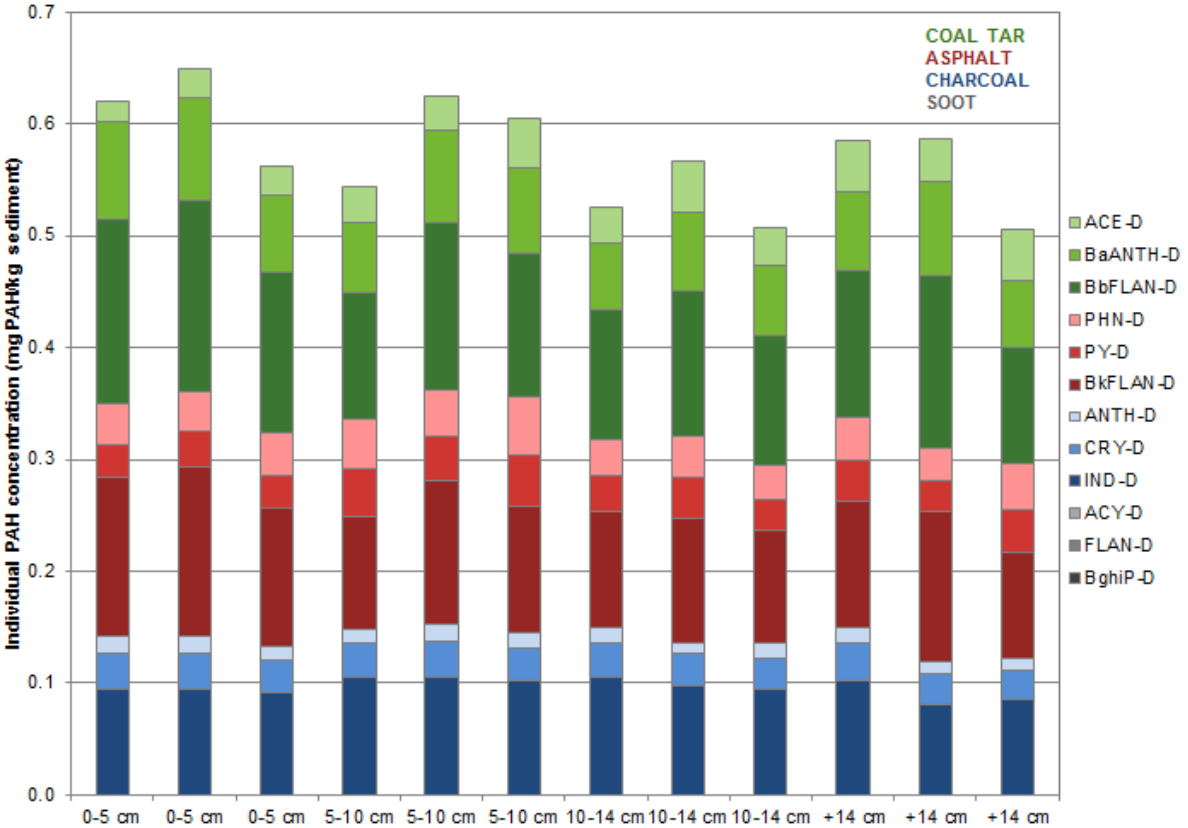

Figure 7: Spiked PAH concentrations in sample core sediment after 1.5 years in the lake (credit: Victoria Boyd, UIUC)

Concentration response curves are shown in Figure 8 for mutagenicity induced by benzo(α)pyrene and coal tar extract containing polyaromatic hydrocarbons in *S. typhimurium*, strain TA100, with and/or without mammalian hepatic microsomal activation. Benzo(a)pyrene with microsomal activation shows a linear increase in histidine revertants with increasing benzo(a)pyrene concentration. Coal tar extract with microsomal activation shows high numbers of histidine revertants as compared to coal tar extract without microsomal activation. Also, the response is nonlinear, showing a plateau at high loadings of extract.

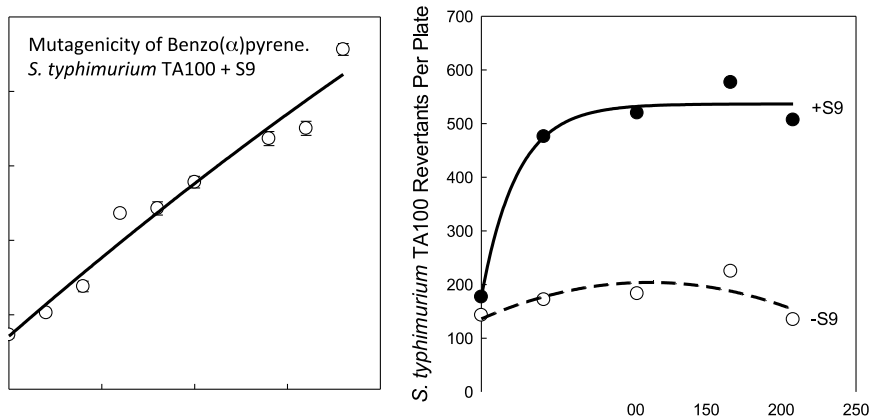

Figure 8: Mutagenic response of *S. typhimurium* to benzo(α)pyrene and a coal tar extract containing PAHs (credit: Azra Dad, UIUC).

Notable Achievements:

The conclusion of the field sampling in July, 2015 was a significant achievement in the project. The analysis of the retrieved field samples shows the movement of spiked PAHs between different CMs and sediment. The most significant trend in this data is the high mobility of spiked PAHs associated with coal tar and asphalt particles compared to those with charcoal and soot.

Students supported with funding:

In the summer of 2012 two graduate students were hired. Ms. Tory Boyd was hired to perform all work except toxicity testing. Ms. Boyd obtained her MS degree at Illinois, and the work in this proposal represents the bulk of her PhD thesis. The other graduate student is Ms. Azra Dad, who is performing the toxicity testing as part of her PhD thesis.

Publications and presentations:

This work was presented at the Environmental Engineering and Science Symposium at the University of Illinois on April 3, 2014 and at the Society of Environmental Toxicology and Chemistry in Vancouver, BC on November 10, 2014.

Photos and figures credited to Boyd, Dad, and Van Metre can be used in IWRC publications.

Year-round wetland microbial activity impacts on nitrogen cycling annual budgets: is restoration impacting greenhouse gas emissions in wetlands?

Basic Information

Title:	Year-round wetland microbial activity impacts on nitrogen cycling annual budgets: is restoration impacting greenhouse gas emissions in wetlands?
Project Number:	2014IL283B
Start Date:	5/1/2014
End Date:	12/31/2015
Funding Source:	104B
Congressional District:	IL-013
Research Category:	Water Quality
Focus Category:	Water Quality, Wetlands, Nutrients
Descriptors:	None
Principal Investigators:	Angela Kent

Publications

There are no publications.

The Effect of Agricultural Management Regimes on the Soil Microbial Denitrification Community Structure and its Impact on Nitrous Oxide Emissions

Summary:

Production agriculture to provide food for an ever-growing world population has resulted in the large scale use of inorganic fertilizers (Erisman, Sutton et al. 2008). The resulting increase of nitrogen in soil has far-reaching consequences (Canfield, Glazer et al. 2010). Nitrogen availability is regulated by microbial transformations in the nitrogen cycle, and agricultural inputs can disrupt the natural cycle (Galloway, Dentener et al. 2004). Important microbial transformations of the nitrogen cycle are nitrification and denitrification. Nitrification converts ammonium to nitrate, which presents pollution risks for groundwater and aquatic ecosystems. Denitrification can remove reactive N from terrestrial ecosystems through conversion of nitrate to molecular nitrogen via a stepwise process ($NO_3^- \rightarrow NO_2^- \rightarrow NO \rightarrow N_2O \rightarrow N_2$) but can also produce nitric oxide/nitrous oxide during incomplete denitrification (Zumft 1997). Nitrous oxide (N_2O) is an extremely potent greenhouse gas (Canfield, Glazer et al. 2010). A range of organisms are capable of denitrification including archaea, bacteria and fungi. The efficiency of denitrification (and production of GHG through incomplete denitrification) is influenced by the composition of the microbial community. Denitrification in soil also depends on oxygen availability, available carbon, redox conditions, pH, nitrate, and temperature, but most importantly on soil moisture, which plays a determining role in the other factors (Butterbach-Bahl, Baggs et al. 2013). The presence of more carbon and nitrogen substrates increases the rates of denitrification, which in turn increases the rate of incomplete denitrification and its byproduct of nitrous oxide. These factors can also influence the composition of soil microbial communities. These drivers of microbial communities and their denitrification processes are influenced by land use and management practices, thus investigating how microbial community structure and function differ among types of land use and also their response to specific ecological drivers can lead to better management of nitrous oxide emissions in intensively managed agricultural landscapes.

Methodology:

Soil samples will be obtained from fields that are managed with the following practices: chisel plow and ridge till, with and without cover cropping. We will also obtain soil samples from agricultural wetlands that treat agricultural runoff, and from denitrifying bioreactors that treat nitrate-laden tile drain effluent. The agricultural plots are located at the University of Illinois South Farm. The plots to be used are planted in a maize/soybean rotation and are fertilized with a surface liquid urea ammonium nitrate (UAN) broadcast application just prior to planting. The two denitrifying bioreactors planned for this study are also located at the University of Illinois South Farm. They consist of lined trenches filled with wood chips and receive effluent from a tile drain system from the study field. PVC sampling ports allow access for collecting woodchips from the depths of the bioreactor. The wetland sites are located on the Franklin Research and Demonstration Farm in McLean County, and these wetlands receive tile drain effluent for treatment. We will carry out sample collection over six sampling dates per management regime per year; the dates will be split between times expected to have relatively high N_2O emissions, such as following fertilizer application or incorporation of cover crop residues or during periods of high flow for the bioreactors, as well as during periods expected to have relatively low N_2O

emissions. A standard suite of soil chemical and physical parameters will be measured at the time of each sampling, including soil moisture, pH, SOM, total N and total C, and ammonium and nitrate concentrations.

Standard denitrification studies of soil or woodchip samples will be modified using several known methods to distinguish between contributions of bacteria and fungi. A modified acetylene inhibition method allows the measurement of the nitrous oxide produced by specific blockage of the last step of denitrification (Tiedje, Simkins et al. 1989, Royer, Tank et al. 2004). N_2O concentrations will be determined by use of gas chromatography using an electron capture detector.

A variety of microbial functional groups are involved in nitrogen cycle activities including archaeal and bacterial and fungal denitrifiers, and nitrous oxide consuming bacteria which are not denitrifiers (Butterbach-Bahl, Baggs et al. 2013). We can assess the abundance of these groups using quantitative PCR (qPCR) of functional genes specific to them. We will use Illumina MiSeq amplicon sequencing of diagnostic functional genes to compare community composition of all abundant functional groups across management practices.

We will relate specific microbial populations or specific microbial assemblages to production of nitrous oxide by multivariate analysis of the sequencing and qPCR data. The analysis will also identify ecological drivers or management practices that influence microbial community structure and function.

Objectives and Expected Results

Objectives

The methods described above will allow us to analyze the soil and woodchip samples from a variety of agricultural management practices (and runoff mitigation strategies) for denitrification potential and nitrous oxide emissions. The molecular microbial ecology methods and ecological analyses will produce detailed information about size and composition of the microbial population present in those samples, and the ecological drivers that shape the communities and their functions. Our 4 major objectives for this work are listed below:

Objective 1: Measure N_2O emissions for different agricultural and nutrient management practices (ridge till and chisel plow with and without cover cropping; wetlands; and denitrifying bioreactors) for at least 6 sample dates over the course of the season.

Objective 2: Characterize the microbial community associated with production and consumption of N_2O in each management regime using functional gene markers for nitrifiers, denitrifiers, and N_2O-consuming microorganisms (including fungi). Characterize seasonal variations in the microbial community.

Objective 3: Determine the potential denitrification and incomplete denitrification rates for denitrifiers in soil or bioreactor woodchip samples from each management regime, and also determine the contributions of bacterial and fungal denitrifiers.

Objective 4: Determine the management factors and specific ecological drivers that have the

greatest influence on microbial community composition, denitrification, and N2O production in each management practice.

Expected Results

- We will be able to compare denitrifying activity in agricultural production to that of wetlands and bioreactors.
- Fungal denitrifiers will be important in wetlands and bioreactors since they are more abundant in less physically disturbed environments.
- The expectation for the nitrous oxide emissions is that soil in the agricultural fields will have a higher output than wetlands or bioreactors due to fertilization. Among agricultural management practices fertilized fields should have higher nitrous oxide emissions due to increased available nutrients.
- Seasonal patterns will be evident when soils are flooded and more denitrification can take place in the anoxic conditions. However, seasonal trends in agricultural fields will correspond more highly to nutrient inputs. It has also been noted that fungal populations increase over time following planting which may mean N_2O production will increase correspondingly.
- Understanding the abundance of and diversity of the microbes responsible for the production and consumption of nitrous oxide will be important in determining the best management regime.
- High nitrous oxide production will be correlated to low abundance of *nosZ*.

Conclusions

The relationship between the soil microbial community, agricultural nitrogen inputs, and management practices to the reactive nitrogen pollution produced from farming needs to be addressed. While some strategies have been developed to mitigate the runoff of nitrate into the aquatic environment (for example, denitrifying bioreactors and agricultural wetlands), their potential to generate nitrous oxide is a concern which needs to be more fully investigated. We propose that studying the microbial community composition in soil samples from a variety of agricultural management regimes along with analysis of denitrification potential and N_2O emissions will help us determine meaningful relationships of the community to GHG emissions. Combining these findings with results from other expert teams at the University of Illinois will allow an overarching model to be developed that can identify management practices for farmers which minimize soil, air, and water reactive nitrogen pollution while retaining good crop yields and revenue potential. The synergy from a multidisciplinary analysis of the problem by groups that have not traditionally worked together should advance our understanding of how to abate pollution caused by reactive nitrogen from agriculture.

Participants

The work will be carried out by graduate student Natalie Stevenson under the supervision of Professor Angela Kent. Two undergraduate students will participate in this project in Summer 2015.

References

Butterbach-Bahl, K., E. M. Baggs, M. Dannenmann, R. Kiese and S. Zechmeister-Boltenstern (2013). "Nitrous oxide emissions from soils: how well do we understand the processes and their controls?" Philosophical Transactions of the Royal Society B-Biological Sciences **368**: 20130122.

Canfield, D. E., A. N. Glazer and P. G. Falkowski (2010). "The Evolution and Future of Earth's Nitrogen Cycle." Science **330**: 192-196.

Erisman, J. W., M. A. Sutton, J. Galloway, Z. Klimont and W. Winiwarter (2008). "How a century of ammonia synthesis changed the world." Nature Geoscience **1**: 636-639.

Galloway, J. N., F. J. Dentener, D. G. Capone, E. W. Boyer, R. W. Howarth, S. P. Seitzinger, G. P. Asner, C. C. Cleveland, P. A. Green, E. A. Holland, D. M. Karl, A. F. Michaels, J. H. Porter, A. R. Townsend and C. J. Vorosmarty (2004). "Nitrogen cycles: past, present, and future." Biogeochemistry **70**: 153-226.

Royer, T. V., J. L. Tank and M. B. David (2004). "Transport and fate of nitrate in headwater agricultural streams in Illinois." Journal of Environmental Quality **33**: 1296-1304.

Tiedje, J. M., S. Simkins and P. M. Groffman (1989). "Perspectives on Measurement of Denitrification in the Field Including Recommended Protocols for Acetylene Based Methods." Plant and Soil **115**: 261-284.

Zumft, W. G. (1997). "Cell biology and molecular basis of denitrification." Microbiology and Molecular Biology Reviews **61**: 533-616.

Improving Morphodynamic Predictions in Rivers

Basic Information

Title:	Improving Morphodynamic Predictions in Rivers
Project Number:	2014IL292S
USGS Grant Number:	
Sponsoring Agency:	USGS
Start Date:	8/16/2015
End Date:	8/15/2016
Funding Source:	104S
Congressional District:	IL-015
Research Category:	Climate and Hydrologic Processes
Focus Category:	Models, Geomorphological Processes, Solute Transport
Descriptors:	None
Principal Investigators:	Gary Parker

Publications

There are no publications.

Progress Report

Improving Morphodynamic Predictions in Rivers

Gary Parker
Dept. of Civil & Environmental Engineering and Dept. of Geology
University of Illinois Urbana-Chanmpaign, Urbana, IL USA

I hereby submit the text of a technical paper, “Numerical simulation of large-scale bedload particle traceradvection-dispersion in rivers with free bars” by Toshiki Iwasaki, Jonathan Nelson, Yasuyuki Shimizu and Gary Parker, which was submitted for publication in the Journal of Geophysical Research in May, 2016.

The paper is simultaneously in review by the US Geological Survey. This paper represents the major achievement of our project, and also a major personal achievement of Dr. Iwasaki.

Numerical simulation of large-scale bedload particle tracer advection-dispersion in rivers with free bars

Toshiki IWASAKI[1,2], Jonathan NELSON[2], Yasuyuki SHIMIZU[3] and Gary PARKER[1,4]

[1]Department of Civil and Environmental Engineering, University of Illinois at Urbana-Champaign, 205 N Mathews Avenue, Urbana, Illinois, 61801, USA

[2]U.S. Geological Survey, Geomorphology and Sediment Transport Laboratory, Golden, Colorado, 80403, USA

[3]Laboratory of Hydraulic Research, Graduate School of Engineering, Hokkaido University, N13, W8, Kita-ku, Sapporo, 0608628, Japan

[4]Department of Geology, University of Illinois at Urbana-Champaign, 156 Computing App. Bldg., 605 E. Springfield Avenue, Champaign, Illinois, 61820, USA

*Corresponding author: Toshiki IWASAKI, toshia413@gmail.com

Key points:

- Tracer pebbles both advect and disperse over a plane, mobile bed, but the dispersion rate is dramatically increased by the alternate bars
- We show how the scour and fill associated with alternate bars achieves this asymptotic bedload tracer advection-dispersion

ABSTRACT

Asymptotic characteristics of the transport of bedload tracer particles in rivers have been described by advection-dispersion equations. Here we perform numerical simulations designed to study the role of free bars, and more specifically single-row alternate bars, on streamwise tracer particle dispersion. In treating the conservation of tracer particle mass, we use two alternative formulations for the Exner equation of sediment mass conservation; the flux-based formulation, in which bed elevation varies with the divergence of the bedload transport rate, and the entrainment-based formulation, in which bed elevation changes with the net deposition rate. Under the condition of no net bed aggradation/degradation, a 1D flux-based deterministic model that does not describe free bars yields no streamwise dispersion. The entrainment-based 1D formulation, on the other hand, models stochasticity via the PDF of particle step length, and as a result does show tracer dispersion. When the formulation is generalized to 2D to include free alternate bars, however, both models yield almost identical asymptotic advection-dispersion characteristics, in which streamwise dispersion is dominated by randomness inherent in free bar morphodynamics. This randomness can result in a heavy-tailed PDF of waiting time. In addition, migrating bars may constrain the travel distance through temporary burial, causing a thin-tailed PDF of travel distance. The superdiffusive character of streamwise particle dispersion predicted by the model is attributable to the interaction of these two effects.

Index terms:

0744 Rivers, 1825 Geomorphology: fluvial, 1862 Sediment transport

Keywords:

bedload tracers, advection-dispersion, free single-row alternate bars, normal dispersion, anomalous dispersion

1. INTRODUCTION

An understanding of the detailed mechanisms of bedload transport is of central importance for elucidating a wide spectrum of morphodynamic processes in rivers [e.g., *Einstein*, 1937; *Meyer, Peter and Müller*, 1948; *Nakagawa and Tsujimoto*, 1978; *Ashida and Michiue*, 1972; *Kovacs and Parker*, 1994; *Parker et al.*, 2000; *Seminara et al.*, 2002; *Parker et al.*, 2003; *Ancey*, 2010; *Furbish et al.*, 2010; *Schmeeckle*, 2015], as well as the fate of sediment-bound substances such as nutrients, metals, and radionuclides in river systems [e.g., *Falkowska and Falkowski*, 2015; *Iwasaki et al.*, 2015]. Tracer particles that are distinguishable from the ambient bed sediment only via passive markers that do not affect transport dynamics (e.g. color, magnetic properties, radioisotope signature, etc.) have been widely used to measure and quantify bedload transport. The tracking of tracer particles that are initially deployed on the bed surface provides data regarding temporal and spatial changes in tracer distribution [*Sayre and Hubbell*, 1965; *Hoey*, 1996], and gives insight into characteristics of bedload transport, such as travel distance and waiting time distribution [*Einstein*, 1937; *Ferguson and Hoey*, 2002; *Pyrce and Ashmore*, 2003; *Wong et al.*, 2007; *Martin et al.*, 2012; *Roseberry et al.*, 2012; *Hassan et al.*, 2013; *Haschenburger*, 2013]. Such measurements have shown that tracers advect downstream, and disperse in space in the streamwise, transverse and vertical directions. The collective asymptotic behavior of tracers has been described in terms of advection-dispersion. An understanding of this advection-dispersion allows better understanding of bedload transport itself and

associated bed morphodynamics and is central to the estimation of how fast and far sediment-bound substances can be transported.

Einstein [1937] first treated the bedload transport phenomenon as a stochastic process using the statistical characteristics of bedload, i.e., travel distance and waiting time. These statistical quantities are key factors for modeling the streamwise advection-dispersion of bedload tracers. *Einstein* [1937] suggested an exponential distribution of travel distance and waiting time based on experiments. In the context of a random walk model, thin-tailed PDF's of travel distance and waiting time asymptotically results in normal advection-dispersion [*Schumer et al.*, 2009; *Ganti et al.*, 2010], according to which the streamwise standard deviation σ of an ensemble of tracers increases as $t^{1/2}$, where t denotes time. However, recent detailed measurements of tracers in experiments and field studies have suggested the possibility of heavy-tailed PDF's for step length and waiting time (e.g. power distributions) that, for example, do not have finite second moments. This can lead anomalous dispersion instead of normal dispersion, leading to faster (superdiffusive, i.e. $\sigma \sim t^{\gamma}$, where $\gamma > 1/2$) or slower (subdiffusive, i.e. $\gamma < 1/2$) dispersion of tracers than normal dispersion [*Schumer et al.*, 2009; *Bradley et al.*, 2010; *Ganti et al.*, 2010; *Zhang et al.*, 2012]. Since differences in the dispersion rate are critical to a full understanding of bedload transport and subsequent bedload-bound substances dispersal in rivers, there has been a long debate as to what factors control travel distance, waiting time distribution and the associated characteristics of tracer advection-dispersion.

Several experimental, numerical, and field studies have been performed to address

these issues. These studies have yielded, however, different results for travel distance and waiting time, and therefore different dispersion features. This is in part because of differences in the temporal and spatial scales considered. *Nikora et al.* [2002] proposed a framework to describe tracer dispersion regime over a broad range of temporal and spatial scales, suggesting three diffusive regimes for bedload particles, i.e. local (ballistic diffusion), intermediate (normal or superdiffusion), and global (subdiffusion) regimes. Although this framework needs to be validated based on several datasets, it is novel in that it suggests that scale dependency is a dominant mechanism controlling the characteristics of bedload transport. In their model, the local regime explains bedload motion due to the collision of two particles, and the intermediate regime describes bedload transport within at least two successive rests. This indicates that the diffusive mechanisms at these scales might be related to microscopic (particle scale) phenomena such as particle-particle or particle-bed interactions, as well as turbulent structures in the flow near the bed surface. Recent advances in measurement techniques [e.g., *Roseberry et al.*, 2012; *Campagnol et al.*, 2015] and computational technologies using highly resolved detailed physically-based numerical models [e.g., *Schmeeckle*, 2014, 2015] have contributed to a comprehensive understanding of the bedload transport phenomena at these scales. Conversely, the global regime is associated with a large collection of particle motions at the intermediate regime, so that this regime represents particle behaviors associated with tens to millions of steps and rests. As a consequence, the dominant diffusive mechanisms at the global scale are more complex; in addition to particle-scale phenomena, the complexity of the system associated with the bed and planform

morphology and morphodynamics, sediment composition, and unsteady flow regimes in rivers all affect tracer behavior. Because of this, the scale dependence of the dominant diffusive mechanism is poorly understood. An understanding of streamwise tracer dispersion at the global scale remains one of the challenges in the field of geomorphology and river engineering.

Dynamic measurements of large-scale bedload motions are required in order to understand the characteristics of bedload transport at the global scale [*Hassan et al.*, 2013]. However, detailed measurements of particle motion with sufficient temporal and spatial resolution are still limited to experimental scales [*Lajeunesse et al.*, 2010; *Roseberry et al.*, 2012; *Campagnol et al.*, 2015]. Alternative advanced methods, such as accelerometer-embedded cobble tracers [*Olinde and Johnson*, 2015] are necessary at field scale. In general, measurable quantification of tracer behavior at field scale correspond to cumulative quantities evaluated over specified durations. These quantities and their statistical features are strongly affected by a larger variety of physical mechanisms than those at intermediate scale. For instance, *Philips et al.* [2013] and *Olinde and Johnson* [2015] measured long-term and large-scale tracer behaviors using active and passive tracer techniques under the influence of unsteady flows. The results showed a thin-tailed travel distance and heavy-tailed waiting time, suggesting superdiffusive dispersion. Effects of graded sediment, in which each particle size has different mobility, result in more complex patterns of total grain displacement [e.g., *Hashenburger*, 2013], resulting in anomalous dispersion of the grain size mixture even when each grain size range disperses normally [*Ganti et al.*, 2010] and significant streamwise advective slowdown of tracers [*Ferguson and Hoey*,

2002]. Among the many relevant factors affecting tracer transport, however, bed surface morphology and its dynamics are likely to be the most important. Bed morphology is the main factor affecting storage of sediments in rivers, so this strongly affects the waiting time characteristics [*Hashenburger*, 2013]. Moreover, large-scale bedforms and planform features (i.e., dunes, bars, meandering) constrain the length scale of bedload motion [*Pyrce and Ashmore*, 2003, 2005; *Kasprak et al.*, 2015], thus controlling cumulative travel distance. Analysis by *Hassan et al.* [2013] of large field measurement datasets regarding tracer transport in several rivers have indicated that bed geometry impacts travel distance more significantly than flow regime. The same authors also showed that the PDF of travel distance is likely to be thin-tailed rather than heavy-tailed because of separate transport events during multiple floods. In addition to the effect of bed geometry, dynamic morphological changes of the bed surface cause vertical mixing of bedload particles [*Hassan and Church*, 1994; *Parker et al.*, 2000; *Ferguson and Hoey*, 2002; *Blom and Parker*, 2004; *Wong et al.*, 2007; *Blom et al.*, 2008], which complicates the pattern of overall tracer transport and dispersal. Bedload transport at the global scale, therefore, is a multi-scale phenomenon associated with the complexity of the system at a broad range of temporal and spatial scales, rendering the identification of a single dominant mechanism of tracer advection-dispersion problematic. Field measurements often fail to provide the instantaneous location of all tracers, because some of tracers are lost via deep burial or leave the reach of interest. These limitations to field studies makes this large-scale and long-term phenomenon difficult to understand. In small-scale experimental flumes on the other hand, we can measure detailed flow structures, tracer dispersal, and

morphodynamics under well-controlled conditions, but the inherent limitation on spatial scale places a severe constraint on the understanding of dispersal at a global scale.

Numerical models are powerful tools used to overcome these limitations. Because bedload tracer transport can be treated as a random process, simple stochastic models (e.g., Markov process, random walk model) have been proposed to capture the horizontal and vertical mixing of tracers [*Sayre and Hubbell*, 1965; *Yang and Sayre*, 1971; *Hassan and Church*, 1994; *Ferguson and Hoey*, 2002; *Schumer et al.*, 2009]. Physically based models that include the origin of this stochasticity, for instance, the probability of bed surface fluctuation, entrainment, and deposition [*Parker et al.*, 2000; *Ancey*, 2010; *Pelosi et al.*, 2014; *Pelosi et al.*, 2016]; the irregularity of bedform dimensions [*Blom and Parker*, 2004]; and the velocity variability of bedload particles [*Furbish et al.*, 2012], have led to the derivation of master equations describing tracer dispersal. A key question for each of these approaches is how to model the stochasticity of bedload motion under the influence of physical phenomena such as bedforms and planform variation. On the other hand, recent advances in numerical modeling have made it possible to directly resolve complex phenomena such as bars. In particular, the modeling framework for reproducing reach-scale morphological changes of bed surfaces such as bars, meandering and braiding, have been well documented in the literature, and a variety of numerical models that capture morphodynamic complexity are now available publicly such as Delft3D (http://www.deltares.nl) [e.g., *Lesser et al.*, 2004], TELEMAC (http://www.opentelemac.org) [e.g., *Langendoen et al.*, 2016], iRIC

(http://www.i-ric.org) [*Nelson et al.*, 2016]. A coupled model that includes a sophisticated morphodynamic submodel such as one of the above and a tracer transport submodel may capture the physics of long-term and large-scale tracer behavior under the influence of complex bed geometry and its morphological change, so yielding new insight into advection-dispersion characteristics at the global scale. As far as we know, however no numerical models have been proposed for capturing tracer advection-dispersion under the influence of complex bed morphodynamics generated within the model itself.

Here we present a first step toward combining a submodel that captures self-formed morphodynamic complexity at global scale with two alternative submodels that describe tracer dispersal. Our morphodynamic model captures self-formed free alternate bars at field scale, as earlier described by e.g. *Tubino et al.* [1999], that is, under typical reach-scale dynamic bed morphodynamics in rivers. We adopt two different submodels describing sediment tracer conservation: a flux-based model and an entrainment-based model [*Parker et al.*, 2000]. Our bedload transport model employ captures the tracer behavior induced by bedload motion (intermediate regime), and the combination of the tracer conservation and morphodyamic submodels directly resolve large-scale tracer transport associated with mutual interactions among flow, bedload, and free bar dynamics (global regime).

In this paper, we 1) illustrate how the flux- and entrainment-based tracer conservation models affect tracer advection-dispersion, 2) describe effects of dynamic bed evolution associated with migrating free bars on large-scale tracer

advection-dispersion, and 3) quantify dominant mechanisms controlling asymptotic tracer dispersion features under the influence of free bars. This is a first attempt to explicitly resolve the effects of dynamic bed evolutions on tracer advection-dispersion at global scales.

2. MODEL

The numerical model used in this study consists of a morphodynamic module and a tracer transport module. A key element of these modules is the treatment of bedload transport; this determines the tracer advection-dispersion associated with the bedload, as well as how bedload transport affects free bar dynamics. Two different formulations have been proposed to handle sediment conservation under the condition of bedload transport, i.e. a flux-based model and an entrainment-based model [*Parker et al.*, 2000]. Below, we address how these models describe tracer transport.

2.1 Flux- and entrainment-based models: Tracer advection-dispersion

Exner [1925] proposed the first morphodynamic model that takes into account morphological changes of the bed surface associated with bedload transport. A 1D version of the model, which corresponds to sediment mass conservation, can be written as:

$$\frac{\partial \eta}{\partial t} + \frac{1}{1-\lambda_p}\frac{\partial q_b}{\partial x} = 0, \tag{1}$$

where t is time, x is the streamwise coordinate, η is the bed surface elevation, q_b is the volume bedload transport rate per unit width, and λ_p is the porosity of bed. (In the above form, the model described sediment volume conservation; this translates to sediment mass conservation assuming that the sediment has constant density.) This model treats bedload transport in terms of the differential flux of sediment volume parallel to the bed. The divergence of the flux drives bed elevation change. This classical flux-based model for sediment conservation [e.g. *Parker et al.*, 2000] is the most common one used in morphodynamic calculations, and has been widely applied within mathematical and numerical models to describe fluvial and related processes on the Earth's surface. The flux-based, however, is limited in its ability to handle the dispersion of bedload tracers, because the bedload transport rate q_b inherently represents a bulk average that does not account for stochastic variations.

Here we show that this limitation precludes the quantification of tracer dispersion in a simple 1D model. By introducing an active layer model [*Hirano*, 1971], we can obtain a flux-based relation for the conservation of tracer volume that corresponds precisely to Eq. (1) [*Parker et al.*, 2000]:

$$L_a \frac{\partial f_a}{\partial t} + f_I \frac{\partial \eta}{\partial t} + \frac{1}{1-\lambda_p}\frac{\partial q_b f_a}{\partial x} = 0, \tag{2}$$

where f_a is the fraction of tracers in the active layer, L_a is the active layer thickness, and f_I is the fraction of tracers exchanged at the interface between the active layer and

the substrate as the bed aggrades or degrades. This fraction is given by the following relation:

$$f_I = \begin{cases} f_a & , \quad \dfrac{\partial \eta}{\partial t} > 0 \\ f_t & , \quad \dfrac{\partial \eta}{\partial t} < 0 \end{cases}, \tag{3}$$

where f_t is the fraction of tracers in the substrate at the interface between the active layer and the substrate. The second and third terms on left-hand side of Eq. (2) represent the exchange of tracers between the active layer and the substrate as a result of bed elevation change and volumetric gradient in the bedload flux of tracers respectively. Experiments have demonstrated that tracers in the bedload disperse by stochastic motion, even under the condition of dynamic equilibrium of the bed surface (i.e., $\partial \eta / \partial t = 0$) [e.g., *Wong et al.*, 2007; *Martin et al.*, 2013]. This dispersion, however, cannot be captured by Eq. (2), because it reduces precise to the kinematic wave equation with no diffusive term at dynamic equilibrium:

$$\frac{\partial f_a}{\partial t} + \frac{q_b}{L_a\left(1-\lambda_p\right)} \frac{\partial f_a}{\partial x} = 0. \tag{4}$$

The classic flux-based model thus cannot explain tracer dispersion.

Several attempts have been made to include stochastic behavior of particles moving as bedload into morphodynamic models [e.g., *Einstein*, 1937; *Nakagawa and Tsujimoto*, 1980; *Parker et al.*, 2000; *Ancey*, 2010; *Furbish et al.*, 2012; *Bohorquez and Ancey*, 2015]. This has most commonly been done in terms of an entrainment-based form for the Exner equation of sediment conservation:

$$\frac{\partial \eta}{\partial t} = \frac{1}{1-\lambda_p}\left(D-E\right), \tag{5}$$

where E is the volumetric entrainment rate of sediment per unit bed area into the bedload, and D is the volumetric deposition rate of sediment per unit area onto the bed. In this model framework, an imbalance of the vertical flux of sediment volume between the bedload and the substrate causes bed elevation change. Stochastic behavior is brought into the model in terms of the deposition rate. A particle entrained into the bedload is assumed to travel a distance, i.e. step length r before depositing again, where r is assumed to be a random variable with PDF $f_p(r)$. The deposition rate $D(x)$ is then given as:

$$D\left(x\right) = \int_0^\infty E\left(x-r\right) f_p\left(r\right) dr. \tag{6}$$

The corresponding relation for conservation of tracers can be written as follows [*Parker et al.*, 2000]:

$$\left(1-\lambda_p\right)\left(L_a \frac{\partial f_a}{\partial t} + f_1 \frac{\partial \eta}{\partial t}\right) = \int_0^\infty f_a\left(x-r\right) E\left(x-r\right) f_p\left(r\right) dr - f_a\left(x\right) E\left(x\right). \tag{7}$$

At dynamic equilibrium, i.e. $\partial\eta/\partial t = 0$, this relation reduces to:

$$\left(1-\lambda_p\right)\frac{L_a}{E}\frac{\partial f_a}{\partial t} = \int_0^\infty f_a\left(x-r\right) f_p\left(r\right) dr - f_a\left(x\right). \tag{8}$$

Taylor expanding for f_a $(x\text{-}r)$ in Eq. (8) and dropping terms higher than 2nd order term yields:

$$\left(1-\lambda_p\right)\frac{L_a}{E}\frac{\partial f_a}{\partial t}=-\mu_1\frac{\partial f_a}{\partial x}+\frac{\mu_2}{2}\frac{\partial^2 f_a}{\partial x^2}, \tag{9}$$

where μ_1 and μ_2 are the first and second moments of the step length PDF, respectively. In the case of an exponential (thin-tailed) PDF for step length [e.g., *Nakagawa and Tsujimoto*, 1980], i.e.:

$$f_p\left(r\right)=\frac{1}{L_s}\exp\left(-\frac{r}{L_s}\right), \tag{10}$$

it is found that μ_1 and μ_2 take the values L_s and $2L_s^2$, respectively, in which L_s denotes the mean step length. At dynamic equilibrium, the bedload transport rate is given by the following relation [*Nakagawa and Tsujimoto*, 1980]:

$$q_b = EL_s. \tag{11}$$

Consequently, Eq. (9) reduces as follows at dynamic equilibrium:

$$\frac{\partial f_a}{\partial t}+\frac{q_b}{L_a\left(1-\lambda_p\right)}\frac{\partial f_a}{\partial x}=\frac{q_b L_s}{L_a\left(1-\lambda_p\right)}\frac{\partial^2 f_a}{\partial x^2}. \tag{12}$$

As opposed to the flux-based kinematic wave equation corresponding to Eq. (4), Eq. (12) is an advection-diffusion equation, so demonstrating that the entrainment-based model does indeed describe the dispersion of tracers associated with bedload transport [*Ganti et al.*, 2010; *Lajeunesse et al.*, 2013]. The scale of step length is intermediate in the sense of *Nikora et al.* [2002], so the diffusion effect in Eq. (12) may be related to dispersion at the intermediate scale.

2.2 Model framework and numerical technique

Here we couple the Exner relations for morphodynamics and tracer conservation with an unsteady shallow water flow model. The model we use, which can be implemented in both 1D and 2D models is essentially the same as *Jang and Shimizu* [2005], to which we refer the reader for details. The Manning roughness closure is used to evaluate the bed shear stress. The governing equations are discretized on a staggered grid system based on a finite difference scheme. The momentum equations of the flow model are decomposed into advective and non-advective terms that include the pressure and roughness terms, and the continuity equation of water and the non-advective terms are solved implicitly by an iterative method. The flow velocities predicted in this way are then updated using the advection terms with the Constrained Interpolation Profile (CIP) method to minimize numerical diffusion [*Yabe et al.*, 1991].

In the entrainment-based model, we evaluated the local entrainment rate from the following relation based on Eq. (11);

$$E = \frac{q_{be}}{L_s}, \tag{13}$$

where q_{be} is the local bedload transport rate that would prevail were it to be in equilibrium with the local bed shear stress (as is assumed in the flux-based model). We further computed q_{be} from the Meyer-Peter and Müller formula [*Meyer, Peter and Muller*, 1948]. The effect of transverse bed slope on bedload is taken into account using the linearized formula proposed by *Hasegawa* [1981] (see also *Kovacs and Parker* [1994] and *Parker et al.* [2003] for fully nonlinearized formulations). The

effect of secondary flow on the bedload transport direction is neglected herein for simplicity, since it plays only a minor role in free bar dynamics in a straight channel at the nonlinear level. The divergence of the bedload fluxes yields bed elevation changes for the flux-based model. In addition, the vector field of the bedload flux is used to calculate the trajectory of the bedload particles in the entrainment-based model. In a 1D model, a single bedload step is directed downstream. In a 2D model, however, the trajectory of a step is described by a 2D path. The appropriate trajectories are most easily described in terms of what might be called "bedload streamlines" (in analogy to flow streamlines), along which the path is everywhere parallel to the local bedload vector. The model framework and detailed numerical procedures used to discretize the entrainment-based model are presented in Appendix A.

To reduce the computational cost of simulating long-term morphological changes of free bars and the associated pattern of asymptotic tracer advection-dispersion, we introduce a morphological factor that accelerates bed evolution changes. This numerical parameter, as defined in e.g. *Roelvink* [2006], *Nabi et al.* [2013a], and *Schuurman et al.* [2016] does not play a critical role in the governing bed morphodynamic processes as long as it is not too large. We set this parameter as 5, which is reasonable for free bar simulations [*Crosato et al*., 2011; *Schuurman et al.*, 2013; *Duro et al.*, 2016].

A constant discharge and a corresponding bedload supply necessary to maintain the elevation of the upstream end set in the initial conditions are imposed at the upstream boundary. Numerical models generally need a perturbation as a trigger for the

inception of free bars [e.g., *Defina*, 2003]. In addition, to get continuous bar inception, the perturbation needs to be maintained over the entire calculation [*Federici and Seminara*, 2003]. In this study, we maintain a small perturbation with a random transverse distribution into the water discharge at the upstream end. Free flux boundary conditions for both flow and bedload are employed at the downstream boundary. The sidewall boundary conditions are set those of vanishing transverse flux of water and bedload.

As mentioned in the model explanation, the flux-based model does not yield a diffusion term for tracer transport for the case of dynamic equilibrium. However, since the governing equation of tracer volumetric conservation in the active layer (i.e., Eq. (2)) is a pure advection equation, an inappropriate numerical scheme will yield numerical diffusion. For example, a low order scheme (e.g., first order upwind scheme) introduces non-negligible numerical diffusion for tracers. We thus use a discretization of the divergence term of tracer flux (last term of left hand side of Eq. (2)) chosen for optimal accuracy but minimal numerical diffusion. More specifically, we use the 5th order Weighted Essentially Non-Oscillatory (WENO) scheme [*Liu et al.*, 1994] to discretize that term to minimize numerical diffusion and achieve stable computations.

Aggradation/degradation causes volumetric exchange of tracers between the active layer and the substrate in this model framework, so we need to store a fraction of the tracers on the substrate. For this, we use a simple multi-layer approach proposed by *Ashida et al.* [1990], which was proposed for computing size-sorting of graded

sediment. This model is similar to the stratigraphy-storing models of *Viparelli et al.* [2010], *Stecca et al.* [2014] and *Stecca et al.* [2016]. The model discretizes the substrate as a number of layers with constant thickness, and calculates the exchange of tracers between the active layer and only the top layer of the substrate, which is called the transition layer. The treatment of the substrate in model of *Ashida et al.* [1990] is more similar to the model of *Viparelli et al.* [2010] than either that of *Stecca et al.* [2014], which generalizes the exchange of sediment between the active layer and other substrate layers, or the model proposed by *Pelosi et al.* [2014], which does not use any active layer assumption.

3. RESULTS

We perform 1D and 2D calculations of tracer advection-dispersion, using the flux- and entrainment-based models described above, under equivalent conditions. Since the 1D model cannot capture free bars, comparison of the 1D and 2D results demonstrates how the presence of single-row free bars affects the characteristics of tracer advection-dispersion.

We use a straight channel that is 62.5 m wide and 20 km long for the computations. The hydraulic conditions are determined in accordance with a linear stability analysis of free bars so that the initial state is indeed subject to single-row alternate bar instability. We performed this linear stability analysis using the relations presented above, with the methodology of *Colombini et al.* [1987]. We accordingly selected constant flow discharge of 305.7 m^3/s, an initial bed slope (S) of 0.00461, and a grain

size of 44.25 mm. These correspond to an initial Froude number (F_r) of 0.85, an initial Shields number (θ) of 0.095, and an initial width-to-depth ratio (β) of 41.7, all computed for the initial flat-bed case (i.e., in the absence of free bars). At the dynamic equilibrium attained in the presence of free bars, the values of S, Fr, θ and β based on cross-sectionally averaged parameters did not deviate strongly from these initial values, although in some local shallow zones Fr deviated significantly from the initial value. The grid sizes in the streamwise and transverse direction are 5 and 2.5 m, respectively. The active layer thickness is twice the grain size. The mean step length used for the entrainment-based model is set to be 100 times the grain size [*Einstein*, 1950]. With these conditions, we first run the models to obtain well-developed single-row alternate bars in the computational domain. These bars appear clearly only after a relaxation distance from the inlet. A rectangular patch of tracers is then placed in the active layer at the upstream end of the simulated free bar train. The discretized step size used to calculate the deposition rate for the entrainment-based model is set to be half of the minimum grid size, which is 1.25 m in this case. We found through trial runs that this step size needs to be smaller than at least either half of the minimum grid size or one tenth of the mean step length.

Figures 1 and 2 show the temporal changes of alternate bar morphology and the spatial distribution of vertically integrated tracer amounts simulated by the 2D entrainment- and flux-based models, respectively. These figures demonstrate that simulated alternate bar morphology and its development between the two models are consistent. Tracer transport characteristics, on the other hand, are somewhat different, particularly in the early stage of the computations. The tracer transport in these

simulations can be categorized into three stages: 1) absence of the bars (a-2, b-2 of Figures 1 and 2), 2) when the tracer plume just encounters the bars (c-2 of the same two figures), and 3) in the presence of bars (d-2, e-2 of the same two figures). In the first stage, the tracer plume advects downstream. This advecting tracer plume is seen to disperse in the streamwise direction in the entrainment-based model, but is seen to translate without dispersion in the flux-based model, as demonstrated in the model explanation above. By comparing (a-2) and (b-2) of Figure 2 with the corresponding panels of Figure 1, it can be clearly seen that at dynamic equilibrium in the absence of bars (i.e. equivalent to 1D conditions) we need a stochastic bedload transport model to reproduce the tracer dispersion; the entrainment-based model is an appropriate approach to model this dispersion.

Since there is only a minor transverse component of bedload in the first stage, the tracer plume simply advects downstream, and the shape of the tracer plume does not change, except for the streamwise dispersion of the entrainment-based model. The migrating alternate bars, however, significantly deform the shape of the tracer plume. The alternate bars generate a meandering flow and associated complex bedload transport and bed elevation variation in the streamwise and transverse directions; as such, the tracer plume is horizontally stretched. In addition, because of the dynamic bed evolution processes (i.e., migrating bars), the tracers in the active layer deposit within the substrate (i.e., within the bars) and spend a longer waiting time before re-entrainment than the tracers in the active layer. The tracer transport in the second stage corresponds to a transition phase from the first to the third stage. The tracer distribution in the second stage is thus discontinuous in space. After this transition

process, the migrating alternate bars mix the tracers well. Thus at the third stage, tracers buried in the bars are re-entrained because of their migration, and then transported again on the bed surface. Consequently, the tracer distribution becomes spatially smooth, tending to converge to a distribution that is symmetrical in the streamwise direction.

We define the vertical integral of tracer fraction F as:

$$F(x,y)=\int_{-\infty}^{\eta} f(x,y,z)\,dz, \tag{14}$$

where f is the local fraction of tracers within the layer corresponding to elevation z, and the corresponding width-averaged value $\overline{F}(x)$ as:

$$\overline{F}(x)=\frac{1}{B}\int_{-B/2}^{B/2}\int_{-\infty}^{\eta} f(x,y,z)\,dzdy, \tag{15}$$

where B is the channel width.

Figure 3 shows the temporal change of vertically-integrated, width-averaged tracer amount $\overline{F}$ in the longitudinal direction at this stage (i.e., stage 3, when the alternate bars are significantly affecting the tracers). The figure demonstrates that the fluctuations associated with bars drives a spatial distribution of tracers that asymptotically approaches a bell-shaped distribution at time passes. This implies that the long-term influence of the bars leads to an asymptotic pattern of dispersion of the tracers. Interestingly, the asymptotic behavior obtained from the flux-based and entrainment-based models are very similar, indicating the dominant role of alternate

bars in driving dispersion.

To discuss the results in detail, we quantify the tracer transport characteristics using the tracer plume advection velocity, c and the standard deviation of the plume of tracers in the longitudinal direction, σ. These are obtained from the 2D calculation results as follows:

$$c = \frac{d\bar{x}}{dt}, \qquad \bar{x} = \frac{\int_0^\infty \int_{-B/2}^{B/2} xF(x,y)\,dydx}{\int_0^\infty \int_{-B/2}^{B/2} F(x,y)\,dydx}, \tag{16}$$

$$\sigma^2 = \frac{\int_0^\infty \int_{-B/2}^{B/2} (x-\bar{x})^2 F(x,y)dydx}{\int_0^\infty \int_{-B/2}^{B/2} F(x,y)dydx}, \tag{17}$$

where $\bar{x}$ is the centroid of tracers in the longitudinal direction. The temporal change of the standard deviation of tracers can be used to characterize streamwise dispersion. A pattern of normal dispersion (normal diffusion) leads to the power relationship, $\sigma \sim t^{\gamma}$, with $\gamma = 0.5$. Here, γ is a scaling exponent characterizing the pattern of dispersion. As noted above, deviation of the scaling exponent from 0.5 indicates anomalous dispersion, specifically, superdiffusive dispersion for $\gamma > 0.5$, and subdiffusive dispersion for $\gamma < 0.5$; superdiffusive (subdiffusive) dispersion results in faster (slower) dispersion of tracers than normal dispersion [*e.g. Schumer et al., 2009*].

Figure 4a shows the temporal change of the advection velocity of the tracer plume in all of four cases (i.e., 1D and 2D, flux- and entrainment-models). This figure

demonstrates that 1) in the absence of bars, the advection velocity is constant and same for all cases, and 2) alternate bars slow the tracer plume down significantly. This velocity slowdown is attributed to the intermittent burial of tracers within the bars (i.e., increasing waiting time).

We explain this by first considering the case of 1D dunes. If every bedload particle is captured on the lee side of a dune, without throughput transport, then the bedload transport rate can be calculated directly from the product of the mean dune height and migration rate [*Simons et al.,* 1965]. This means that every particle is buried after traveling the length of one dune. Here we find that alternate bars play a similar role to dunes. That is, most of the bedload is bound up in bar migration rather than throughput, thus implying repeated burial after transport on the order of one bar wavelength. This makes the plume advection velocity extremely slow, since most of tracer transport is bound up in bar migration. When stage 3 is reached, the deposition rate of tracers within the bars coincides with their re-entrainment rate as bars pass through, exposing zones of low elevation. After a sufficiently long time, the mean advection velocity approaches a constant value which is considerably slower than the early (stage 1) velocity, as well as the velocity simulated by the 1D models.

The presence of the bars plays a key role in the dispersion of tracers as well. Figure 4b shows that 1) in the absence of bars, the 1D and 2D models yield identical patterns of dispersion features, i.e., no dispersion for the flux-based model and normal dispersion for the entrainment-based model; 2) the onset of the influence of bars greatly disperses the trace plume, causing a deviation from the 1D calculation; and

most importantly 3) the asymptotic pattern of dispersion after a sufficiently long time is somewhat superdiffusive dispersion, regardless of whether a flux-based or entrainment-based model is used.

At stage 1, e.g. hours 1 – 3 in Figure 4b, bars are absent, and the asymptotic pattern of dispersion obtained from the numerical model is consistent with the analytical forms of Eqs. (4) and (12); advection without dispersion in the flux-based model, and advection with normal dispersion in the entrainment-based model. During stage 2, when the tracer plume encounters bars, the dispersion becomes strongly superdiffusive (e.g. hours 7 – 20 in Figure 4b), followed by a short period of slightly subdiffusive behavior (e.g. hours 20 – 40 in Figure 4b). The strongly superdiffusive behavior is caused by horizontal stretching of the tracer plume and deposition of tracers within the bars, and the subsequent short period of slightly subdiffusive behavior may be attributed to the fact that most of the tracers stay within a bar until new bars migrate from upstream and re-entrain them. After that, repeated of transport, deposition, and re-entrainment events during stage 3 lead asymptotically to mildly superdiffusive behavior (e.g. after 100 hours in Figure 4b). Importantly, the flux-based model shows the same asymptotic behavior as the entrainment-based model. This indicates that the migrating alternate bars themselves drive dispersion much more effectively than particle-scale stochastic motion of the bedload.

This implication motivates us to perform numerical experiments for a sensitivity analysis of tracer advection-dispersion associated with single-row free bars. For this analysis, we use the flux-based model only, as the entrainment-based model shows

similar behavior at large times (Figure 4). Hereafter, we define the 2D flux-based run above as Case 1; Table 1 summarizes the set of parameters and cases for the analysis. We choose cases corresponding to three dimensionless parameters, i.e., the Froude number, Shields number, and width-to-depth ratio. The other parameters, conditions, and grid sizes used for all the cases are identical to those of Case 1. To make the morphodynamic features in all cases consistent, the combination of parameters has been specifically chosen to yield migrating alternate bars. Figure 5 shows the combination of parameters for all cases of bar regime criteria delineated based on the linear stability analysis of *Kuroki and Kishi* [1984], confirming our result that all the runs of Table 1 do indeed fall within the single-row alternate bar regime.

Figure 6 shows the tracer plume advection-dispersion characteristics for all cases. Their general characteristics are quite consistent. The migrating bars cause the slowdown of advection velocity and disperse the tracers. With passage of sufficient time, the tracer transport approaches an asymptotic form corresponding to constant advection velocity and the power dependence $\sigma \sim t^{\gamma}$ characterizing dispersion. Table 2 summarizes the results of asymptotic advection velocity and the scaling exponent, γ. With respect to tracer dispersion, the results suggest that 1) the scaling exponent is slightly different in each case, but nevertheless 2) the asymptotic dispersive behavior is either normal or weakly superdiffusive, but not subdiffusive. A high Froude number Fr and width/depth ratio β, and a low Shields number θ tend to increase the scaling exponent, and thus superdiffusive behavior.

The concepts embodied in the random walk model allow interpretation of the

physical mechanisms governing this large-scale dispersion and the origin of superdiffusive behavior. In the framework of random walk model, random motion of the walkers asymptotically leads to normal diffusion in accordance with Central Limit Theorem (CLT) [e.g., *Schumer et al.*, 2009]. Anomalous diffusion is associated with conditions that break the CLT. In linear and nonlinear stability theory, single-row and multiple-row alternate bars are idealized as phenomena that show purely deterministic spatiotemporal variation [*e.g. Colombini et al.,* 1987]. Such bars have no random element, and cannot be expected to cause asymptotic tracer dispersion that is either normal or anomalous. Indeed free bars and associated tracer transport are not purely random and stochastic processes; migrating bars tend to be relatively well-ordered, and the bars constrain the length scale of tracer motion [*Pyrce and Ashmore*, 2003, 2005]. Nevertheless, the properties of free bars (i.e., wavelength, waveheight, celerity, and transverse mode) generally show some stochastic variation in space and time. Even under the simple conditions adopted herein (i.e., steady water discharge and bedload supply, uniform grain size, and straight channel with constant slope), our model reproduces this stochasticity. The irregularity of individual bars gives some randomness to the system, resulting in tracer dispersion. This randomness inherent to the model can be expected to cause normal diffusion, as would be the case with a random walk model, as long as the CLT is satisfied. We investigate whether or not this is the case below. While doing this, it is worthwhile to investigate the probability density functions (PDFs) of tracer of travel distance and waiting time, because whether or not the tails of these distributions are heavy or thin can influence whether or not dispersion is normal or anomalous. With this in mind, we interpret the

simulation results in the context of probability.

The model we use for the simulations is Eulerian-based, so we cannot calculate the precise probability distributions of the travel distance and waiting time. In principle, we would need to track all individual particles to do so [*Lajeunesse et al.*, 2010; *Roseberry et al.*, 2012; *Campagnol et al.*, 2015]. We describe alternatives to such a Lagrangian description below.

Voepel et al. [2013] estimated a PDF of particle waiting time from an experimental time series data of bed surface elevation. They assumed that when the local bed surface rises at a given elevation, a tracer particle must have deposited onto the bed at that elevation, and when the bed surface falls at a given elevation, a bed particle there must have been entrained. The duration between these events characterizes particle waiting time. By discretizing the bed elevation between the maximum and minimum elevation recorded within a sampling period, they calculated the conditional probability of waiting time for a bed particle at each discretized elevation. This probability is in turn weighted based on the probability $p_e(z)$ of the bed surface elevation being at each discretized elevation z when calculating an unconditional waiting time for a bed particle. We apply this method to time series data of bed elevation generated by the numerical model at each grid point along a cross section where bars are well developed. In principle, the relevant PDF's should be based on averaging over the entire reach along which alternate bars are developed. If, however, the statistical characteristics of the alternate bars (e.g. average bar height, wavelength and migration speed) are invariant along the reach in question, it suffices to obtain the

PDF's characterizing waiting time based on data corresponding to grid points along a single cross-section.

We denote the probability density that the bed is at elevation z at transverse position y on the cross-section as $p_e(z,y)$, and the corresponding conditional probability that waiting time T exceeds τ at elevation z and transverse position y as $P(T>\tau|\, z, y)$. Figure 7 shows two examples of time series of bed elevation variation produced by the model for Case 1. The left-hand side of panel a) corresponds to the time series for left bank of a cross section, and the left-hand side of panel b) corresponds to channel center. The corresponding time series of waiting times are denoted by the lengths of the gray lines connecting times when the bed moves upward across a given elevation z to when the bed subsequently next moves downward across this same elevation. Illustrated on the right-hand side for each panel in the figure is the corresponding PDF p_e for elevation. Note that since our simulation is 2D horizontal, the probability of bed surface elevation becomes a function of both the transverse (y) and vertical (z) coordinates. The unconditional exceedance probability distribution of waiting time can be calculated as follows:

$$P(T>\tau)=\int\int P(T>\tau \mid z,y)\, p_e(z,y)\, dzdy \tag{18}$$

where τ is the waiting time, $p_e(z,y)$ is the probability density that of the bed surface is at (z, y), and $P(T>\tau)$ is the exceedance probability of waiting time.

We can now obtain an estimate of the probability distribution of travel distance in one transport "event". In order to do this, we repeat the calculation of Cases 1 – 7

above, but with the following constraint; once a tracer particle is deposited in the substrate (i.e. buried within the bars), it is not allowed to be re-entrained (i.e., by setting f_l in Eq. (2) equal to zero whenever the bed degrades due to bar passage). We then define the duration of the "event" as the time required for a specified large fraction (e.g. 0.999) such that nearly all of the initially deployed particles are buried in the substrate. The spatial variation of distance to burial at the end of this "event" then serves as a surrogate for the PDF of travel distance. That is, the simulated tracer distribution at the end of the "event" normalized by the total amount of tracers serves as the probability density function of the travel distance within that "event". This, of course does not represent the true travel distance in the system, because re-entrainment is not allowed. The cumulative travel distance distribution, however, can be approximated as the sum of many such single transport "events" [*Hassan et al.*, 2013]. Since the flux-based model does not calculate the trajectory of tracers, we cannot measure the exact travel distance along any bedload streamline (i.e. path everywhere parallel to the bedload vector). With this in mind, we define travel distance in terms of downstream distance as measured along the x coordinate rather than path length.

Figure 8 shows the estimated exceedance probability of travel distance, l, and waiting time, τ, from the calculation results for all seven runs. The slope of this log-log plot, α, indicates the characteristics of the tails associated with long travel distance or waiting time; a slope with $\alpha < 2$ implies a heavy-tailed distribution; whereas a slope with $\alpha > 2$ implies a thin-tailed distribution. The threshold slope between thin- and heavy-tailed feature (e.g., $P(L>l) \sim l^{-2}$) is also shown on the figure.

The figures exhibits thin-tailed behavior for travel distance distribution in all cases, implying that the PDF of travel distance feature is unlikely to be the origin of anomalous dispersion. On the other hand, the exceedance probability distribution of waiting time shows more complex behavior than that of the travel distance. The tails for Cases 2, 3 and 5 appear to be thin in Figure 8. In Case 1 there are likely two slope breaks in the tail, similar to a truncated Pareto distribution (combination of exponential and power functions) [*Aban et al.*, 2006], and the tails for Cases 4, 6, and 7 appear to be heavy. This heavy-tailed waiting time may be the origin of the anomalous dispersion seen in Cases 1, 4, 6 and 7.

Schumer et al. [2009] show that in cases when the travel distance distribution is thin-tailed, a heavy-tailed waiting time PDF causes subdiffusive dispersion in the context of a Continuous Time Random Walk (CTRW) model. *Weeks et al.* [1996], on the other hand, suggest that a heavy-tailed waiting time PDF could result in either super- or sub-diffusive dispersion depending on the heaviness of the tail (i.e., α). Both suggest that the tail of waiting time required to generate subdiffusive dispersion needs to be extremely heavy (e.g., $\alpha < 0.5$ [*Weeks et al.*, 1996]), which is unlikely in the present simulations. Our results suggest that a moderately heavy-tailed waiting time (i.e. α slightly less than 2), may be the cause of superdiffusive dispersion, in line with *Weeks et al.* [1996]. This is consistent with the superdiffusive exponent γ in the relation $\sigma \sim t^{\gamma}$ found for several of the results, e.g. 0.68 for Case 1 and 0.63 for Case 4.

A physically based description of the behavior generating such PDF tail may be as follows. The free bar morphology and its migration strongly restrict the travel distance

of tracers due to the frequent passage of troughs [*Pyrce and Ashmore*, 2003, 2005], so travel distance is strongly bounded by the frequency of encounter with a trough. Although the randomness of free bars gives a certain stochasticity to tracer motion, well-regulated migrating bars act to inhibit the preferential tracer motion necessary to generate a heavy-tailed pattern of tracer dispersal. On the other hand, the randomness of free bars, especially in terms of bar height, plays an important role in the tail of the PDF of waiting time. The randomness of free bar properties introduces a large stochastic variability in bed surface elevation. The PDF of trough elevation in particular plays an important role in this regard [*Blom et al.*, 2003; *van der Mark et al.*, 2008]. Deeply-buried particles are only infrequently re-entrained into the active layer, so generating a very long waiting time. Randomness sufficient to generate a heavy-tailed waiting time in the simulation may be, for example a result of nonlinear interaction among different bar modes [*Pornprommin et al.*, 2004; *Watanabe*, 2007]. Interestingly, the scaling exponent γ in the dispersion relation tends to be high (i.e., more superdiffusive) when the flow conditions approach the threshold between alternate bars and multiple bars (Fig. 5), corresponding to a sufficiently wide channel.

4. DISCUSSION

The computational conditions of this study are somewhat extreme in terms of the morphological changes of the bed surface, in so far as the alternate bars continue migrating downstream in a relatively regular way. This notwithstanding, the model does capture a stochastic element to bed deformation by alternate bars, particularly in

terms of minimum trough elevation. The results reported here are consistent with several important findings based on field observations of long-term tracer advection-dispersion. *Hassan et al.* [2013] suggest that bed morphology is more important for controlling tracer motion than hydraulic regime. They summarize a number of field datasets, showing that the travel distance distribution could be heavy-tailed in a single flood event, but is unlikely to be heavy-tailed after multiple flood events. As we have shown, this is because the bed elevation variation (in this case associated with alternate bars) eventually results in capture of the tracers within the bed, so constraining the length scale of travel distance.

The superdiffusive behavior seen in several of the runs reported here, and the associated heavy-tailed waiting time qualitatively agrees with several field observations [e.g., *Phillips et al.*, 2013; *Olinde and Johnson*, 2015]. It should be kept in mind, however, that only the morphodynamics of a single morphological unit, i.e., that of alternate bars, is considered here. In reality, however, morphological units coevolve in a system and control the overall morphodynamic features. For instance, bedforms (ripples, dunes, and antidunes) [*Blom and Parker*, 2004], multiple-row bars [*Fujita*, 1985; *Shuurman et al.*, 2013], braiding [*Kasprak et al.*, 2015], and meandering [*Asahi et al.*, 2013] are dynamic components that add complexity the problem of tracer dispersal. Corresponding static components include curvature-induced forced bars [*Blondeaux and Seminara*, 1985], mid-channel bars driven by channel width variation [*Zolezzi et al.*, 2012], and floodplains occasionally accessed by the flow [*Lauer and Parker*, 2008]. Interactions among components of dynamic bed evolution at different spatial and temporal scales can result in a complex pattern of bed surface elevation

variability, and static components can serve to store large amounts of sediment. These factors all complicate the issue of waiting time distribution. A thorough understanding of how the interaction of multiscale bed morphologies and their dynamics affect tracer advection-dispersion would be key to explaining crucial phenomena we have not touched upon in this paper, including subdiffusive dispersion [*Nikora et al.*, 2002; *Schumer et al.*, 2009; *Zhang et al.*, 2012] and advective slowdown [*Ferguson et al.*, 2002; *Haschenburger*, 2013; *Pelosi et al.*, 2016].

As we have shown in our simulations, the waiting time distribution associated with the randomness of free bars is not simply thin-tailed, but neither is it extremely heavy-tailed. This is because the randomness of the simulated alternate bars is not extreme, so that the migrating bars eventually transport all the tracers we deploy. Such conditions are insufficient to achieve a strongly heavy-tailed waiting time distribution leading to subdiffusive dispersion, as suggested by *Weeks et al.* [1996] and *Schumer et al.* [2009]. Extra randomness associated with morphodynamics at different scales may affect the heaviness of the waiting time, possibly pushing the pattern of dispersion from superdiffusive to subdiffusive. Additionally, the migration speed of free bars in nature tends to be relatively slow, even in straight channels, and free bars may in some cases stop migrating [*Crosato et al.*, 2011; *Eekhout et al.*, 2013; *Rodrigues et al.*, 2015]. The retention of tracers in a quasi-static bed morphology would constrain tracer motion, eventually resulting in subdiffusion and advective slowdown as all tracer particles eventually become trapped and stop moving.

Some tracer particles in transport are trapped in the downstream faces of alternate

bars, and thus buried, whereas other particles find trajectories that allow them to bypass one or more bars without being trapped. The dispersal pattern of bedload particle tracers under the influence of migrating alternate bars is likely sensitive to the degree of bar trapping versus bypassing. More specifically, the relative importance of these two patterns of behavior likely affect both travel distance and waiting time. For instance, stronger trapping should reduce travel distance and cause longer waiting times, possibly resulting in more subdiffusive behavior. In morphodynamic models such as the present one, this behavior is determined by the aggregate of multiple physical submodels (e.g, gravitational effects acting on bedload transport and three dimensional flow structures such as topographically-induced secondary flow at the downstream side of bars), and is also affected by the numerical scheme itself. Such factors contribute to alternate bar characteristics such as wavelength, wave height and migration speed [e.g., *Nelson*, 1990; *Schuurman et al.*, 2013; *Iwasaki et al.*, 2016]. However, it is in general not possible to accurately simulate numerically the full range of behavior observed in experiments or field rivers in the framework of a 2D morphodynamic model [e.g., *Shimizu and Itakura*, 1989; *Defina*, 2003]. Further model validation in terms of a comparison with experimental or field measurements of spatiotemporal changes in alternate bar characteristics, as well as the pattern of tracer particle dispersal among them, are desirable.

A critical model constraint of the present analysis is the assumption that the sediment consists of material of uniform grain size. In the case of graded sediment, variability of particle mobility according to size class further complicates tracer transport and dispersion [*Ganti et al.*, 2010; *Hashenburger*, 2013]. In addition to the

effects of varying mobility, sediment size gradation also plays a role in shaping bedform characteristics [*Lanzoni and Tubino*, 1999; *Lanzoni*, 2000; *Blom et al.*, 2003] by generating stronger randomness of bedforms than those generated under the constraint of uniform sediment [*Takebayashi and Egashira*, 2008]. All these factors will impact tracer advection-dispersion. The present model thus invites extension to the case of sediment size mixtures [*Blom and Parker*, 2004; *Blom et al.*, 2006; *Blom et al.*, 2008; *Viparelli et al.*, 2010; *Stecca et al.*, 2016].

Lastly, another model limitation is our use of a discretized layer model (i.e., an active layer and several substrate layers) to calculate tracer transport and to store the stratigraphic record of tracer deposition. *Parker et al.* [2000] showed that the active layer model approximates the probability density function for entrainment as a step-like function, i.e., constant probability within the active layer and no possibility for entrainment in the substrate. Moreover, discretized layer models inject numerical dispersion into any numerical calculation. This creates difficulties in treating deposition and re-entrainment accurately. A more general treatment in terms of a formulation of the Exner equation of sediment continuity that is intrinsically continuous in the vertical, with no active layer, would be of value in future numerical models [*Parker et al.*, 2000; *Blom and Parker*, 2004; *Blom et al.*, 2008; *Stecca et al.*, 2016; *Pelosi et al.*, 2016].

5. CONCLUSIONS

In this paper we present numerical simulations of large-scale tracer particle

advection-dispersion in alluvial rivers. We specifically focus on conditions for which bedload is the dominant mode of sediment transport, and for which the river is subject to the formation of free, migrating alternate bars. We apply two formulations of the Exner equation of sediment conservation; a standard flux form, in which bed elevation change is related to the divergence of the vector of sediment transport rate, and a stochastic entrainment form, in which bed elevation change is related to the net entrainment rate of particles into bedload. In modeling tracer advection-dispersion, we use a single grain size, as well as an active layer formulation in which active layer thickness scales with grain size. We specifically consider conditions so that no bed aggradation or degradation occurs when averaged over the bars.

We find that the presence of bars has a dramatic effect on streamwise advection-dispersion of tracer particles. When the flux form of Exner equation is used for the case of a flat bed (no bars), tracer particles advect without dispersing. When the entrainment formulation is applied to the same condition, the particles also disperse, in response to the stochasticity associated with the PDF of particle step length. The effect of bars is to substantially increase the streamwise dispersion rate. The statistics of the pattern of advection-dispersion seen in the presence of bars are to a large degree independent of whether the flux or entrainment forms of Exner equation are used, indicating that dispersion is dominated by the bars themselves.

The simulated asymptotic pattern of streamwise tracer advection-dispersion under the influence of free bars is either normal or weakly superdiffusive. The numerical model self-generates stochasticity in bar properties, including wavelength, wave

height, and celerity. This in turn imparts a randomness to tracer behavior, resulting in large-scale dispersion. More specifically, the randomness of the alternate bar dimensions renders local bed surface elevation a stochastic quantity. In some cases, the probability distribution of trough elevation is such that it results in a heavy-tailed waiting time distribution; a deeply-buried particle must wait an anomalously long time before it is re-entrained. Migrating bars strongly constrain the length-scale of tracer transport, likely causing a thin-tailed distribution of travel distance. The combination of thin-tailed travel distance and heavy-tailed waiting time may be the cause of the simulated superdiffusive dispersion when it occurs.

The morphological evolution of bed surface we consider in the simulation is that of alternate bars only, in the absence of bed aggradation or degradation when averaged over the bars. However, the coexistence of several static and dynamic morphological elements might make the waiting time distribution more complex, perhaps causing other dispersion behavior (e.g., subdiffusive dispersion) and perhaps affecting advection (e.g., advective slowdown), which are not illustrated in this paper. The effects of different bed morphologies (e.g., multiple-row bars, braiding and 3D dunes) and channel planform (e.g., meandering, systematic width variation, and interacting channel and floodplain) on tracer advection-dispersion invite further investigation. In addition, model extensions including e.g. sediment size mixtures, and also describing the bed in terms of a continuous vertical structure rather than the active layer formulation so as to better simulate vertical mixing of tracers in the bed [*e.g. Pelosi et al.*, 2014, 2016], are future challenges in the pursuit of a comprehensive understanding of bedload tracer advection-dispersion in nature. This study contributes to a better

understanding of tracer advection-dispersion in the global regime [*Nikora et al.,* 2002].

APPENDIX

A. Flux- and entrainment-based model: Free bar simulation

In this appendix we show how the flux- and the entrainment-based morphodynamic models work for free bar simulations. The model framework using the flux-based model to reproduce free bar inception and development has been well documented in the literature [e.g., *Callendar*, 1969; *Parker*, 1976; *Fredsøe*, 1978; *Kuroki and Kishi*, 1984; *Colombini et al.*, 1987; *Shimizu and Itakura*, 1989; *Nelson*, 1990; *Schielen et al.*, 1993; *Defina*, 2003; *Federici and Seminara*, 2003; *Pornprommin and Izumi*, 2011; *Crosato et al.*, 2012]. A horizontal 2D morphodynamic model, which consists of a shallow water flow model and a flux-based Exner equation with the appropriate bed slope effect on bedload transport (especially in the transverse direction) is sufficient for reproducing the linear and nonlinear free bar dynamics. As far as we know, however, there has been no attempt to use entrainment-based models for free bar simulations in rivers. A model framework and sensitivity analysis of the results of these morphodynamic models is thus of use.

One-dimensional flux- and entrainment-based models of morphodynamics are essentially identical under dynamic equilibrium conditions [*Nakagawa and Tsujimoto*, 1980]. Both types of formulations have been coupled with hydrodynamic models to simulate 1D bed evolution (e.g., bedform dynamics and bed aggradation/degradation)

[e.g., *Giri and Shimizu*, 2006; *Yamaguchi et al.*, 2009; *Pelosi and Parker*, 2014]. We address the 2D case in this appendix.

A key issue for solving the 2D entrainment-based model is the determination of how to compute the deposition rate. The deposition rate at (x, y) is the total amount of bedload that is transported from upstream of (x, y) and deposited onto the bed at (x, y); thus, this term must be calculated based on the trajectory of motion of the bedload particles themselves [*Nagata et al.*, 2000]. The flow velocity near the bed surface, as well as the local bed slope, consideration of the effect of which is necessary to achieve a finite wavelength [*Engelund and Skovgaard*, 1973; *Fredsøe*, 1978; *Kuroki and Kishi*, 1984], determine the motion of bedload particles on the bed surface. Transverse bedload transport formulas [*Ikeda*, 1982; *Hasegawa*, 1989; *Sekine and Parker*, 1992; *Talmon et al.*, 1995] have been used to describe the direct gravitational effect of bed slope on bedload transport in flux-based morphodynamic models. This suggests that the use of such bedload formulas to compute the trajectory of bedload particles (and thus their deposition rate) would be sufficient to reproduce free bar instability in an entrainment-based model. We thus consider a bedload vector field defined as:

$$\frac{dx}{q_{bx}} = \frac{dy}{q_{by}} = \frac{ds}{q_{bs}}, \tag{A1}$$

where s is the local "bedload streamline" coordinate (i.e. coordinate along which the differential arc length vector is everywhere parallel to the bedload vector), q_{bs} is the bedload transport rate in the s direction, and q_{bx}, q_{by} are the bedload transport rates in the x and y directions (Cartesian coordinate system) that are obtained in a manner

identical to the flux-based model. Integrating the deposition rate with respect to particle trajectory leads to the following 2D entrainment-based Exner equation:

$$\left(1-\lambda_p\right)\frac{\partial \eta}{\partial t} = -E\left(x,y\right) + \int_0^\infty E\left[x - x'\left(s\right), y - y'\left(s\right)\right] f_p\left(s\right) ds, \tag{A2}$$

where x' and y' are the particle locations along the trajectory of bedload motion. Taylor-expanding E in the integral for deposition rate and retaining only the 1st order term gives, it is found that:

$$\left(1-\lambda_p\right)\frac{\partial \eta}{\partial t} = -\frac{\partial E}{\partial x} L_x - \frac{\partial E}{\partial y} L_y, \tag{A3}$$

in which:

$$L_x = \int_0^\infty x'\left(s\right) f_p\left(s\right) ds, \qquad L_y = \int_0^\infty y'\left(s\right) f_p\left(s\right) ds. \tag{A4}$$

We linearize the problem by considering a locally constant angle of bedload transport direction with respect to the x-axis, θ_s, defined as:

$$\frac{dy}{dx} = \frac{q_{by}}{q_{bx}} = \tan\theta_s. \tag{A5}$$

This gives the following relationships:

$$L_x = L_s \cos\theta_s, \qquad L_y = L_s \sin\theta_s. \tag{A6}$$

This simplification reduces Eq. (A2) to:

$$\left(1-\lambda_p\right)\frac{\partial \eta}{\partial t}=-\frac{\partial}{\partial x}\left(EL_x\cos\theta_s\right)-\frac{\partial}{\partial y}\left(EL_x\sin\theta_s\right)=-\frac{\partial q_{bx}}{\partial x}-\frac{\partial q_{by}}{\partial y}. \tag{A7}$$

The derivation above suggests that in correspondence to the 1D case, under the constraint of mobile-bed equilibrium the flux- and entrainment-based models are essentially identical in the 2D case as well. This correspondence implies that in a linear stability analysis, the entrainment formulation predicts the formation of alternate bars similarly to the flux formulation.

We elaborate on more specific calculation procedures for the deposition rate as follows. We assume that a bedload particle, which is entrained at the center of each computational cell, represents the motion of all bedload particles that are entrained in each cell, meaning that we calculate the trajectory of each cell [*Nabi et al.*, 2013b] as follows:

$$\begin{aligned} x_p{}^n &= x_{entrained}+\sum_{i=1}^{n-1}\Delta s\left(\frac{q_{bx}}{q_{bs}}\right)_{x=x_p{}^i,\,y=y_p{}^i}, \\ y_p{}^n &= y_{entrained}+\sum_{i=1}^{n-1}\Delta s\left(\frac{q_{by}}{q_{bs}}\right)_{x=x_p{}^i,\,y=y_p{}^i}, \end{aligned} \tag{A8}$$

where $x_{entrained}$, $y_{entrained}$ is the location where the particle is entrained, Δs is the discretized step size used to compute the trajectory, n is the index number of the discretized steps, and x_p and y_p are the particle locations at the nth discretized step. We continue increasing the number of steps n until the cumulative PDF of step length f_p reaches almost unity, meaning that the entrained bedload has all deposited onto the bed along the computed trajectory so as to satisfy mass conservation of bedload tracer

particles. At each nth step, the cell we track in principle overlaps with four computational cells. We compute the deposition rate for these four cells based on the percentage of overlapped area. Note that for this procedure, we calculate q_{bx} and q_{by} at x_p^i and y_p^i based on the exact location of the particle we track. According to our trial calculations, a simple interpolation of bedload fluxes computed at other locations (e.g., center of cell or boundary of cell) to x_p^i and y_p^i can cause development of very small bars with high transverse mode. This may be because such an interpolation results in use of a wide discrete points in computing the local bed slope, leading to inaccuracy in a parameter that plays an important role in the inception of free bars [*Kuroki and Kishi*, 1984] as well as in the stabilization of the computation of bed evolution [*Mosselman and Le*, 2016].

Lastly, we illustrate the sensitivity of free bar formation to the type of Exner formulation (flux versus entrainment), and to variation in mean step length. The calculations here are at experimental scale: channel width is 0.48 m, grain size is 1.3 mm, bed slope is 0.075, and water discharge is 3 *l*/s, corresponding to a Froude number of 0.88, a Shields number of 0.06, and a width-to-depth ratio of 27.7. Mean step length characterizes a lag effect on bedload transport; the longer the step length, the more stable bed perturbations become [*Mosselman and Le*, 2016], suppressing the conditions for the linear development of free bars [*Kuroki and Kishi*, 1984]. Figure A1 shows the sensitivity of the wavelength and wave height of free bars to the type of morphodynamic model (flux versus entrainment) and variation in mean step length. According to this sensitivity analysis, the lag effect on the initially selected bar wavelength is fairly strong, whereas the effect on the equilibrium wavelength and

wave height is minor.

Notations

B : channel width [L]

c : tracer plume advection velocity [L/T]

D : volumetric deposition rate of sediment per unit area onto the bed [L/T]

E : volumetric entrainment rate of sediment into the bedload per unit bed area into the bedload [L/T]

F : vertically-integrated tracer amount at (x,y) [L]

$\bar{F}(x)$: width-averaged value of vertical integral of tracer fraction [L]

F_r : initial Froude number [-]

f : the local fraction of tracers [-]

f_a : fraction of tracers in the active layer [-]

f_I : fraction of tracers exchanged at the interface between the active layer and the substrate [-]

f_p : probability density function (PDF) of step length [1/L]

f_t : fraction of tracers in the substrate at the interface between the active layer and the substrate [-]

l : travel distance [L]

L_a : active layer thickness [L]

L_s : mean step length [L]

n : index number of the discretized steps [-]

$P(L>l)$: exceedance probability of travel distance [-]

$P(T>\tau)$: exceedance probability of waiting time [-]

$p_e(z)$: probability of bed surface elevation being at each discretized elevation [1/L]

q_b : volume bedload transport rate per unit width [L^2/T]

q_{be} : equilibrium local bedload transport rate per unit width [L^2/T]

q_{bx} : volume bedload transport rate per unit width in x direction [L^2/T]

q_{by} : volume bedload transport rate per unit width in y direction [L^2/T]

q_{bs} : volume bedload transport rate per unit width in s direction [L^2/T]

S : initial bed slope [-]

s : streamwise coordinate [L]

t : time [T]

x : streamwise coordinate [L]

$\bar{x}$: centroid of tracers in terms of streamwise direction [L]

$x_{entrained}$: x where the particle is entrained [L]

x_p ,y_p : particle location at n^{th} discretized step [L]

y : transverse coordinate [L]

$y_{entrained}$: y where the particle is entrained [L]

z : vertical coordinate [L]

α : indicator of power relation of exceedance probability distribution [-]

β : initial width-to-depth ratio (aspect ratio) [-]

γ : scaling exponent characterizing the pattern of tracer dispersion in a relation, $\sigma \sim t^{\gamma}$ [-]

Δs : discretized step size to compute the trajectory in entrainment-based model [L]

η : bed surface elevation [L]

θ : initial Shields number [-]

θ_s : angle of streamline to x axis [rad]

λ_p : porosity of bed [-]

μ_1 : first moment of step length PDF [L]

μ_2 : second moment of step length PDF [L^2]

σ : standard deviation of the plume of tracers in longitudinal direction [L]

τ : waiting time [L]

ACKNOWLEDGEMENTS

T.I. was supported by a research project "Improving Morphodynamic Predictions in Rivers" funded by the U.S. Geological Survey National Research Program. Y.S. was supported by Grant-in-Aid for Scientific Research on Innovative Areas (Grant Number 24110006) of the Ministry of Education, Culture, Sports, Science, and Technology in Japan. G.P. was in part supported by the US National Science Foundation (grant no. EAR-1124482).

REFERENCES

Aban, I.B., M.M. Meerschaert, and A.K. Panorska (2006), Parameter estimation of the truncated Pareto distribution, *J. Amer. Statist. Assoc.*, 101, doi: 10.1198/016214505000000411.

Ancey, C. (2010), Stochastic modeling in sediment dynamics: Exner equation for planar bed incipient bed load transport conditions, *J. Geophys. Res.*, 115, F00A11, doi:10.1029/2009JF001260.

Asahi, K., Y. Shimizu, J. Nelson, and G. Parker (2013), Numerical simulation of river meandering with self-evolving banks, *J. Geophys. Res.*, 118(4), 2208–2229, doi:10.1002/jgrf.20150.

Ashida, K., and M. Michiue (1972), Hydraulic resistance and bed transport rate in alluvial stream, *Proc. of JSCE*, 201, 59–69. (in Japanese)

Ashida, K., S. Egashira, B. Liu, and M. Umemoto (1990), Sorting and bed topography in meander channels, *Annuals, Disaster Prevention Research Institute*, Kyoto University, 33(B-2), 1-19 (in Japanese).

Blom, A., J.S. Ribberink, and H.J. de Vriend (2003), Vertical sorting in bed forms: Flume experiments with a natural and a trimodal sediment mixture, *Water Resour. Res.*, 39(2), 1025, doi:10.1029/2001WR001088.

Blom, A., and G. Parker (2004), Vertical sorting and the morphodynamics of bed form-dominated rivers: A modeling framework, *J. Geophys. Res.*, 109, F02007, doi:10.1029/2003JF000069.

Blom, A., G. Parker, J. S. Ribberink, and H. J. de Vriend (2006), Vertical sorting and the morphodynamics of bed-form dominated rivers: An equilibrium sorting model, *J. Geophys. Res.*, 111, F01006, doi:10.1029/2004JF000175.

Blom, A., J.S. Ribberink, and G. Parker (2008), Vertical sorting and the morphodynamics of bed form-dominated rivers: A sorting evolution model, *J. Geophys. Res.*, 113, F01019, doi:10.1029/2006JF000618.

Bohorquez, P., and C. Ancey (2015), Stochastic-deterministic modeling of bed load transport in shallow water flow over erodible slope: Linear stability analysis and numerical simulation, *Adv. Water Resour.*, 83, 36-54, doi: 10.1016/j.advwatres.2015.05.016.

Bradley, D.N., G.E. Tucker, and D.A. Benson (2010), Fractional dispersion in a sand bed river, *J. Geophys. Res.*, 115, F00A09, doi:10.1029/2009JF001268.

Callander, R.A. (1969), Instability and river channels, *J. Fluid Mech.*, 36, 465-480, doi:10.1017/S0022112069001765.

Campagnol, J., A. Radice, F. Ballio, and V. Nikora (2015), Particle motion and diffusion at weak bed load: accounting for unsteadiness effects of entrainment and disentrainment, *J. Hydraul. Res.*, 53(5), 633-648, doi: 10.1080/00221686.2015.1085920.

Colombini, M., G. Seminara, and M. Tubino (1987), Finite amplitude alternate bars, *J. Fluid Mech.*, 181, 213-232, doi:10.1017/S0022112087002064.

Crosato, A., E. Mosselman, F.B. Desta, and W.S.J. Uijttewaal (2011), Experimental and numerical evidence for intrinsic nonmigrating bars in alluvial channels, *Water Resour. Res.*, 47, W03511, doi:10.1029/2010WR009714.

Defina, A. (2003), Numerical experiments on bar growth, *Water Resour. Res.*, 39(4), 1092, doi:10.1029/2002WR001455.

Duro, G., A. Crosato, and P. Tassi (2016), Numerical study on river bar response to spatial variations of channel width, *Adv. Water Resour.*, doi:10.1016/j.advwatres.2015.10.003.

Eekhout, J.P.C., A.J.F. Hoitink, and E. Mosselman (2013), Field experiment on alternate bar development in a straight sand-bed stream, *Water Resour. Res.*, 49, 8357-8369, doi:10.1002/2013WR014259.

Einstein, H. 1937. Bedload transport as a probability problem, Ph.D thesis, Colorado State University, Fort Collins, Colorado.

Einstein, H. (1950), The bed-load function for sediment transportation in open channel flows, *Technical Bulletin 1026*, *US Dept. of the Army*, *Soil Conservation Service*, *Washington*, *DC*.

Engelund, F. and O. Skovgaard (1973), On the origin of meandering and braiding in alluvial streams, *J. Fluid Mech.*, 57(2), 289-302, doi: 10.1017/S0022112073001163.

Exner, F. M. (1925), U ber die wechselwirkung zwischen wasser undgeschiebe in flussen, Akad.Wiss.Wien Math. Naturwiss. Klasse,134, 165– 204.

Falkowska, E. and T. Falkowski (2015), Trace metals distribution pattern in floodplain sediments of a lowland river in relation of contemporary valley bottom morphodynamics, *Earth Surf. Proc. Land.*, 40, 876-887, doi: 10.1002/esp.3680.

Federici, B. and G. Seminara (2003), On the convective nature of bar instability, *J. Fluid Mech.*, 487, 125-145, doi:10.1017/S0022112003004737.

Ferguson, R.I. and T.B. Hoey (2002), Long-term slowdown of river tracer pebbles: Generic models and implications for interpreting short-term tracer studies, *Water Resour. Res.*, 38(8), 1142, doi:10.1029/2001WR000637.

Fredsøe, J. (1978), Meandering and braiding of rivers, *J. Fluid Mech.*, 84, 609-624, doi:10.1017/S0022112078000373.

Furbish, D., P. Haff, J. Roseberry, and W. Schmeeckle (2012), A probabilistic

description of the bed load sediment flux: 1. Theory, *J. Geophys. Res.*, 117, F03031, doi: 10.1029/2012JF002352.

Ganti, V., M.M. Meerschaert, E. Foufoula-Georgiou, E. Viparelli, and G. Parker (2012), Normal and anomalous diffusion of gravel tracer particles in rivers, *J. Geophys. Res.*, 115, F00A12, doi:10.1029/2008JF001222.

Giri, S. and Y. Shimizu (2006), Numerical computation of sand dune migration with free surface flow, *Water Resour. Res.*, 42(10), doi: 10.1029/2005WR004588.

Hashenburger, J.K. (2013), Tracing river gravels: Insights into dispersion from a long-term field experiment, *Geomorphology*, 200, 121-131, doi:10.1016/j.geomorph.2013.03.033.

Hassan, M.A. and M. Church (1994), Vertical mixing of coarse particles in gravel bed rivers: A kinematic model, *Water Resour. Res.*, 30(4), 1173-1185, doi: 10.1029/93WR03351.

Hassan, M.A., H. Voepel, R. Schumer, G. Parker, and L. Fraccarollo (2013), Displacement characteristics of coarse fluvial bed sediment, *J. Geophys. Res.*, 118, 155-165, doi: 10.1029/2012JF002374.

Hirano, M. (1971), River bed degradation with armoring. *Proc., JSCE*, 195, 55–65. (in Japanese)

Hoey, T.B. (1996), Sediment dispersion and duration of storage in a model braided river, *J. Hydrol. NZ*, 35(2), 213-237.

Iwasaki, T., M. Nabi, Y. Shimizu, and I. Kimura (2015), Computational modeling of

^{137}Cs contaminant transfer associated with sediment transport in Abukuma River, *J. Environ. Radioactiv.*, 139, 416-426, doi:10.1016/j.jenvrad.2014.05.012.

Iwasaki, T., Y. Shimizu, and I. Kimura (2016), Sensitivity of free bar morphology in rivers to secondary flow modeling: Linear stability analysis and numerical simulation, *Adv. Water Resour.*, 92, 57-72, doi:10.1016/j.advwatres.2016.03.011.

Jang, C. and Y. Shimizu (2005), Numerical simulation of relatively wide, shallow channels with erodible banks, *J. Hydraul. Eng.*, 131(7), 565–575. doi:10.1061/(ASCE)0733-9429(2005)131:7(565).

Kasprak, A., J.M. Wheaton, P.E. Ashmore, J.W. Hensleigh, and S. Peirce (2015), The relationship between particle travel distance and channel morphology: Results from physical models of braided rivers, *J. Geophys. Res.*, 120, 55-74, doi:10.1002/2014JF003310.

Kovacs, A. and G. Parker (1994), A new vectorial bedload formulation and its application to the time evolution of straight river channels, *J. Fluid Mech.*, 267, 153-183, doi:10.1017/S002211209400114X.

Kuroki, M. and T. Kishi (1984), Regime criteria on bars and braids in alluvial straight channels, *Proc. of JSCE*, 342, 87-96. (in Japanese)

Lajeunesse, E., L. Malverti, and F. Charru (2010), Bed load transport in turbulent flow at the grain scale: Experiments and modeling, *J. Geophys. Res.*, 115, F04001, doi:10.1029/2009JF001628.

Lajeunesse, E., O. Devauchelle, M. Houssais, and G. Seizilles (2013), Tracer

dispersion in bedload transport, *Adv. Geosci.*, 37, 1-6, doi: 10.5194/adgeo-37-1-2013.

Langendoen, E.J., A. Mendoza, J.D. Abad, P. Tassi, D. Wang, R. Ata, K. El Kadi Abderrezzak, and J. Hervouet (2016), Improved numerical modeling of morphodynamics of rivers with steep banks, *Adv. Water Resour.*, doi:10.1016/j.advwatres.2015.04.002.

Lanzoni, S. and M. Tubino (1999), Grain sorting and bar instability, *J. Fluid Mech.*, 393, 149-174, doi: 10.1017/S0022112099005583.

Lanzoni, S. (2000), Experiments on bar formation in a straight flume. Part II: Graded sediment, *Water Resour. Res.*, 36(11), 3351-3363, doi: 10.1029/2000WR900161.

Lauer, J.W. and G. Parker (2008), Modeling framework for sediment deposition, storage, and evacuation in the floodplain of a meandering river: Theory, *Water Resour. Res.*, 44, W04425, doi:10.1029/2006WR005528.

Lesser, G.R., J.A. Roelvink, J.A.T.M. van Kester, G. Stelling (2004), Development and validation of a three-dimensional morphological model, *Coast. Eng.*, 51, 883-915, doi:10.1016/j.coastaleng.2004.07.014.

Lui, X.D., S. Osher, and T. Chan (1994), Weighted essentially non-oscillatory schemes, *J. Comput. Phys.*, 115, 200-212, doi:10.1006/jcph.1994.1187.

Martin, R.L., D.J. Jerolmack, and R. Schumer (2012), The physical basis for anomalous diffusion in bed load transport, *J. Geophys. Res.*, 117, F01018, doi: 10.1029/2011JF002075.

Meyer-Peter, E. and R. Muller (1948), Formulas for bedload transport, IAHSR, Report on the second Meeting, 3, 39-64.

Mosselman, E. and T.B. Le (2016), Five common mistakes in fluvial morphodynamic modeling, *Adv. Water Resour.*, doi:10.1016/j.advwatres.2015.07.025.

Nabi, M., H.J. de Vriend, E. Mosselman, C.J. Sloff, and Y. Shimizu (2013a), Detailed simulation of morphodynamics: 3. Ripples and dunes, *Water Resour. Res.*, 49, doi:10.1002/wrcr.20457.

Nabi, M., H.J. de Vriend, E. Mosselman, C.J. Sloff, and Y. Shimizu (2013b), Detailed simulation of morphodynamics: 2. Sediment pickup, transport, and deposition, *Water Resour. Res.*, 49, doi:10.1002/wrcr.20303.

Nakagawa, H. and T. Tsujimoto (1980), Sand bed instability due to bed load motion, *Journal of the Hydraulics Division*, 106(12), 2029-2051.

Nagata, N., T. Hosoda, and Y. Muramoto (2000), Numerical analysis of river channel processes with bank erosion, *J. Hydraul. Eng.*, 126(4), 243-252, doi: 10.1061/(ASCE)0733-9429(2000)126:4(243).

Nelson, J.M. (1990), The initial instability and finite-amplitude stability of alternate bars in straight channels, *Earth-Sci. Rev.*, 29, 97–115, doi:10.1016/0012-8252(0)90030-Y.

Nelson, J.M., Y. Shimizu, T. Abe, K. Asahi, M. Gamou, T. Inoue, T. Iwasaki, T. Kakinuma, S. Kawamura, I. Kimura, T. Kyuka, R.R. McDonald, M. Nabi, M. Nakatsugawa, F.R. Simoes, H. Takebayashi, and Y. Watanabe (2016), The

International River Interface Cooperative: Public Domain Flow and Morphodynamics Software for Education and Applications, *Adv. Water Resour.*, doi:10.1016/j.advwatres.2015.09.017.

Nikora, V., H. Habersack, T. Huber, and I. EcEwan (2002), On bed particle diffusion in gravel bed flows under weak bed load transport, *Water Resour. Res.*, 38(6), doi: 10.1029/2001WR000513.

Olinde, L. and J.P.L. Johnson (2015), Using RFID and accelerometer-embedded tracers to measure probabilities of bed load transport, step lengths, and rest times in a mountain stream, *Water Resour. Res.*, 51, 7572-7589, doi: 10.1002/2014WR016120.

Parker, G. (1976), On the cause and characteristic scales of meandering and braiding in rivers, *J. Fluid Mech.*, 76, 457-480, doi:10.1017/S0022112076000748.

Parker, G., C. Paola, and S. Leclair (2000), Probabilistic Exner sediment continuity equation for mixtures with no active layer, *J. Hydraul. Eng.*, 126(11), 818-826, doi: 10.1061/(ASCE)0733-9429(2000)126:11(818).

Parker, G., G. Seminara, and L. Solari (2003), Bed load at low Shields stress on arbitrarily sloping beds: alternative entrainment formulation, *Water Resour. Res.*, 39, 1183-1192, doi: 10.1029/2001WR001253.

Pelosi, A., G. Parker, R. Schumer, and H.-B. Ma. (2014), Exner-Based Master Equation for transport and dispersion of river pebble tracers: Derivation, asymptotic forms, and quantification of nonlocal vertical dispersion, *J. Geophys.*

Res., 119, doi:10.1002/2014JF003130.

Pelosi, A. and G. Parker (2014), Morphodynamics of river bed variation with variable bedload step length, *Earth Surf. Dynam.*, 2, 243-253. doi:10.5194/esurf-2-243-2014.

Pelosi, A., R. Schumer, G. Parker, and R.I. Feruson (2016), The cause of advective slowdown of tracer pebbles in rivers: Implication of Exner based master equation for coevolving streamwise and vertical dispersion, *submitted to J. Geophys. Res.*, doi: 10.1002/2015JF003497

Phillips, C.B., R.L. Martin, and D.J. Jerolmack (2013), Impulse framework for unsteady flows reveals super-diffusive bed load transport, *Geophys. Res. Lett.*, 40, 1328-1333, doi: 10.1002/grl.50323.

Pornprommin, A., N. Izumi, and T. Tsujimoto (2004), Weakly nonlinear analysis of multimodal fluvial bars, *Annual Journal of Hydraulic Engineering*, *JSCE*, 1009-1014.

Pornprommin, A. and N. Izumi (2011), Stability analysis of sand bars using amplitude expansion method, *Proceedings of 6th international symposium on River, Coastal and Estuarine Morphodynamics, RCEM2011*, Tsinghua University Press, 1624-1638.

Pyrce, R. and P. Ashmore (2003), The relation between particle path length distribution and channel morphology in gravel-bed streams: a synthesis, *Geomorphology*, 56, 167-187, doi:10.1016/S0169-555X(03)00077-1.

Pyrce, R. and P. Ashmore (2005), Bedload path length and point bar development in gravel-bed river models, *Sedimentology*, 52, 839-857, doi: 10.1111/j.1365-3091.2005.00714.x.

Rodrigues, S., E. Mosselman, N. Claude, C.L. Wintenberger, and P. Juge (2015), Alternate bars in a sandy gravel bed river: generation, migration and interactions with superimposed dunes, *Earth Surf. Proc. Land.*, 40, 610-628, doi:10.1002/esp.3657.

Roelvink, J.A. (2006), Coastal morphodynamic evolution techniques, *Coast. Eng.*, 53, 277-287, doi;10.1016/j.coastaleng.2005.10.015.

Roseberry, J.C., M.W. Schmeeckle, and D.J. Furbish (2012), A probabilistic description of the bed load sediment flux: 2. Particle activity and motions, *J. Geophys. Res.*, 117, F03032, doi:10.1029/2012JF002353.

Sayre, W. and D. Hubbell (1965), Transport and dispersion of labeled bed material, North Loup River, Nebraska, *U.S. Geol. Surv. Prof. Pap.*, 433-C, 48pp.

Schielen, R., A. Doelman, and H.E. de Swart (1993), On the nonlinear dynamics of free bars in straight channels, *J. Fluid Mech.*, 252, 325-356, doi:10.1017/S0022112093003787.

Schmeeckle, M. (2014), Numerical simulation of turbulence and sediment transport of medium sand, *J. Geophys. Res.*, 119(6), 1240-1262, doi:10.1002/2013JF002911

Schmeeckle, M. (2015), The role of velocity, pressure, and bed stress fluctuations in bed load transport over bed forms: numerical simulation downstream of a

backward-facing step, *Earth Surf. Dynam.*, 3, 105-112, doi: 10.5194/esurf-3-105-2015.

Schumer, R., M.M. Meerschaert, and B. Baeumer (2009), Fractional advection-dispersion equations for modeling transport at the Earth surface, *J. Geophys. Res.*, 114, F00A07, doi:10.1029/2008JF001246.

Schuurman, F., M.G. Kleinhans, and W.A. Marra (2013), Physics-based modeling of large braided sand-bed rivers: bar pattern formation, dynamics, and sensitivity, *J. Geophys. Res.*, 118, 2509-2527, doi:10.1002/2013JF002896.

Schuurman, F., Y. Shimizu, T. Iwasaki, and M.G. Kleinhans (2016), Dynamic meandering in response to upstream perturbations and floodplain formation, *Geomorphology*, 253, 94-109, doi:10.1016/j.geomorph.2015.05.039.

Shimizu, Y. and T. Itakura (1989), Calculation of bed variation in alluvial channel, *J. Hydraul. Eng.*, 115, 367-384. doi:10.1061/(ASCE)0733-9429(1989)115:3(367).

Simons, D.B., E.V. Richardson, and C.F. Nordin Jr. (1965), *Bedload equation for ripples and dunes*, *U.S. Geol. Surv. Prof. Pap.*, *462-H*, 1-9.

Stecca, G., A. Siviglia, and A. Blom (2014), Mathematical analysis of the Saint-Venant-Hirano model for mixed-sediment morphodynamics, *Water Resour. Res.*, 50, doi:10.1002/2014WR015251.

Stecca, G., A. Siviglia, and A. Blom (2016), An accurate numerical solution to the Saint-Venant-Hirano model for mixed-sediment morphodynamics in rivers, *Adv. Water Resour.*, doi:10.1016/j.advwatres.2015.05.022.

Takebayashi, H. and S. Egashira (2008), Non-equilibrium characteristics of bar geometry on bed with non-uniform sediment, *J. Hydrosci. Hydraul. Eng.*, 26(2), 1-14.

Tubino, M., R. Repetto, and G. Zolezzi (1999), Free bars in rivers, *J. Hydraul. Res.*, 37(6), 759–775, doi:10.1080/00221689909498510.

van der Mark, C.F., A. Blom, and S.J.M.H. Hulscher (2008), Quantification of variability in bedform geometry, *J. Geophys. Res.*, 113, F03020, doi:10.1029/2007JF000940.

Viparelli, E., O.E. Sequeiros, A. Cantelli, P.R. Wilcock, and G. Parker (2010), River morphodynamics with creation/consumption of grain size stratigraphy 2: numerical model, *J. Hydraul. Res.*, 48(6), 727-741, doi: 10.1080/00221686.2010.526759.

Voepel, H., R. Schumer, and M.A. Hassan (2013), Sediment residence time distributions: Theory and application from bed elevation measurements, *J. Geophys. Res.*, 118, 2557-2567, doi: 10.1002/jgrf.20151.

Watanabe, Y. (2007), A weakly nonlinear analysis of bar mode reduction process, *J. Hydrosci. Hydraul. Eng.*, 25(1), 107-122, doi: 10.2208/prohe.50.967.

Weeks, E.R., J.S. Urbach, and H.L. Swinney (1996), Anomalous diffusion in asymmetric random walks with a quasi-geostrophic flow example, *Physica D*, 97, 291-310, doi:10.1016/0167-2789(96)00082-6.

Wong, M., G. Parker, P. DeVries, T. M. Brown, and S. J. Burges (2007), Experiments

on dispersion of tracer stones under lower-regime plane-bed equilibrium bed load transport, *Water Resour. Res.*, 43, W03440, doi:10.1029/2006WR005172.

Yabe, T., T. Ichikawa , P.Y. Wang, T. Aoki, Y. Kadota, and F. Ikeda (1991), A universal solver for hyperbolic equations by Cubic-Polynomial Interpolation II. two and three-dimensional solvers, *Comput. Phys. Commun.*, 66(2-3), 233-242, doi:10.1016/0010-4655(91)90072-S.

Yamaguchi, S., Y. Shimizu, I. Kimura, and S. Giri. (2009), Significance of bed slope effect and non-equilibrium sediment transport on bed form evolution process: A numerical analysis using detailed hydrodynamics, Proceedings of the 6th IAHR symposium on River, Coastal and Estuarine Morphodynamics (RCEM2009), *Universidad Nacional Del Litoral, Santa Fe*, *Argentina*, *21-25*, September, 2009, 659-666.

Yang, C.T., and W.W. Sayre (1971), Stochastic model for sand dispersion, *Proc. ASCE*, *Journal of the Hydraulics Division*, 97(2), 265-288.

Zhang, Y., M.M. Meerschaert, and A.I. Packman (2012), Linking fluvial bed sediment transport across scales, *Geophys. Res. Lett.*, 39, L20404, doi:10.1029/2012GL053476.

Zolezzi, G., R. Luchi, and M. Tubino (2012), Modeling morphodynamic processes in meandering rivers with spatial width variations, *Rev. Geophys.*, 50, 1-24, doi: 10.1029/2012RG000392.

Tables

Table 1. Nondimensional parameters for the sensitivity analysis of tracer advection-dispersion associated with free bars.

	Froude number, F_r	Shields number, θ	Width/depth, β
Case 1	0.85	0.095	41.7
Case 2	0.6	0.095	41.7
Case 3	0.45	0.095	41.7
Case 4	0.6	0.075	41.7
Case 5	0.6	0.141	41.7
Case 6	0.6	0.095	33.3
Case 7	0.6	0.095	50

Table 2. Tracer plume transport characteristics: asymptotic advection velocity with respect to initial velocity and the scaling exponent, γ, in the relationship, $\sigma \sim t^{\gamma}$.

	Asymptotic velocity/initial velocity (%)	Scaling exponent, γ
Case 1	6.1	0.69
Case 2	2.6	0.59
Case 3	1.2	0.52
Case 4	3.1	0.63
Case 5	1.5	0.50
Case 6	2.8	0.55
Case 7	2.3	0.59

Figures

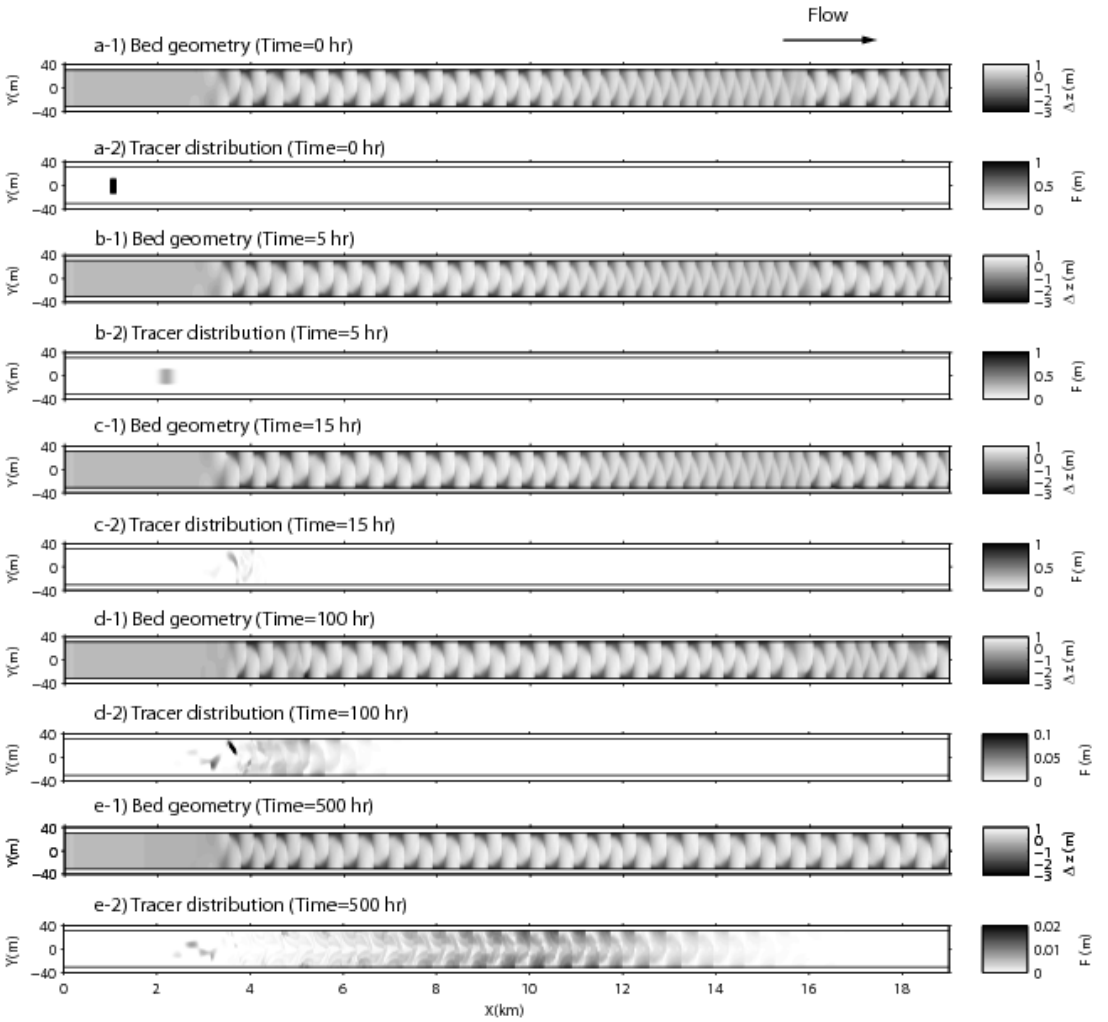

Figure 1. Temporal changes of alternate bar morphology and tracer distribution simulated by the entrainment-based model. Hydraulic conditions are: $F_r = 0.85$, $\theta = 0.095$, $S = 0.00461$, and $\beta = 41.7$. Flow is from left to right. A detailed view of the spatiotemporal evolution of bar morphology and tracer concentration can be seen in Video S1, a link to which is given in the Supporting Information.

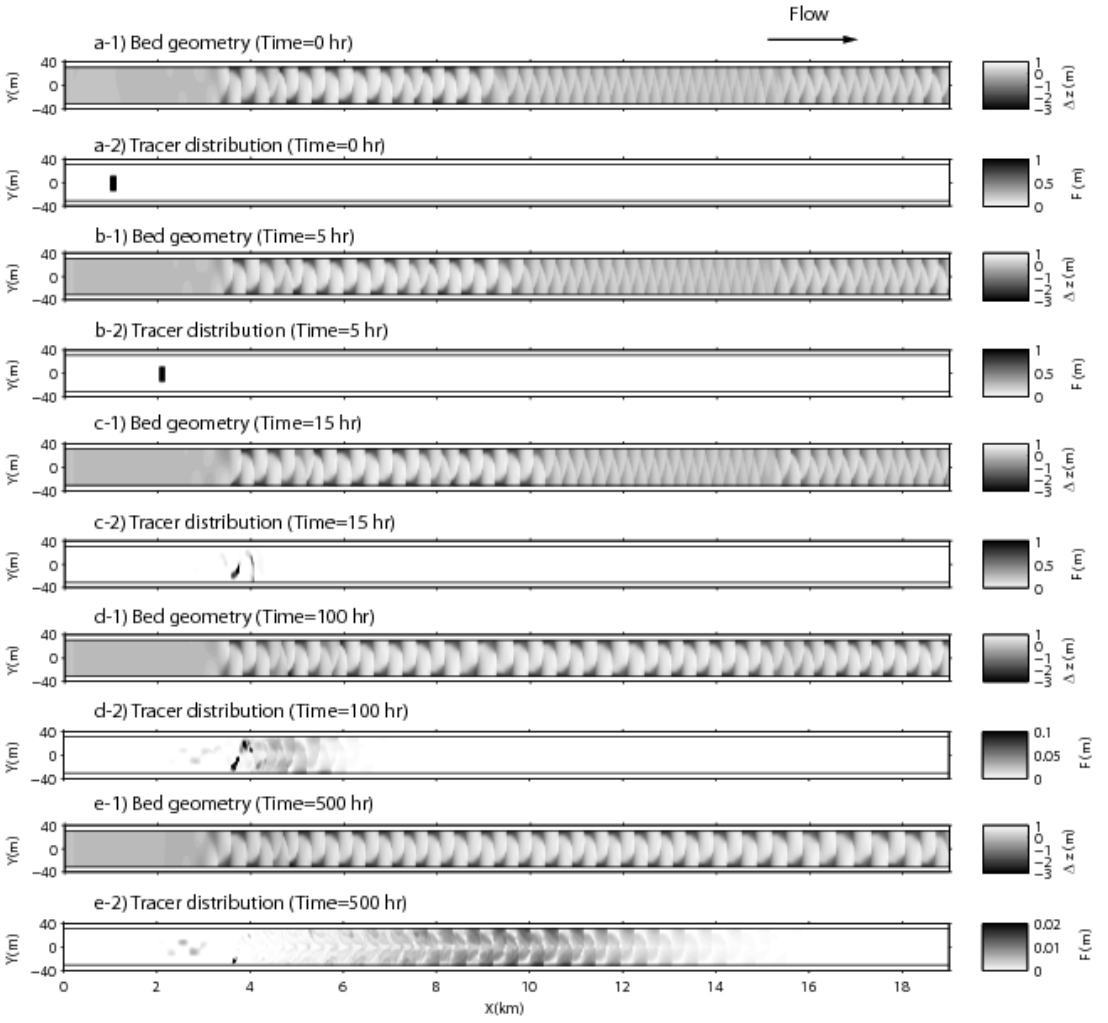

Figure 2. Temporal changes of alternate bar morphology and tracer distribution simulated by the flux-based model. Hydraulic conditions are: $F_r = 0.85$, $\theta = 0.095$, $S = 0.00461$, and $\beta = 41.7$. Flow is from left to right. Details of the spatiotemporal evolition of bar morphology and tracer concentration can be seen in Video S1 in the Supporting Information.

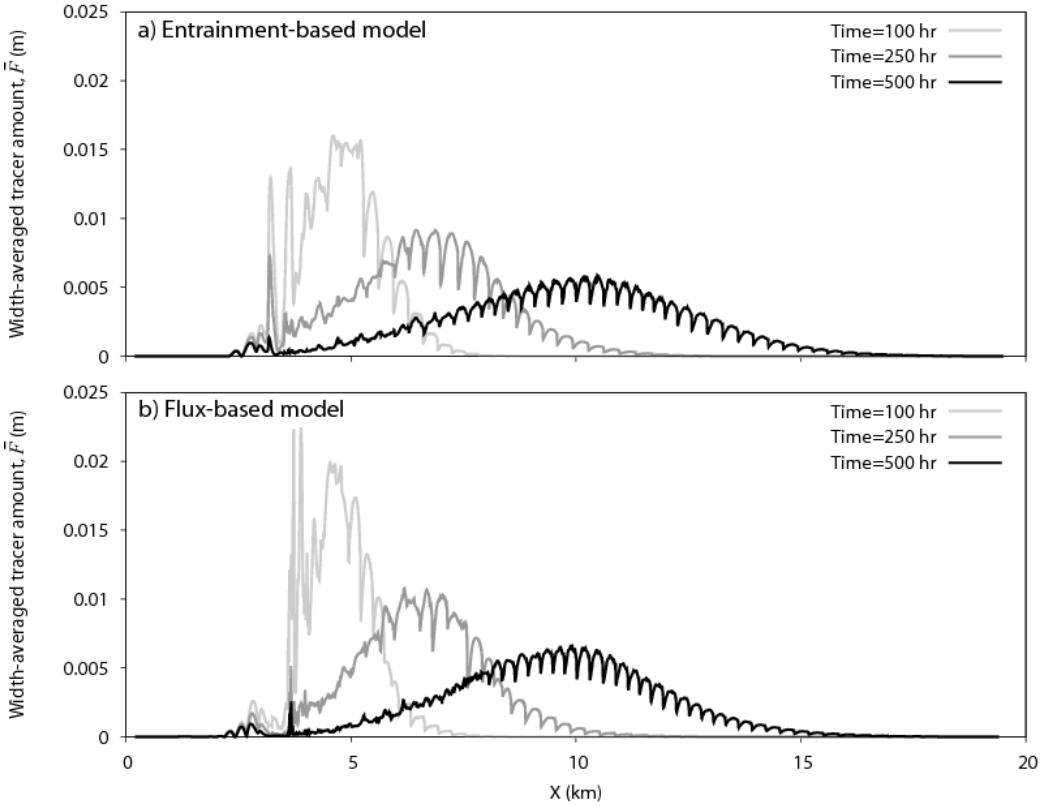

Figure 3. Temporal change of the width-averaged tracer amount $\bar{F}$ in the longitudinal direction, as simulated by a) the entrainment-based model and b) the flux-based model. Flow is from left to right.

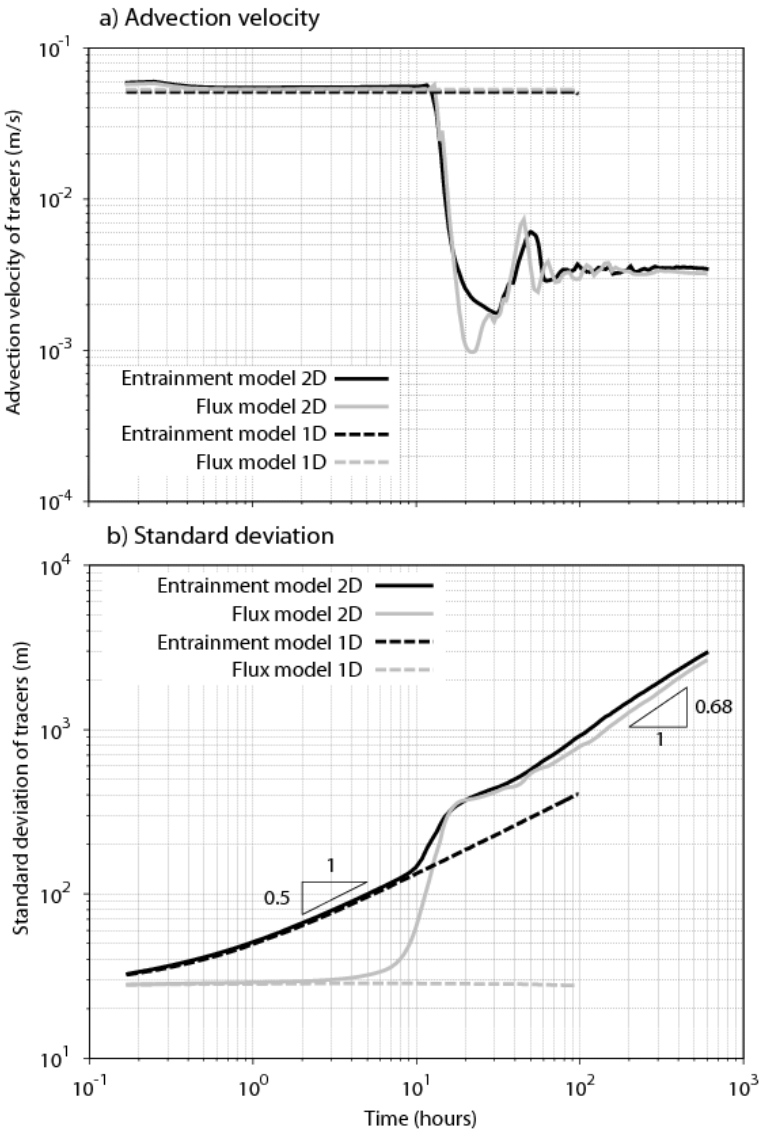

Figure 4. a) Advection velocity and b) standard deviation of the plume of tracers in the longitudinal direction. The dashed and solid lines represent the 1D and 2D calculations, respectively, and the black and gray lines denote the entrainment- and flux-based models, respectively.

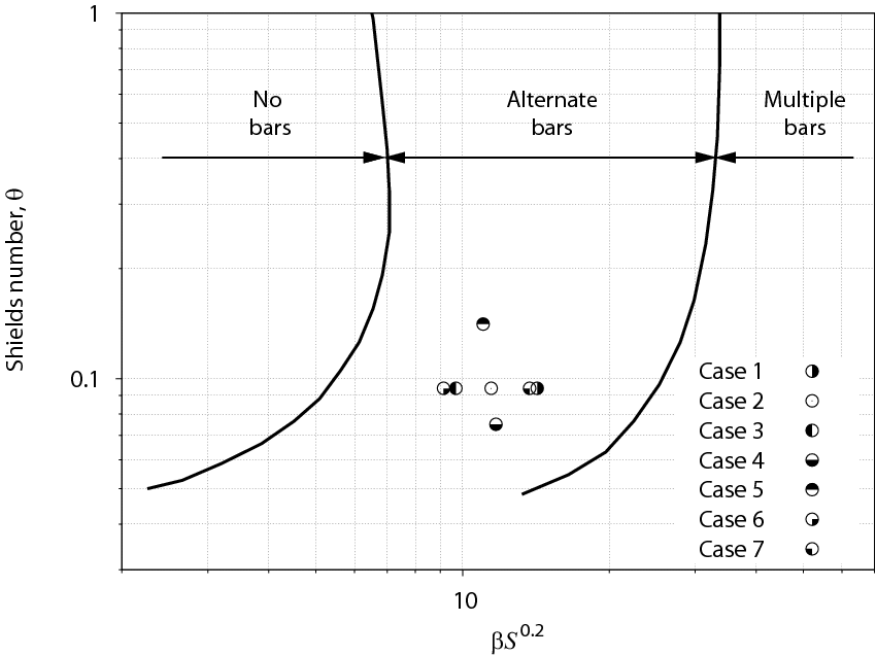

Figure 5. Regime criteria of free bar mode based on a linear stability analysis [*Kuroki and Kishi*, 1984]. All runs performed for the sensitivity analysis are categorized in the single-row alternate bar regime.

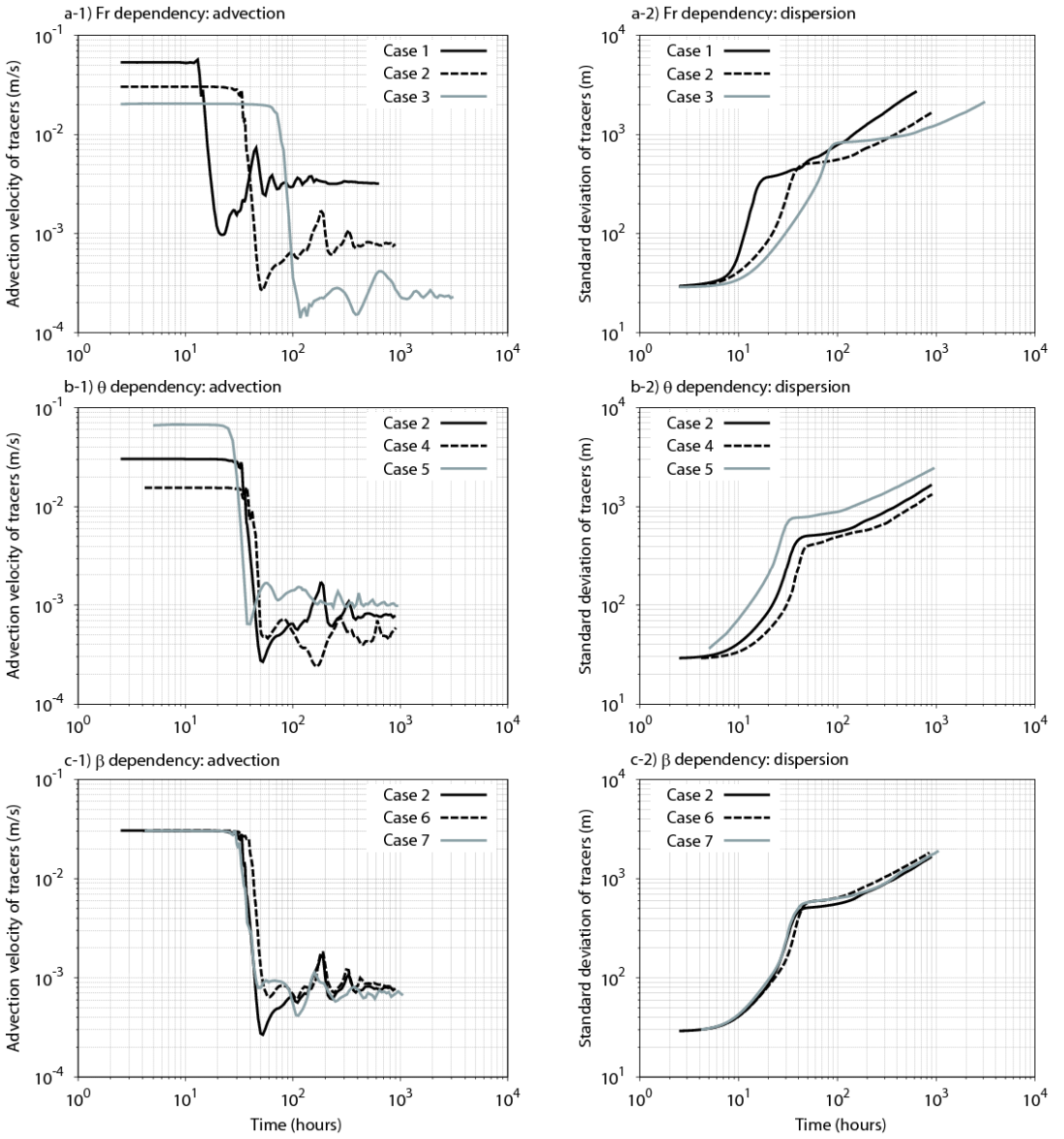

Figure 6. Sensitivity analysis of advection and dispersion characteristics. The figures in the left and right columns show the advection velocity and standard deviation of the tracer plume, respectively. The notations a), b), and c) in the upper left-hand side of each panel indicate that variation in Froude number *Fr*, Shields number θ, and width/depth ratio β, respectively, are studied.

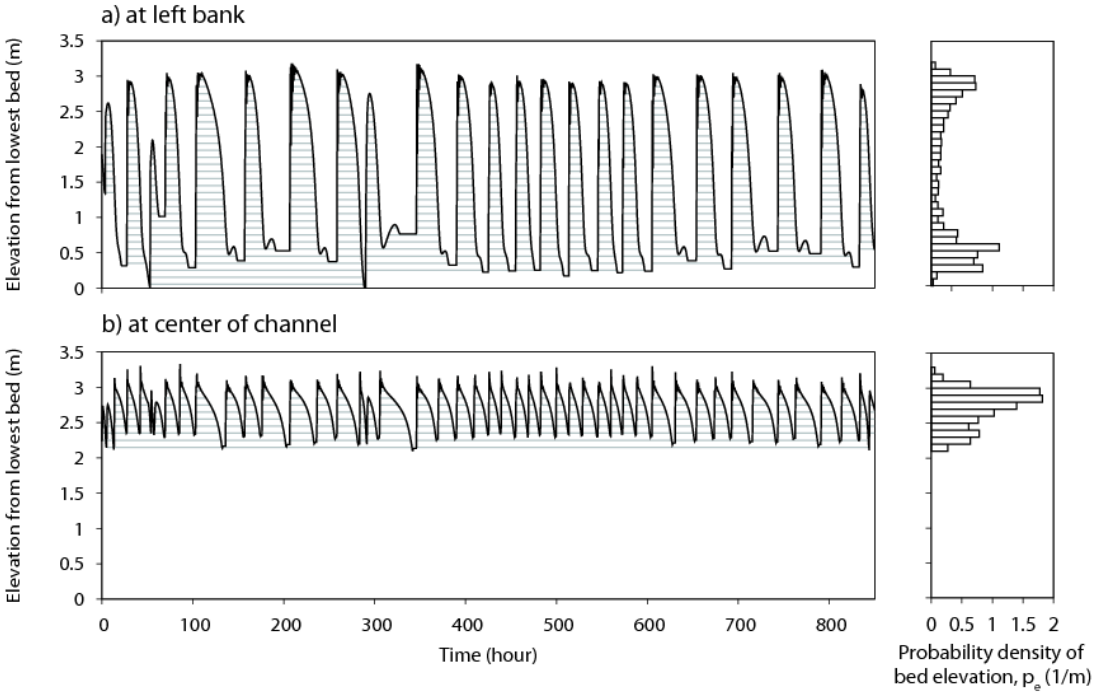

Figure 7. Time series of bed surface elevation (black line) and the corresponding waiting time (gray line) (left), and the probability of bed surface elevation (right) at the a) left bank and b) center of the channel in Case 1.

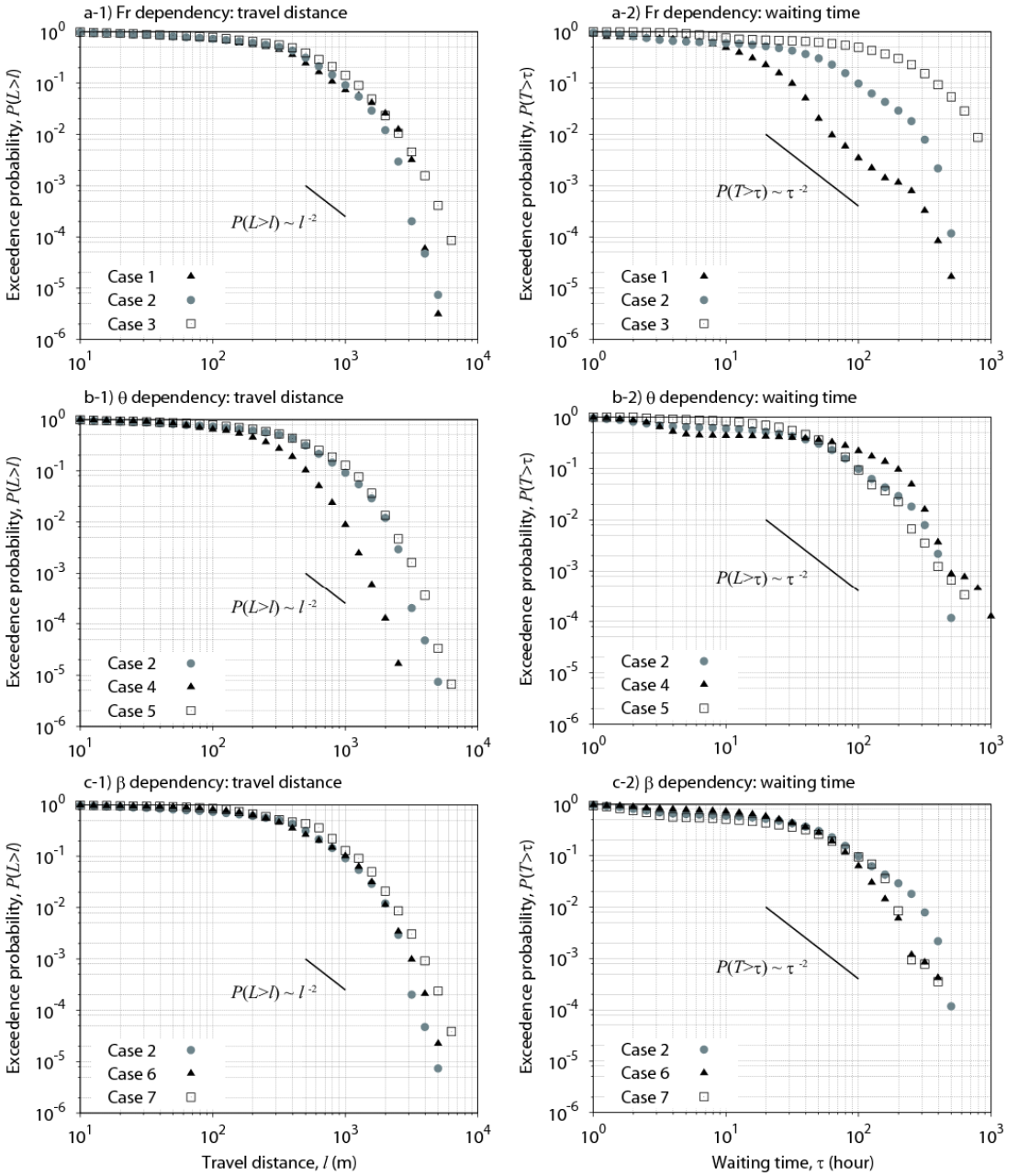

Figure 8. Exceedance probability distribution of the travel distance (a-1, 2, 3) and waiting time (b-1, 2, 3) in each the seven numerical runs.

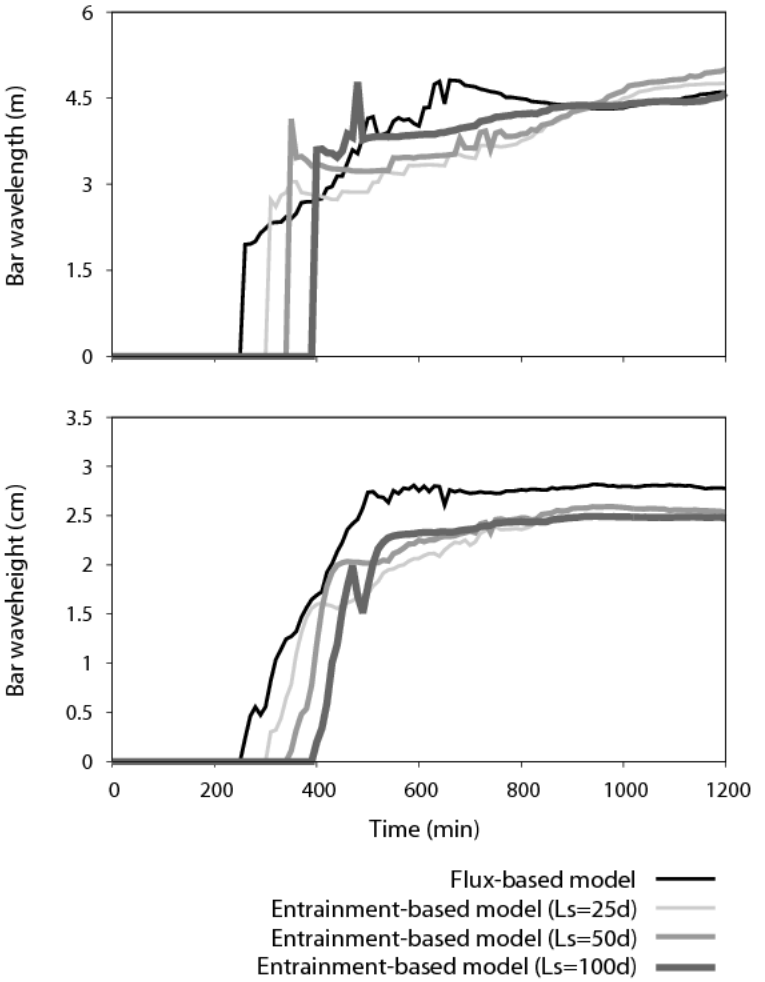

Figure A1. Sensitivity of the simulated free bar dimensions, i.e., wavelength (top), and b) wave height (bottom), to the type of morphodynamic model (flux or entrainment) and mean step length.

Effects of structural rehabilitation on nutrient retention and uptake, community assemblages, and functional morphology of biotic communities in a small Midwestern stream

Basic Information

Title:	Effects of structural rehabilitation on nutrient retention and uptake, community assemblages, and functional morphology of biotic communities in a small Midwestern stream
Project Number:	2015IL293B
Start Date:	3/1/2015
End Date:	2/28/2016
Funding Source:	104B
Congressional District:	IL-15
Research Category:	Biological Sciences
Focus Category:	Ecology, Geomorphological Processes, Nutrients
Descriptors:	None
Principal Investigators:	Anabela Maia, Anabela Maia

Publications

There are no publications.

Effects of structural rehabilitation on nutrient retention and uptake, community assemblages, and functional morphology of biotic communities in a small Midwestern stream

Biological Sciences

Graduate (M.S.)

Keywords: Instream rehabilitation, restoration, nutrient retention, fish communities, macroinvertebrate communities

PI: Anabela Maia, PhD, Eastern Illinois University, amresendedamaia@eiu.edu, (217) 581-6360

Congressional District: IL-15

Background

Decades of anthropogenic pressure have devastated lotic ecosystems across the riverscapes of North America, resulting in the degradation of critical habitat and contributing to sharp declines in biotic integrity. For example, agricultural practices in the Midwest have led to increased levels of bank erosion, sedimentation, and nutrient loading, resulting in a loss of critical habitat for aquatic organisms (Berkman and Rabeni, 1987). Small streams are affected considerably by such pressures, with upwards of 85% of ecosystems displaying signs of degraded function (Dahl, 1990). In response, local stream restoration are increasingly frequent, yet comparably little effort has been allocated to monitoring (NRC, 1992; Moerke and Lamberti, 2003), leading to ambiguous results and limited project success. With habitat heterogeneity and biotic integrity being primary goals of rehabilitation (Gorman and Karr, 1978; O'Connor, 1991; Death and Winterbourn, 1995; Walser and Bart, 1999), it is imperative that projects are monitored with increasing frequency, and describe the factors affecting community structure and biotic integrity in impacted waterways to mitigate further loss. Lessons from the long-term rehabilitation and ecological monitoring of Kickapoo Creek in East-Central Illinois highlight some of the complex dynamics driving reach-scale restoration projects.

Kickapoo Creek is a unique system as it encompasses multiple anthropogenic pressures in a relatively small basin – sanitary treatment plant, golf course, and agricultural land. These pressures may stress the local aquatic ecosystem through habitat degradation and nutrient toxicity, and must be assessed. Nitrates from agricultural runoff and sanitary treatment effluent are harmful, and sometimes fatal to aquatic fauna, and must be closely monitored (Mueller et al., 1997; Royer et al., 2004; Camargo et al., 2005). Elevated estradiol (a form of estrogen) levels are also of concern due to the close proximity of the Mattoon sanitary treatment plant. This hormone has been associated with the production of intersex gonads in male fishes and cancer and reproductive abnormalities in humans (Singh et al., 2003; Braga et al., 2005; Shappell, 2006).

Our research looks at long-term effects of a previous instream rehabilitation on fish and macroinvertebrate assemblages in Kickapoo Creek, near Charleston, IL. In addition, this project will monitor a new restoration project, and will examine the effects of sanitary treatment plant effluent, golf course nutrient enrichment and bank erosion on nutrient uptake and fish and macroinvertebrate communities. During this research we will assess the effects of multiple rehabilitations on local biotic communities, and evaluate the overall success of each rehabilitation in regards to community assemblages, physical properties of the habitat and overall health of the system.

To compliment ecological data, laboratory experiments will examine the effects of changes in turbulence regime associated with restoration on selected fish species within Kickapoo Creek. Longear Sunfish (*Lepomis megalotis*) are both widely prevalent in Kickapoo Creek and fill vital roles in stream ecosystems, and thus will be ideal candidates for experimentation. Since fish live in a complex three-dimensional environment, and are affected by both biotic and abiotic variables (Liao, 2007), it is necessary to consider the organismal-level impacts resulting from habitat alterations. Proposed changes in instream structure and resulting changes in velocity could alter behavior and affect the way these fish use their habitat (Liao, 2007). Thus, it will be beneficial to examine the effects of the restoration to fish physiology as well as ecology. The last portion of our project will look at water chemistry, particularly estradiol levels to assess the anthropogenic impacts on the biotic communities. Fish estradiol

levels will also be measured in the aforementioned species and correlated with oxygen consumption and metabolic scope.

If habitat diversity is maintained, we anticipate a continued increase in fish abundance, biomass, and diversity, as well as an increase in macroinvertebrate diversity at previous restored sites. If restoration increases habitat diversity, we expect to see similar post-restoration increases in fish and macroinvertebrate diversity at two new project sites. Each reach will be compared to itself over a period of time, while also being compared to longitudinal changes seen in reference, upstream, and downstream sites along the stream.

During laboratory testing, we expect to observe several physiological responses in wild caught fish. During respirometry testing, we expect to observe increased oxygen consumption under stressed conditions compared to resting metabolic consumption. We also expect increased turbulence to elicit the greatest change in metabolism. In terms of estradiol levels in the water and fish tissue, we expect to see elevated levels only downstream of the sanitary treatment plant (STP). We also expect elevated estradiol levels in the fish caught in reaches downstream of the STP. Lastly, we expect that fish exposed to estradiol will have elevated metabolism under stress conditions.

Methodology

Study Area

Kickapoo Creek (Latitude 39˚27’, Longitude 88˚13’) is a fourth-order, low gradient stream which originates south of Mattoon, Illinois and flows east for nearly 66 km until meeting its confluence with the Embarras River (Figure 1). Draining approximately 265 km^2, this human-impacted stream is subjected to multiple anthropogenic pressures within a relatively small basin, and land use within the Kickapoo Creek watershed consists primarily of agriculture, disconnected fragments of forest, grasslands, and urban stressors (e.g. road crossings, golf course, sewage treatment plant, and residential area). As part of the larger Embarras River watershed, a region which has been identified by the Illinois Environmental Protection Agency (IEPA) as a watershed of concern, this tributary has been a recent hotspot for rehabilitation and mitigation efforts. Prior to an instream rehabilitation project, all study reaches shared similar habitat characteristics, consisting of a shifting sand and gravel substrate regime accompanied by elevated levels of bank erosion and sedimentation (West 2013). Following a chemical-induced fish kill in 2001, mitigation from Illinois Department of Natural Resources (IDNR) enabled the structural rehabilitation of over 400 m of streambank and main channel habitat in September 2010. In an effort to improve habitat heterogeneity, and thus biotic integrity (Palmer et al., 1997) rehabilitation included construction of two artificial Newbury riffles (Newbury Hydraulics, Okanagan Centre British Colombia, Canada), which increased average water depths and simulated scour pool hydraulics within the rehabilitation reach (Pant, 2014). Rip-rap was employed along streambanks in the form of boulder cover and scouring keys to further facilitate geomorphic stabilization and improve hydrologic conditions (West, 2013; Pant 2014). Additionally, streambanks were revegetated with native grasses to further aid the recovery of riparian habitat and to reduce bank erosion and sedimentation.

Habitat Assessment

Stream habitat and integrity were monitored annually in the fall using the Qualitative Habitat Evaluation Index (QHEI; Rankin, 1989). Beginning immediately after the rehabilitation project in summer 2010, we examined habitat in three fixed 200 m sites — two located within the larger rehabilitation reach and associated with each artificial riffle, and one site approximately 1.8 km upstream which served as a reference, or control, for baseline comparisons. In 2012, an additional reach was added 1.8 km downstream of the rehabilitation reach to serve as an added reference. In teams of two researchers, each site was divided into ten equidistant transects where depth and substrate measures were taken at specified intervals along the width of the channel. Relative abundance of instream and riparian habitat was also estimated between each transect using a standard protocol. Water quality variables (dissolved oxygen, specific conductivity, water temperature, and pH) were collected instantaneously during each sampling event using a YSI multimeter probe (YSI Inc., Yellow Springs, OH). Additionally continuous in situ nitrate, temperature, and dissolved oxygen levels in Kickapoo Creek were monitoring by the US Geological Survey (USGS), and recorded using two USGS monitoring stations located within the rehabilitation reach and near the upstream reference. During the 2014 and 2015 sampling periods, ecological monitoring began at an additional three sites located within in the upstream reaches of Kickapoo Creek near Mattoon, Illinois (Figure 1). These areas were identified as impacted regions, characterized by decreased geomorphic stability with heavy amounts of bank erosion and siltation. Habitat assessments were conducted concurrently with our long-term monitoring project, and data were incorporated into ecological models.

Biotic Community Sampling

To ensure all fish were fully recruited to the gear, communities were sampled annually in the fall at baseflow water conditions, and concurrently with QHEI habitat monitoring. Blocking seines (mesh size, 5 mm) were employed during sampling at the upstream and downstream ends of seven 200 m sites, however, fish were only added to the sample from the downstream seine. Teams of six researchers conducted single-pass removal DC barge electrofishing surveys within each site using standardized protocols (Rabeni et al., 2009) where all available habitat within the stream channel was sampled, and fishing time was recorded as a measure of sampling effort. Whenever feasible, fishes were weighed (nearest gram), measured (nearest millimeter), identified to species and released unharmed near each site. Fishes which were unable to be identified in the field were euthanized using a lethal dose of MS-222, fixed in 10% formalin solution and later stored in 75% ethanol before further enumeration and identification using a taxonomic key (Pflieger 1997).

Changes in macroinvertebrate populations were measured using the IEPA's (2007) multihabitat 20-jab method, with jabs allocated using the QHEI as a measure of available habitat. Macroinvertebrate collections were taken in the sediment using an 18 inch rectangular dip net, and an 18x18 inch area was thoroughly aggravated to ensure all insects were suspended and collected within the net. All samples were stored in 90% ethanol until identification and enumeration in the lab. A standard procedure was used to subsample macroinvertebrates within each site, using randomly selected grids to identify approximately 300 ± 40 macroinvertebrates per site. All macroinvertebrates were identified down to family, or lowest taxonomic resolution possible.

Metabolic Scope

To analyze the metabolic changes under stressed (i.e. turbulent) conditions we used standard respirometry techniques developed for aquatic fauna (Svendsen et al. 2014). Longear Sunfish collected from Kickapoo Creek were examined due to their broad distribution in warmwater streams and importance to local ecosystems. After fish were adjusted to being housed in the lab at Eastern Illinois University, they were tested in our sealed flow tank (Loligo® Systems 2016). Fish were first acclimated to the chamber or flume with the lid open for a minimum of two hours prior to testing. The fish were also not fed for a minimum period of 24 hours before testing to ensure oxygen measurements reflected locomotor effort and not digestive processes. Once fish were acclimated, the lid to the flume was closed and sealed, and an oxygen probe inserted into the chamber. During experiments we recorded oxygen levels within the intermittent flow chamber for a minimum of two hours due to the large size of the flume; this interval was chosen to maximize the resolution necessary to assess changes in metabolic oxygen condition. During trials, saturation of dissolved oxygen was not allowed to decrease below 85% due to physiological limitations of fish. Variables being tested in the flume were no turbulence (quasi-laminar), and turbulence (simulated). Turbulence was simulated using three equally spaced vertical cylinders, which produced horizontal streets of vortices similar to fish body depth. Oxygen concentration was plotted against time and the slope used to determine metabolic rates for each organism at varying stress levels (Svendsen et al. 2014). A mixed effects analysis of variance (ANOVA) model was used to test for significant differences between treatment types.

Estradiol analysis

Analysis of estradiol concentrations will be carried out using an Enzyme-Linked Immunosorbent Assay system (ELISA). The prefabricated ELISA system is designed to detect specific chemicals within samples, and the protocol is approved by the United States Environmental Protection Agency for sampling drinking water for a variety of pathogens and chemicals. Dr. Karen Gaines and the Ecotoxicology Laboratory at EIU house all necessary equipment, and has used this technique with success in other studies. She will be a collaborator during the estradiol analysis portion of this project. Estradiol concentration data will later be correlated with physiological and metabolic scope data.

Data Analysis

To analyze community data, fish assemblages were aggregated based upon taxonomic families, while macroinvertebrates were classified based on taxonomic order. As the most robust measure of distance in community ecology (Faith et al., 1987), we employed nonmetric multidimensional scaling (NMDS; Minchin, 1978) based on a Bray-Curtis dissimilarity matrix of scaled assemblage data across two dimensions to examine temporal and spatial trends in biotic communities within rehabilitated and reference sites. Community response to the structural rehabilitation was examined using post-restoration data from 2010 to 2015, and was tested using permutational multivariate analysis of variance (perMANOVA; Anderson, 2001), examining community structure as a factor of both time and treatment type (i.e. rehabilitated vs. reference). Additionally, we calculated a fish Index of Biotic Integrity (fIBI; Karr 1986) along with 95% confidence intervals to estimate changes in health of communities both before, and in years

following instream rehabilitation. Health of macroinvertebrate assemblages were monitored using the macroinvertebrate Index of Biotic Integrity (mIBI; Tetra Tech, 2004).

Additionally, we examined linkages between habitat and distribution of fauna using general linear models (GLM) and multiple linear regression (MLR) analyses. Using stepwise model selection based on Akaike's (1973) Information Criterion (AIC), we assessed relationships between relative abundance of taxonomic families to the QHEI parameters. All modeling was completed in R (R Core Team, 2015), and unless otherwise denoted, results were deemed statistically significant at $\alpha=0.05$.

Principle Findings

Fish Communities

During the seven-year study period, we sampled a total of 79,013 fishes comprising 46 species from nine taxonomic families. Species from families Cyprinidae (85.38%), Centrarchidae (5.6%), Percidae (3.98%), Catostomidae (2.29%), and Ictaluridae (1.46%) accounted for >98% of the total catch, with nominal contributions from Clupeidae, Poeciliidae, Fundulidae, and Atherinidae. Following implementation of artificial riffles, scouring keys, and riparian revegetation, we observed distinct temporal and spatial shifts in community structure in the six years following rehabilitation (Figure 2). Initially, assemblages in all sites were largely comprised of tolerant Cyprinid fishes, however, three years post-rehabilitation there was an apparent shift in community structure characterized by decreased abundance of Cyprinids and increased abundance of Centrarchidae, Catostomidae, Ictaluridae, and Percidae species. This was supported by a perMANOVA (Table 1), which indicated community structure was significantly influenced by the habitat rehabilitation ($F_{1,21}=5.9304$, $R^2=0.1692$, $p=0.012$), and varied over a temporal scale ($F_{5,21}=2.6471$, $R^2=0.3777$, $p=0.045$). We found a similar delayed response in biotic integrity, with fishes responding more than two years post-rehabilitation (Figure 3). While biotic integrity remained moderately low throughout the study in reference reaches, fishes in restored reaches experienced a steady increase in assemblage health, with recent samples reaching the moderate level of IBI classification, and possibly indicating the return of sensitive benthic invertivore species. Further evidence of this fundamental shift in community structure was observed when examining relationships between fish taxa and habitat drivers within the system. We found significant linkages between boulder substrate and mean depth driving relative abundance of Cyprinidae and Centrarchidae taxa in Kickapoo Creek (Figure 4). The implementation of artificial riffles, coarse boulder substrate and rip-rap keys allowed for the formation of deep scour pools which provided necessary refuge to facilitate recovery of degraded fish communities.

Macroinvertebrate Communities

During this study period we also collected and identified 9,310 macroinvertebrates from 20 orders comprising 66 taxonomic families. Seven orders accounted for >98% of the total catch, including Diptera flies (30.24%), Ephemeroptera mayflies (29.29%), Trichoptera caddisflies (13.32%), Oligochaeta worms (10.06%), Odonata dragonflies (9.45%), Basommatophora snails (3.68%), and Coleoptera beetles (1.9%). Other taxa were collected infrequently, and occurred in less than 1% of samples. When examining changes in macroinvertebrate community structure we

did not find any distinct trends resulting from the rehabilitation. Results of a perMANOVA (Table 1) indicated significant effects of habitat rehabilitation ($F_{1,21}$=3.7999, R^2=0.0887, p=0.027) on assemblages in Kickapoo Creek, although the variance attributed to the rehabilitation and explained within the data was nominal (approximately 8% explained). Temporal variation accounted for nearly 55% of the variation within the data, and was found to be significantly driving macroinvertebrate communities ($F_{1,21}$=4.7071, R^2=0.5491, p=0.001). Our NMDS model displayed abundant overlap between communities across treatment types, and no clear temporal trends could be assessed (Figure 5), with communities within a given year appearing more similar than between treatment types. We observed similar trends when examining biotic integrity using the mIBI (Figure 6). Short-term response to the rehabilitation was positive, with community integrity steadily increasing in restored sites as reference assemblages fluctuated. However, recent samples indicate that interannual variation remains a driving force, and similar trends in biotic integrity were visible in both restored and reference communities. Although we did not find substantial long-term response to the rehabilitation project, the macroinvertebrate communities within the study reaches remain in stable fair to good integrity and are capable of supporting a robust and diverse community of fishes.

Metabolic Scope

We successfully observed Longear Sunfish swimming in the lab under a variety of stress conditions. Fish were exposed to quasi-laminar and turbulent flow regimes, and displayed dissimilar swimming abilities within the two regimes. In quasi-laminar flow, Longear Sunfish were able to station hold and maintain position with relative ease. In contrast, swimming in turbulent flow was noticeably disturbed and fish were frequently exposed to forced yaw maneuvering and spills, or loss of heading. Metabolic oxygen consumption was measured in three fish exposed to each flow regime repeated over three trials, for a total of six trials per fish. Mass-corrected oxygen consumption values ($\dot{M}_{O2}$) were obtained for each fish and were corrected for unstressed (i.e. quasi-laminar) condition. We obtained average $\dot{M}_{O2}$ values for Longear Sunfish swimming in quasi-laminar and turbulent flow regimes, and found significant increased cost of transport when navigating complex flow (Figure 7). On average, Longear Sunfish consumed 23% more oxygen when exposed to unsteady flows in the lab. In the field, this sunfish shows high fidelity to deep channels with multiple instream cover types and abundant deep silt-bottom pool habitat; areas characterized by low flow and turbulence. We found significant relationships between Longear Sunfish abundance in Kickapoo Creek and four driving habitat parameters — mean depth, submerged terrestrial vegetation, silt substrate, and boulders (Figure 8). Based on current ecomorphological models, the Longear Sunfish can be described as a habitat specialist, finding refuge in areas of low flow with abundant instream cover structures and deep pools. Given the high energetic costs incurred navigating complex flows, we demonstrate a physiological mechanism driving habitat use and behavior which helps explain shifts in ecology following instream habitat rehabilitation.

Estradiol

The estradiol exposure has not yet started. However, we have successfully established baseline data for geometric morphometrics of body shape and metabolic data. Mass corrected mean oxygen consumption during basal metabolism and maximum metabolism were 207.7

$mgO_2Kg^{-1}.h^{-1}$ and 243.1 $mgO_2Kg^{-1}.h^{-1}$, respectively in fish prior to exposure to estradiol. We show that this species has an aerobic capacity of approximately $35mgO_2.kg^{-1}.h^{-1}$. We are expecting that fish exposed to estradiol will have this scope reduce, which would impair their ability to optimize energy consumption in their daily behaviors and compromise growth.

PCA analysis of geometric morphometric landmarks showed that four principal components explain 74% (PC1 28.9%, PC2 18.5%, PC3 16.7% and PC4 9.5%) of the variation in the body shape of male longear sunfish. PC1 can be explained mostly by a dorsoventral compression, while PC2 is mostly explained by a change in height of the caudal fin. PC3 is related to changes in the caudal peduncle while PC4 highlights shape changes in the ventral region. From the geometric morphometrics data we are expecting that the body shape will show less male related characters (e.g. higher head) in fish exposed to estradiol. Oxygen consumption and geometric morphometric measurements in the E2 exposed fish will be conducted and compared with the baseline values calculated at the beginning of the mesocosm experiment.

Training potential

This project has served as a unique learning tool for students at Eastern Illinois University. This project provided a graduate assistantship and served as a Master's Thesis for Carl Favata. Dr. Anabela Maia has also been able to advise another graduate student, Neeta Parajulee Karki, who, along with Camden Nix (Dr. Gaines advisee) have begun research on the energetic costs of estradiol exposure in stream fish. Dr. Robert Colombo's (co-PI on the IEPA grant), and Dr. Karen Gaines' (collaborator, estradiol) labs at EIU also gained a tremendous amount of field and laboratory experience stemming from this research. Graduate students Alex Sotola, Hanna Kruckman, Zachary Mitchell, Evan Boone, Clint Morgeson, David Petry, Shannon Smith, Dan Roth, Jordan Pesik, Bethany Hoster, and Camden Nix were instrumental in assisting with stream electrofishing, fish identification, habitat surveys, macroinvertebrate collections and identification, and estradiol analysis. Undergraduate students Missy Eaton, Kailee Schulz, Krista Zerrusen, Courtney Deters, Katherine Bottom, Alicia Kellup, Vantasia Joe, Georgina Govostis and Kelly Forbus were trained in and assisted with field work, data collection, lab identifications, and energetics experiments.

Publications

Below are listed the relevant publications and conference papers which were presented at local, state, national, and international scientific meetings during the term of this agreement:

Favata CA, Colombo RE, and Maia A. 2016. Managing structural rehabilitation: Ecological monitoring and factors driving community structure in a restored stream. Symposium presentation, American Fisheries Society Annual Meeting, Kansas City, MO.

Favata, C.A. (in preparation). Effects of habitat alteration on biotic assemblages and ecomorphology of fish in a restored stream. MS Thesis. Eastern Illinois University. Charleston, IL.

Favata CA, Colombo RE, Roseboom DR, Straub TD, and Maia A. (manuscript in preparation). Habitat factors driving fish assemblages in a restored stream.

Favata CA, Colombo RE, Roseboom DR, Straub TD, and Maia A. (manuscript in preparation). Habitat and macroinvertebrate response to stream restoration.

Favata CA and Maia A. (manuscript in preparation). Ecomorphology and energetics of Longear Sunfish (*Lepomis megalotis*) steady swimming in turbulent flow.

Favata CA, Colombo RE, and Maia A. (manuscript in preparation). Sampling selectivity and fish community comparisons for two common stream electrofishing gears.

Karki, NP, Colombo RE, Gaines K, and Maia A. 2016. Effects of 17β estradiol in the metabolism of Sunfish species. Poster presentation, Illinois Chapter of American Fisheries Society Annual Meeting, Springfield, IL.

Favata CA, Colombo RE, Roseboom DR, Straub TD, and Maia A. 2016. Community structure in a restored stream: what is driving dissimilarity? Oral presentation, Illinois Chapter of American Fisheries Society Annual Meeting, Springfield, IL.

Favata CA, Colombo RE, Roseboom DR, Straub TD, and Maia A. 2016. Factors driving fish assemblages in a restored stream. Oral presentation, Midwest Fish and Wildlife Annual Conference, Grand Rapids, MI.

Favata CA, Colombo RE, Roseboom DR, Straub TD, and Maia A. 2016. Ecomorphology and swimming energetics of longear sunfish Lepomis megalotis in turbulent flow. Oral presentation, Society of Integrative and Comparative Biology Annual Meeting, Portland, OR.

Favata CA, Colombo RE, Roseboom DR, Straub TD, and Maia A. 2015. Ecomorphology of fish assemblages in an East-Central Illinois stream. Oral presentation, American Fisheries Society Annual Meeting, Portland, OR.

Favata CA, Colombo RE, Roseboom DR, Straub TD, and Maia A. 2015. Ecomorphology of fish assemblages in an East-Central Illinois stream. Poster presentation, College of Sciences Sciencefest, Eastern Illinois University, Charleston IL.

Favata CA, Colombo RE, Roseboom DR, Straub TD, and Maia A. 2015. Ecomorphology of fish assemblages in an East-Central Illinois stream. Poster presentation, 18th Annual Sigma Xi Banquet, Charleston IL.

Favata CA, Colombo RE, Roseboom DR, Straub TD, and Maia A. 2015. Ecomorphology of fish assemblages in an East-Central Illinois stream. Poster presentation, 53rd Annual Illinois American Fisheries Society Chapter Meeting, Pere Marquette, IL.

Literature Cited

Akaike, H. 1976. An information criterion (AIC). *Mathematical Sciences*, 14(153):5–9.

Anderson, M.J. 2001. A new method for non-parametric multivariate analysis of variance. *Austral Ecology*, 26:32-46.

Berkman, H.E., and Rabeni, C.F. 1987. Effect of siltation on stream fish communities. *Environmental Biology of Fishes*, 18:285-294.

Braga, O., Smythe, G.A., Schafer, I., Feitz, J. 2005. Steroid estrogens in primary and tertiary wastewater treatment plants, *Water Science and Technology*, *52*(8):273–8.

Camargo, J.A., Alonso, A., Salamanca, A. 2005. Nitrate toxicity to aquatic animals: a review with new data for freshwater invertebrates. *Chemosphere*, 58:1255-1267.

Dahl, T.E. 1990. Wetlands–losses in the United States, 1780's to 1980's. U.S. Fish and Wildlife Service report to Congress, Washington, D.C.

Death, R.G., and Winterbourn, M.J. 1995. Diversity patterns in stream benthic invertebrate communities: The influence of habitat stability. *Ecology*, 76(5):1446-160.

Faith, D.P., Minchin, P.R., and Belbin, L. 1987. Compositional dissimilarity as a robust measure of ecological distance. *Plant Ecology*, 69:57-68.

Gorman, O.T., and Karr, J.R. 1978. Habitat structure and stream fish communities. *Ecology*, 59(3):507-515.

IEPA (Illinois Environmental Protection Agency). 2007. Methods of collecting macroinvertebrates in streams. Bureau of Water, Springfield, Illinois.

Karr, J.R., F.D. Fausch, P.L. Angermeier, P.R. Yant, and I.J. Schlosser. 1986. Assessment of Biological Integrity in Running Waters: A Method and its Rationale. Illinois Natural History Survey Special Publication 5, Champaign, Illinois.

Liao, J.C. 2007. A review of fish swimming mechanics and behavior in altered flows. *Philos. Trans. R. Soc. Lond. B. Biol. Sci.*, 362(1487):1973-1993.

Moerke, A.H., and Lamberti, G.A. 2004. Restoring stream ecosystems: lessons from a Midwestern state. *Restoration Ecology*, 12(3):327-334.

Minchin, P.R. 1987. An evaluation of relative robustness of techniques for ecological ordinations. *Plant Ecology*, 69: 89-107.

Mueller, D.K., Ruddy, B.C., Battaglin, W.A. 1997. Logistic model of nitrate in streams of the upper-Midwestern United States. *Journal of Environmental Quality*, 25(5): 1223-1230.

NRC (National Research Council). 1992. Restoration of Aquatic Ecosystems: Science, Technology and Public Policy. National Academy Press, Washington, D.C.

O'Connor, N.A. 1991. The effects of habitat complexity on the macroinvertebrates colonizing wood substrates in a lowland stream. *Oecologia*, 85(4):504-512.

Palmer, M.A., Ambrose, R.F., and Poff, N.L. 1997. Ecological theory and community restoration ecology. *Restoration Ecology*, 5(4):291-300.

Pant, M. 2014. Effects of instream habitat restoration on macroinvertebrate and fish communities in a small Midwestern stream. MS Thesis. Eastern Illinois University. Charleston, IL.

Pflieger, W. L. 1997. The fishes of Missouri. Missouri Department of Conservation, Jefferson City, Missouri. 372 pp.

R Development Core Team. 2008. R: A language and environment for statistical computing. R Foundation for Statistical Computing, Vienna, Austria. ISBN 3-900051-07-0, URL http://www.R-project.org.

Rabeni, C.F., Lyons, J., Mercado-Silva, N., and Peterson, J.T. 2009. Warmwater fish in wadeable streams. Pages 43-56 *in* S.A. Bonar, W.A. Hubert, and D.W. Willis, editors.

Standard methods for sampling North American freshwater fishes. American Fisheries Society, Bethesda, Maryland.

Rankin, E.T. 1989. The qualitative habitat evaluation index [QHEI]: rationales, methods, and application. Ohio Environmental Protection Agency, Columbus.

Royer, T.V., Tank, J.L., David, M.B. 2004. Transport and fate of nitrate in headwater agricultural streams in Illinois. *Journal of Environmental Quality,* 33:1296-1304.

Shappell, N.W. 2006. Estrogenic activity in the environment: municipal wastewater effluent, river, ponds, and wetlands. *Journal of Environmental Quality, 35*(1):122–32.

Sudduth, E. B., B. A. Hassett, P. Cada, and E. S. Bernhardt. 2011. Testing the Field of Dreams Hypothesis: functional responses to urbanization and restoration in stream ecosystems. *Ecological Applications,* 21:1972–1988.

Svendsen, J. C., Genz, J., Anderson, W. G., Stol, J. A., Watkinson, D. A., and Enders, E. C. 2014. Evidence of circadian rhythm, oxygen regulation capacity, metabolic repeatability and positive correlations between forced and spontaneous maximal metabolic rates in lake sturgeon Acipenser fulvescens. *PloS One, 9(4),* e94693.

Tetra Tech Inc. 2004. Illinois Benthic Macroinvertebrate Collection Method Comparison and Stream Condition Index Revision, 2004.

Singh, B., Bhat, T.K., Singh, B. 2003. Potential therapeutic applications of some antinutritional plant secondary metabolites. *Journal of Agricultural and Food Chemistry,* 51(19):5579-5597.

Walser, C.A., and Bart Jr., H.L. 1999. Influence of agriculture on in-stream habitat and fish community structure in Piedmont watersheds of the Chattahoochee River System. *Ecology of Freshwater Fish,* 8(4):237-246.

West, J.L. 2013. Short-term responses of fish assemblages to habitat restoration in a small Midwestern stream. MS Thesis. Eastern Illinois University. Charleston, IL

Table 1—Results of permutational ANOVA testing differences in community structure as a factor of habitat rehabilitation, and accounting for temporal (annual) assemblage variation. Community dissimilarity was monitoring in restored and reference (control) sites in Kickapoo Creek from 2010-2015.

	Term	DF	MS	F	R^2	p-value
Fish	treatment	1	0.0603	5.9304	0.1692	0.012
	year	5	0.0269	2.6471	0.3777	0.045
	interaction	5	0.0120	1.1761	0.1678	0.356
	residuals	10	0.0102			
	total	21				
Macroinvertebrates	treatment	1	0.1975	3.7999	0.0887	0.027
	year	5	0.2446	4.7071	0.5491	0.001
	interaction	5	0.0575	1.1060	0.1290	0.358
	residuals	10	0.0520			
	total	21				

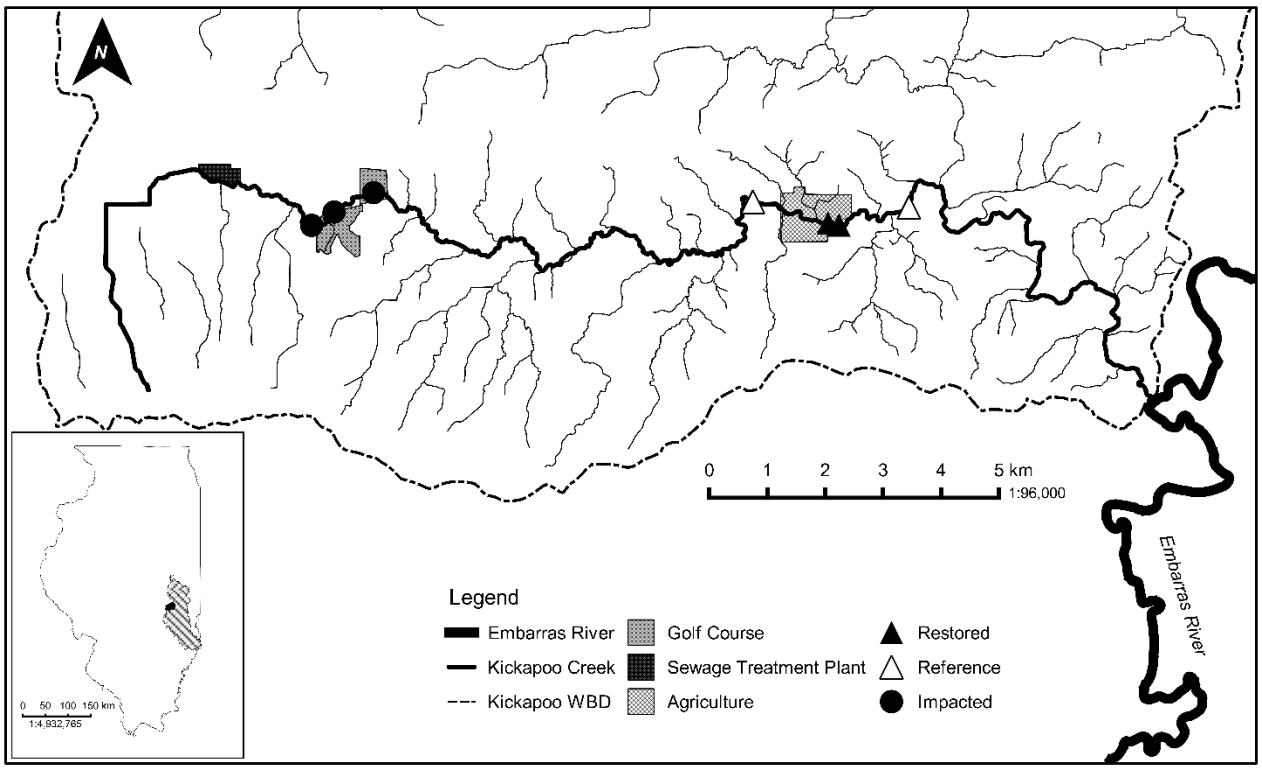

Figure 1—Locations of restoration, reference, and impacted sites monitored within the Kickapoo Creek watershed boundary (WBD) in East-Central Illinois from 2009 to 2015.

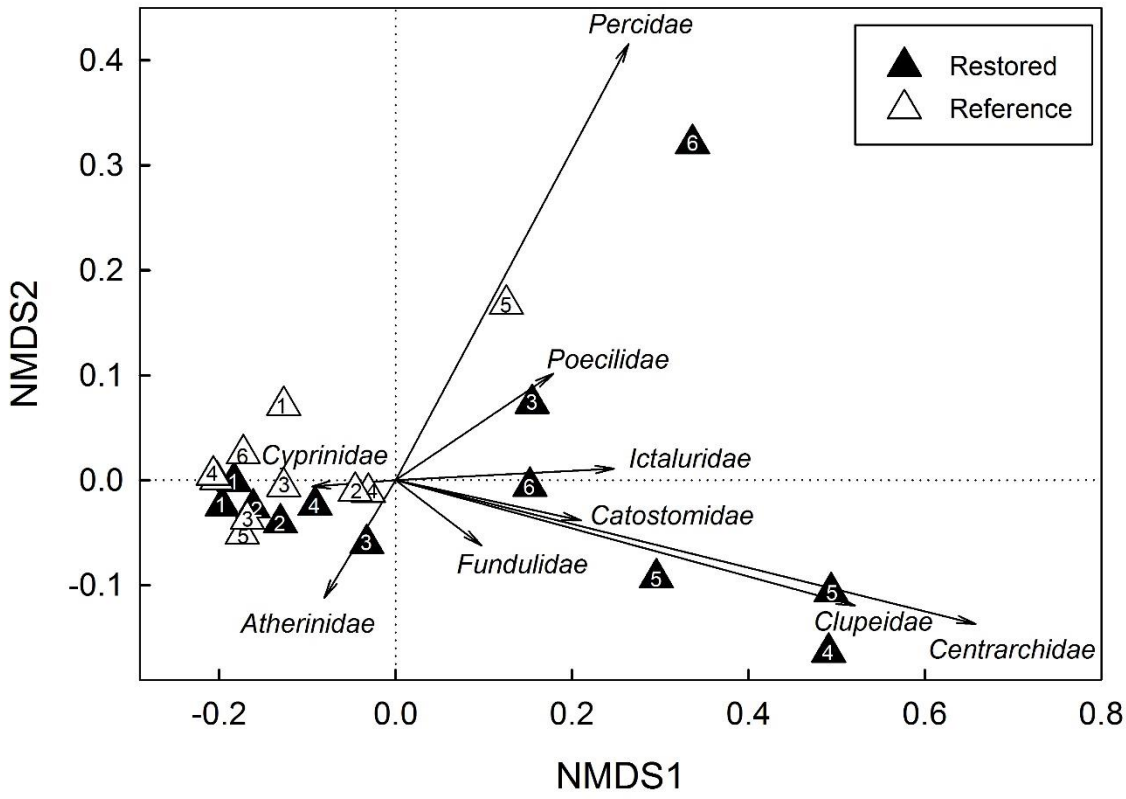

Figure 2—Nonmetric multidimensional scaling (NMDS) plot computed with a Bray-Curtis dissimilarity matrix examining temporal and spatial changes in fish community structure following an instream rehabilitation project in Kickapoo Creek. Assemblages were sampled in restored and reference sites from 2010 to 2015, and numbers within the plot correspond to years post rehabilitation (1-6). Relative loadings of taxonomic groups are represented by solid vectors, with direction and magnitude relating to respective correlations with the community matrix.

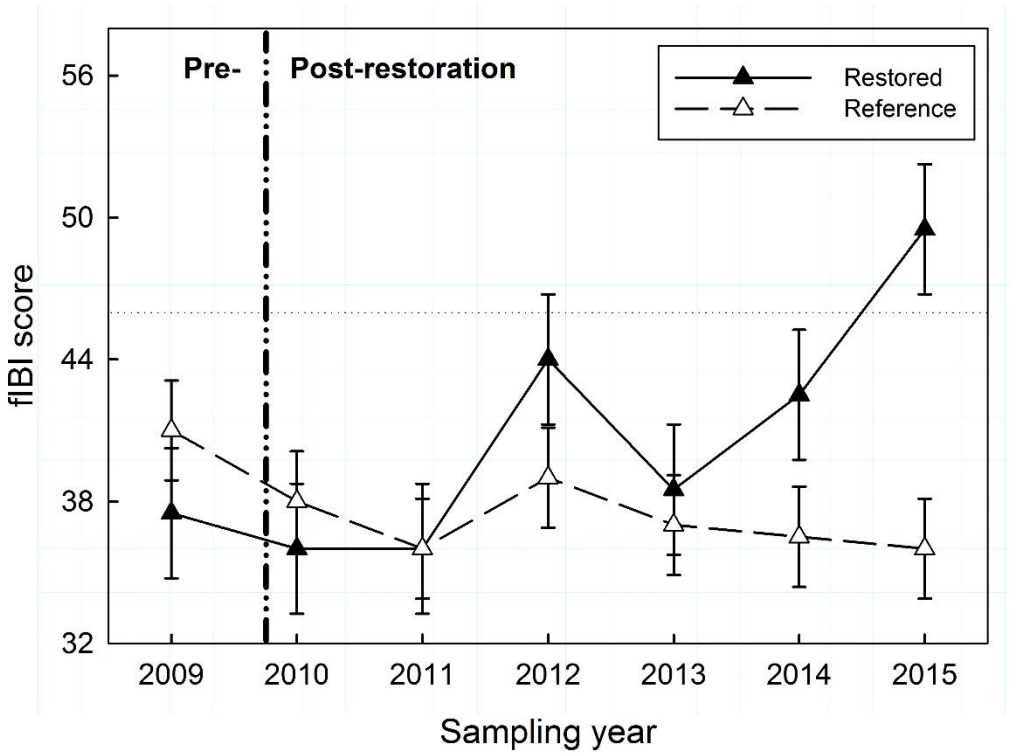

Figure 3—Fish Index of Biotic Integrity (fIBI) scores for fish assemblages in restored and reference sites sampled from 2009 (pre-restoration) to 2015. The vertical dashed line indicates the approximate completion of the rehabilitation project, while the horizontal dotted line separates the 'moderately low' integrity classification from 'moderate' biotic integrity. Error bars represent 95%-confidence intervals computed for assemblages within each of the treatment types.

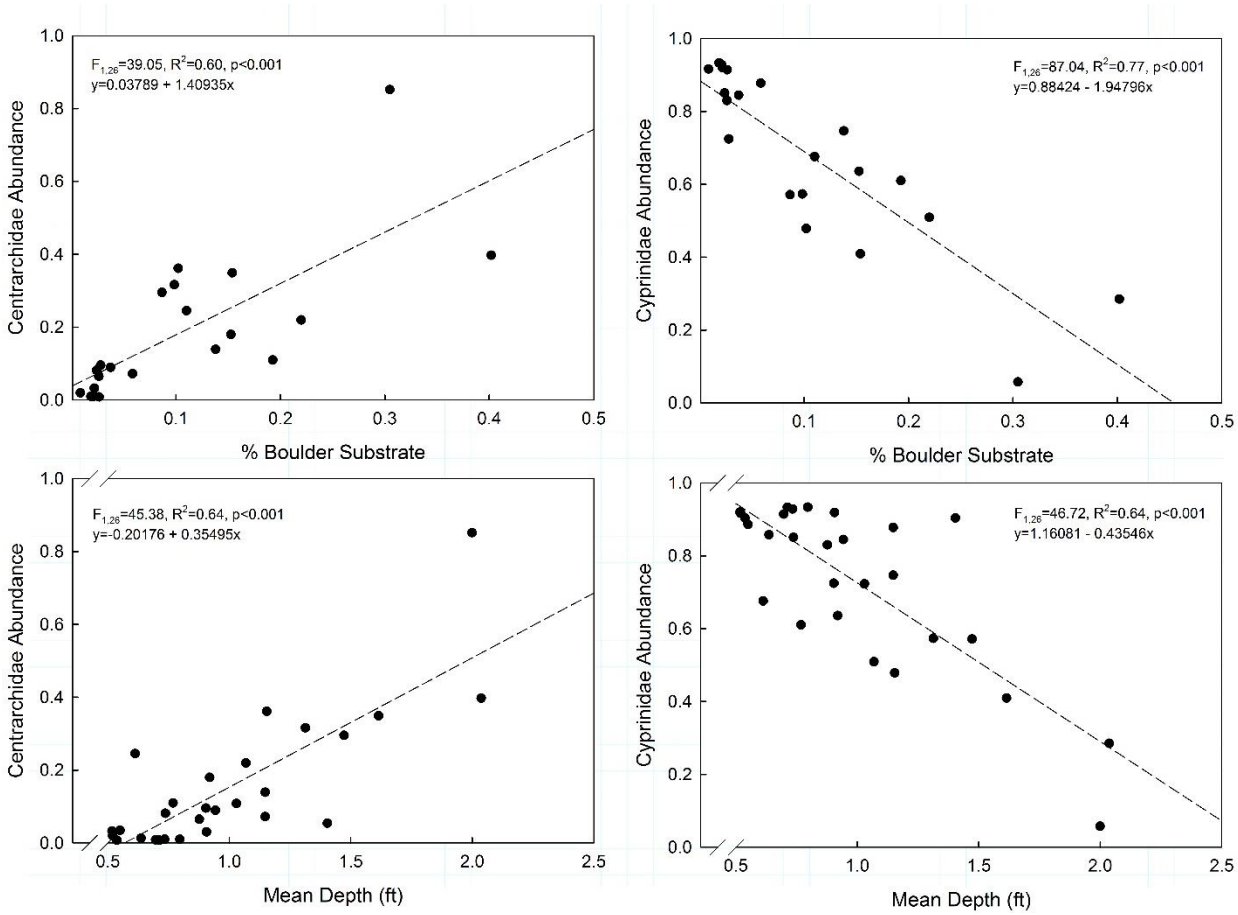

Figure 4—Relationships between relative abundance of Cyprinidae and Centrarchidae taxa with percentage of boulder substrate and mean depth within seven study sites along Kickapoo Creek, sampled from 2009 to 2015. Dashed lines represent best-fit linear regression models. Results of linear regression analysis and equations appear within each respective plot.

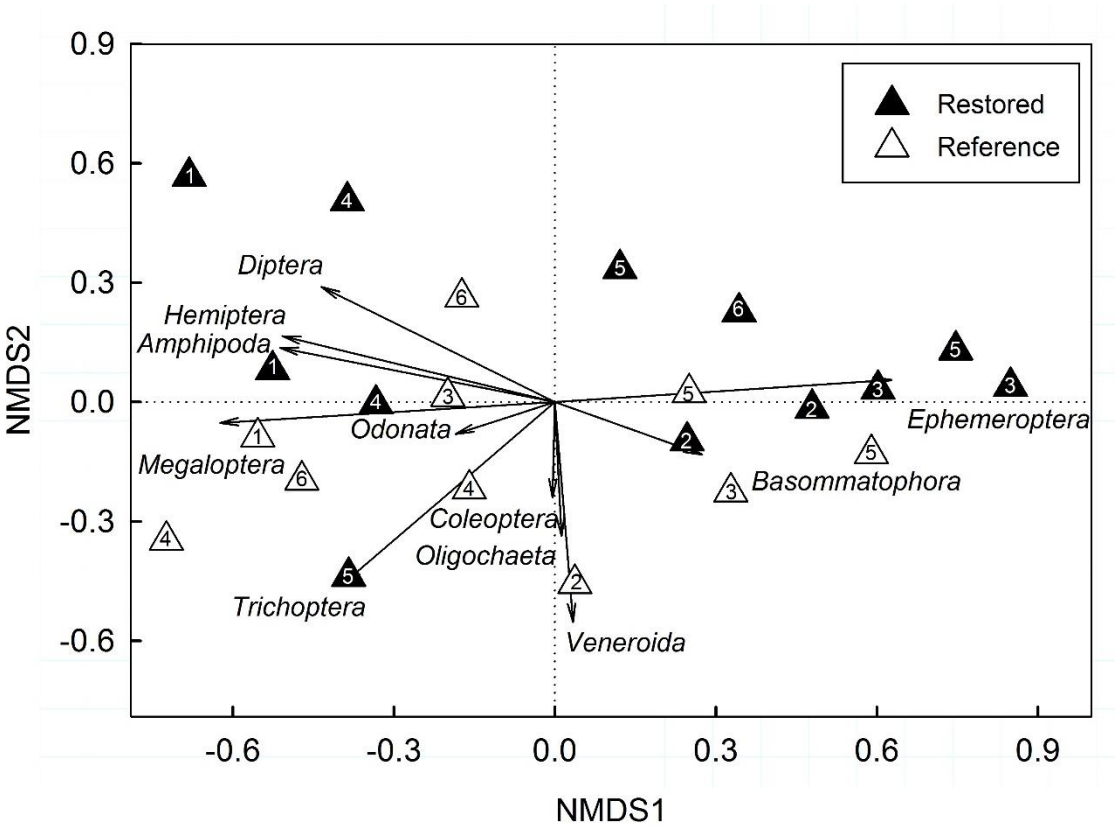

Figure 5— Nonmetric multidimensional scaling (NMDS) plot computed with a Bray-Curtis dissimilarity matrix examining temporal and spatial changes in macroinvertebrate community structure following an instream rehabilitation project in Kickapoo Creek. Assemblages were sampled in restored and reference sites from 2010 to 2015, and numbers within the plot correspond to years post rehabilitation (1-6). Relative loadings of taxonomic groups are represented by solid vectors, with direction and magnitude relating to respective correlations with the community matrix.

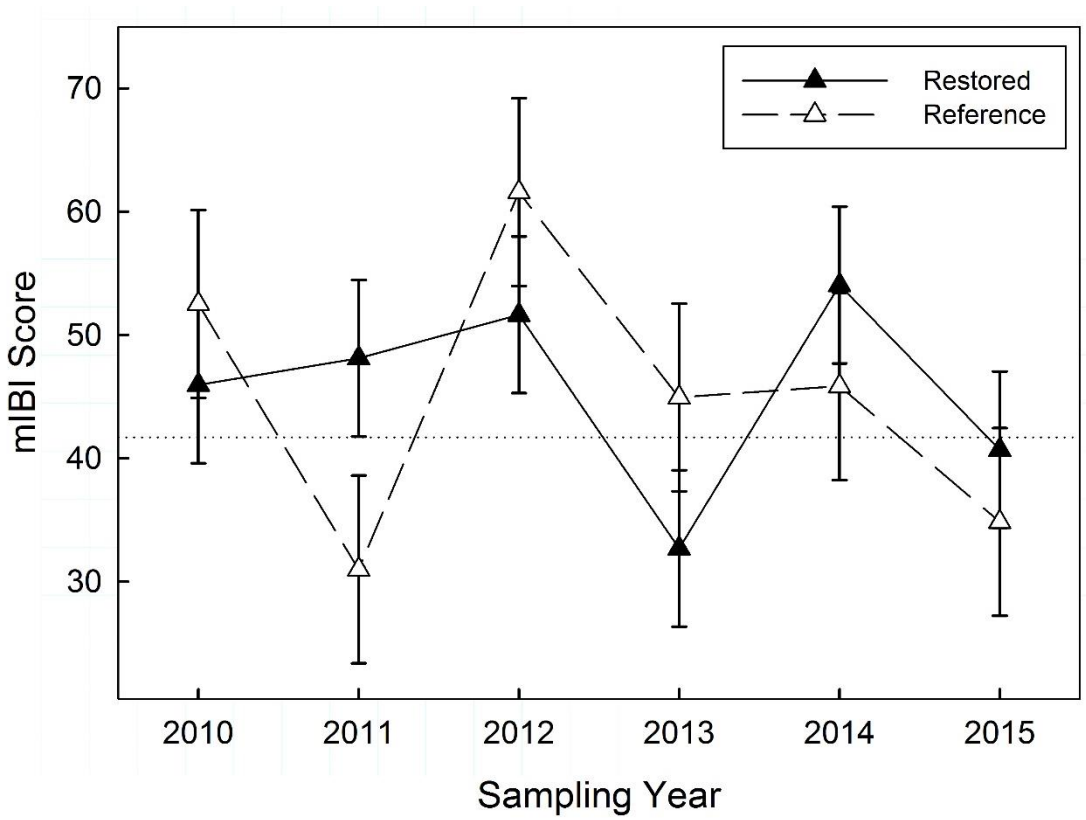

Figure 6—Macroinvertebrate Index of Biotic Integrity (mIBI) scores for fish assemblages in restored and reference sites sampled post-rehabilitation from 2010 to 2015. The horizontal dotted line separates the 'fair' integrity classification from 'good' biotic integrity. Error bars represent 95%-confidence intervals computed for assemblages within each of the treatment types.

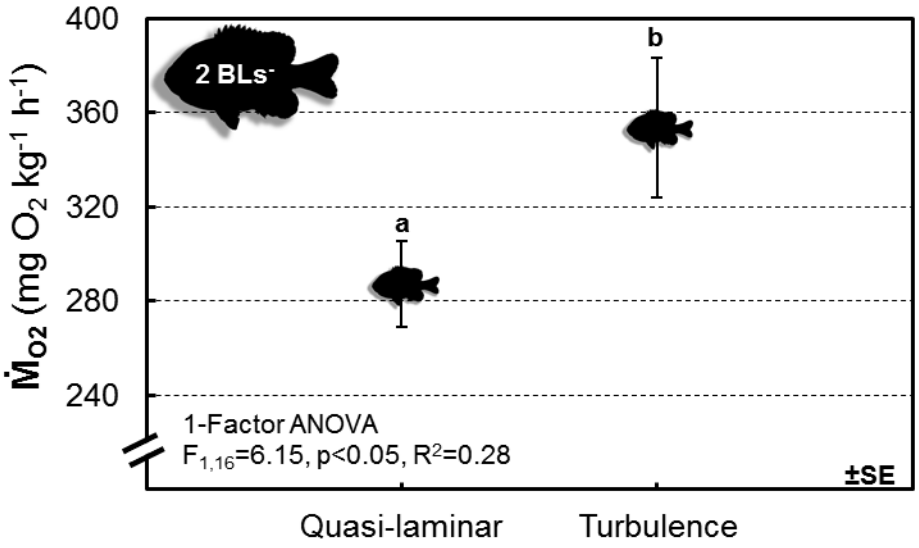

Figure 7—Mass-corrected rates of oxygen consumption ($\dot{M}_{O2}$) for Longear Sunfish swimming in quasi-laminar and turbulent flow. Results of the ANOVA are presented in the figure. Error bars represent ± standard error (SE)

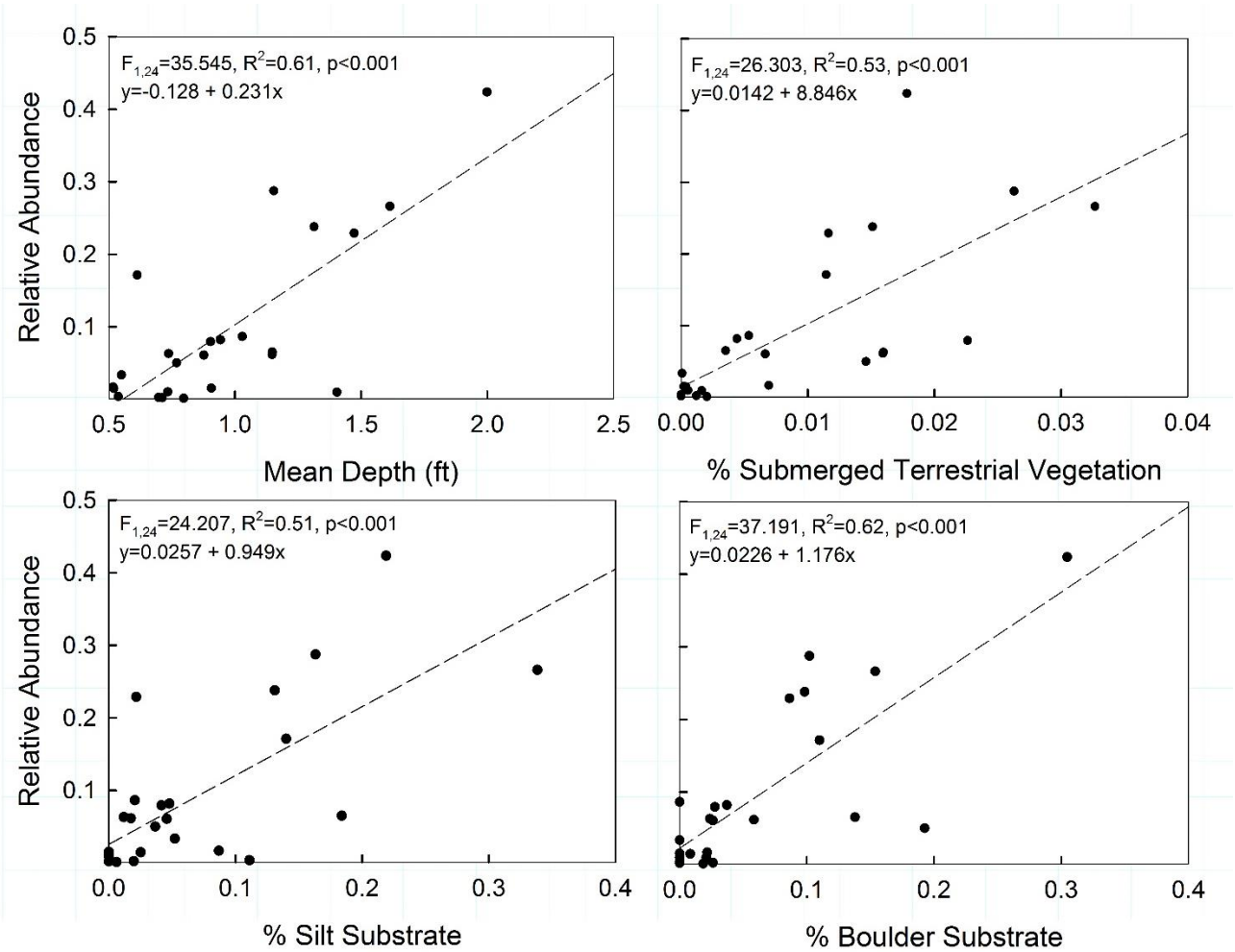

Figure 8—Relationships between relative abundance of Longear Sunfish and driving habitat factors in Kickapoo Creek. Results of linear regressions appear within each respective plot along with an equation for each best-fit dashed line.

Effect of dams on the genetic structure of fish assemblages in the Vermillion River

Basic Information

Title:	Effect of dams on the genetic structure of fish assemblages in the Vermillion River
Project Number:	2015IL294B
Start Date:	3/1/2015
End Date:	2/28/2016
Funding Source:	104B
Congressional District:	IL-15
Research Category:	Biological Sciences
Focus Category:	Ecology, Geomorphological Processes, Management and Planning
Descriptors:	None
Principal Investigators:	Robert Colombo, Devon Keeney, Shannon Smith

Publications

There are no publications.

PROJECT NAME:
Effect of Dams on the Genetic Structure of Fish Assemblages in the Vermilion River

PRINCIPAL INVESTIGATORS:

Dr. Robert Colombo Ph.D
Eastern Illinois University
Email: recolombo@eiu.edu
Phone: (217) 581-3011

Dr. Devon Keeney Ph.D
Le Moyne College
Email: keeneydb@lemoyne.edu
Phone: (315) 445-4508

Shannon C. F. Smith (Co-principal Investigator)
Eastern Illinois University
Email: scsmith3@eiu.edu
Phone: (315) 256-6198

CONGRESSIONAL DISTRICT:
Illinois U.S. District 15 (IL-15)

PROJECT SUMMARY

For the past century river hydrology has been altered by the addition of in-stream structures for industrial, agricultural and recreational purposes. These structures (usually dams) are a major source of anthropogenic disturbance and a decisive impediment to river restoration. The physical effects of dams on a river system are well documented and include converting lotic habitats to lentic habitats, changing flow regimes, and increasing siltation upstream from the dam (Pringle 2003, Bednarek 2001). These habitat alterations can impact aquatic insect and fish assemblages by reducing species richness and abundance and influencing dispersal. Furthermore, dams have been shown to isolate populations and have an impact on genetic structuring and differentiation (Meldgaard et al. 2003). Due to increasing awareness of dams' multifaceted ecosystem impacts, dam removal has been gaining traction in the United States in recent years. However, fewer than 5% of the 500 dams removed nationwide in 2005 underwent ecological studies (Thomson et. al 2005). Additionally, most of the dams monitored were large dams as opposed to low-head dams; the latter are more prevalent in the United States. Approximately 48% of all dams in the U.S. are lower than 25 feet and are often overlooked in terms of their potential ecological impacts due to their relatively small size (USACE 2013). Two of these small dams (classified as low-head dams) are the Danville and Ellsworth Park dams in Danville, IL. The Danville Dam is located on the Vermilion River and is a barrier between the lower 22 miles of Vermilion River mainstem and the 1,290 mi^2 drainage area upstream. The Ellsworth Park Dam is located on the North Fork Vermilion River, approximately 0.53 miles upstream from the confluence of the North Fork River and the Vermilion River. These dams were scheduled for removal between the spring of 2014 and the fall of 2015, but both still stand as a result of budget and funding issues. Since the removal of the dams is on hold indefinitely, the current principal investigator focused on the effects that these low-head dams have on fish population genetics (a topic poorly represented in scientific literature) in addition to the monitoring of habitat and biotic communities. The primary objectives of this study were to 1) assess habitat quality above and below these two low-head dams, 2) assess fish community assemblages above and below the dams, and finally, to evaluate the effects that the dams have on genetic differentiation and dispersal in two fish species: Longear Sunfish (*Lepomis megalotis*) and Bluntnose Minnow (*Pimephales notatus*). We found that the dams have clear impacts on physical river characteristics like habitat quality; upriver sites in both rivers had significantly higher habitat quality compared to pool sites directly above the dams. Fish assemblages reflected these habitat patterns, with riffle specialist species having a significantly higher abundance at the high quality habitat North Fork River upriver sites compared to other sites. However, our genetic data show that dams themselves are not preventing dispersal of the two fish species. There was weak genetic differentiation in Longear Sunfish, and no discernible patterns in F_{ST} values that would indicate that the dams are impeding movement. Bluntnose Minnow had two genetically distinct populations in the study area, but pairwise F_{ST} comparisons reveal that this is likely due to an isolation by distance effect instead of the dams blocking fish dispersal.

METHODOLOGY SUMMARY

Six sites on the Vermilion River and six sites on the North Fork Vermilion River were sampled for habitat quality and fish assemblages twice annually in the fall and spring seasons. On each

river two sites are located below the dam, two in the pool created above the dam, and two are located upriver of the pool extent. To analyze habitat quality at each site, basic habitat metrics were collected and Qualitative Habitat Evaluation Index (QHEI) scores determined for all reaches. Fish communities on each river were sampled using DC boat electrofishing gear with supplemental gears such as seine nets and mini-fyke nets. To investigate the effects of a physical barrier on the genetic composition of populations above and below the dams, targeted fish species for genetic analysis (Longear Sunfish and Bluntnose Minnow) were finclipped. These species are representative of different life histories and movement patterns in order to gain a comprehensive picture of how impoundments may affect genetic structure in fishes.

To determine genetic differentiation in these two species we used microsatellites: non-coding sections of the genome that are highly variable in populations and therefore a good detector of genetic differentiation. We isolated DNA from 426 Longear Sunfish and 374 Bluntnose Minnow collected in different years and sampling seasons in order to account for any seasonal or annual fluctuation in alleles. Novel and preexisting (Landis et. al 2009, Gotoh et. al 2013) microsatellite loci were amplified to examine levels of genetic differentiation among study sites. We tested over 25 loci for each species to ensure that they were suitable for inclusion in the study; testing involved linkage disequilibrium and Hardy-Weinberg equilibrium analyses. Ultimately we used 11 loci for Bluntnose Minnow and 10 loci for Longear Sunfish. Microsatellite amplifications used fluorescent-labeled DNA primers in multiplex polymerase chain reactions (PCR) and fish genotypes were determined on a Li-Cor 4300 DNA Analyzer.

All ecological data analyses were carried out in the statistical software R (version 3.2.1). To analyze ecological data, habitat quality scores for each site were calculated from the QHEI. Relative abundances of fish and macroinvertebrates were calculated for each site and these data were used in non-metric multidimensional scaling (NMDS) analyses in order to examine patterns in biotic assemblages. Environmental variables such as habitat quality scores and flow were correlated with fish assemblage data using permutational analyses and distance matrices. Analysis of variance (ANOVA) with Tukey Honest Significance Difference post-hoc tests were used to test for significant differences.

To analyze genetic data, we used the program FSTAT (version 2.9.3) to calculate F_{ST} values (a measure of genetic differentiation) for each species among all sites (overall) and between sites (pairwise). For overall comparisons an alpha value of 0.05 was used; for pairwise comparisons the B-Y method False Discovery Rate (FDR) adjusted critical value was applied (Narum 2006). The program STRUCTURE (Pritchard et al. 2000) was used to infer the number of genetic populations among all sites and to infer genetic differentiation.

RESULTS AND DISCUSSION

Habitat quality between below dam, above-dam (pool) and upriver sites showed significant patterns in both rivers. The highest habitat quality scores were in the upriver sites farthest from the dams, and upriver sites had significantly higher habitat quality than the pool sites (ANOVA, $P<0.05$). Fish communities showed groupings that reflected this pattern seen in habitat quality among sites. Fish communities aggregated at the family level in NMDS analysis showed a

separation of the North Fork River and Vermilion River sites. Catostomids clustered with below dam sites, which makes sense for a group of fishes that favors areas with noticeable current. Families that prefer riffle habitat clustered with the with the high quality habitat in the North Fork River upriver sites, notably the families Percidae (darter species) and Ictaluridae (madtom species). When fish were grouped into habitat guilds, riffle specialist species had higher abundance in the North Fork upriver sites when compared to North Fork River pool, Vermilion River pool, and Vermilion River below-dam sites (ANOVA, $P<0.05$). Flow was determined to be a significant predictor of habitat guild assemblages (perMANOVA, $P<0.05$). Although QHEI and substrate type were not statistically significant predictors of guild assemblages, both of these physical parameters of river systems are ecologically important factors in fish dispersal.

Genetic data revealed different results for Longear Sunfish and Bluntnose Minnow. For Longear Sunfish, overall F_{ST} was very low yet statistically significant ($F_{ST} = 0.001$, $P<0.05$), indicating very low genetic differentiation in this species among sites. STRUCTURE also indicated that the Longear Sunfish in both rivers are genetically homogenous; there is only one genetic population overall. When comparing Longear Sunfish between sites, pairwise F_{ST} values showed that Longear Sunfish in the North Fork River upriver sites are genetically distinct from Longear Sunfish below the Danville Dam in the Vermilion River ($P<0.01656$), which is not surprising given the distance between these sites. Additionally, Longear Sunfish in the two Vermilion River pool sites were also genetically distinct ($P<0.01656$), which may be due to the small home range of the Longear Sunfish. Although the overall differentiation is very weak, these pairwise comparisons reveal significant differentiation between sites that is likely too weak for STRUCTURE or overall F_{ST} to detect. In summary, Longear Sunfish show very weak genetic differentiation among the study sites, which is likely due to the fact that these low-head dams are completely submerged during periods of high spring flows. This occurs multiple times every spring and allows unimpeded movement of these fish across the dams.

Like Longear Sunfish, Bluntnose Minnow also had a very low F_{ST} value ($F_{ST} = 0.007$, $P<0.01$) indicating weak but significant genetic differentiation overall. However, Bluntnose Minnow data showed a strong pattern when making pairwise site comparisons. Bluntnose Minnow from the North Fork River upriver sites were genetically distinct from every site in the Vermilion River ($P<0.01572$). STRUCTURE corroborated these F_{ST} values and determined that there were two genetically distinct populations of Bluntnose Minnow within the study area. This is likely a genetic isolation-by-distance effect where we see one population in the North Fork River upriver sites and another in the Vermilion River.

In terms of ecological data and physical habitat characteristics, these dams are clearly impacting these two river systems. The dams' presence drives habitat type and habitat quality, which in turn influences the fish communities in that area. However, our genetic analyses show that the dams themselves do not obstruct fish dispersal and movement to the point of genetic isolation. Although Bluntnose Minnow showed strong genetic differences, there were no patterns to suggest that the dams were driving these differences. We conclude that in this system these two species are not reproductively hindered by the dams and that the dams are causing no harm at the population genetic level.

STUDENT INFORMATION

A great many students from Eastern Illinois University and the Fisheries and Aquatic Research Team contributed their time and energy toward this project. M.S. degree candidates (graduate students) past and present include Clint Morgeson, Carl Favata, Zach Mitchell, Evan Boone, Daniel Roth, Hanna Kruckman, V. Alex Sotola, and Samuel Gradle. Undergraduate students who assisted in laboratory work include Kailee Schulz, Kaleb Wood, Pabitra Aryal and Melissa Eaton.

LITERATURE CITED

Bednarek, A. (2001). Undamming Rivers: A Review of the Ecological Impacts of Dam Removal. Environmental Management. 27: 803-814.

Landis, J.B., Grose, M.J., Wiley, E.O., and S.P. Hudman. (2009). Characterization of 35 novel microsatellite loci for ecological and evolutionary studies of the bluntnose minnow (Pimephales notatus). Molecular Ecology Resources. 9: 864-867.

Narum, S.R. (2006). Beyond Bonferroni: Less conservative analyses for conservation genetics. Conservation Genetics. 7:783-787.

Meldgaard, T., Nielsen, E.E., and Loesckcke, V. (2003). Fragmentation by weirs in a riverine system: A study of genetic variation in time and space among populations of European grayling (Thymallus thymallus) in a Danish river system. Conservation Genetics. 4: 735-747.

Pringle, C. (2003). What is hydrologic connectivity and why is it ecologically important? Hydrological Processes. 17: 2685-2689.

Pritchard, J.K., Stephens, M., and P. Donnelly. (2000) Inference of population structure using multilocus genotype data. Genetics. 155: 945-959.

Thomson, J.R., Hart, D.D., Charles, D.F., Nightengale, T.L. and Winter, D.M. (2005). Effects of the Removal of a Small Dam on Downstream Macroinvertebrate and Algal Assemblages in a Pennsylvania Stream. Journal of the North American Benthological Society. 24: 192-207.

United States Army Corps of Engineers (USACE). 2013. National Inventory of Dams database. Available: http://nid.usace.army.mil/cm_apex/f?p=838:3:0::NO. October 2015.

Making up for losses: A critical analysis of Section 404 compensatory stream mitigation banking in Illinois

Basic Information

Title:	Making up for losses: A critical analysis of Section 404 compensatory stream mitigation banking in Illinois
Project Number:	2015IL295B
Start Date:	3/1/2015
End Date:	2/28/2016
Funding Source:	104B
Congressional District:	IL-15
Research Category:	Water Quality
Focus Category:	Wetlands, Management and Planning, Water Quality
Descriptors:	None
Principal Investigators:	Bruce L. Rhoads, Thomas Bassett, Jeffery Matthews, Alex Peimer

Publications

There are no publications.

Title: Making Up for Losses: A Critical Analysis of Section 404 Compensatory Stream Mitigation Banking in Illinois

Submitted: March 25, 2016

Student author: Alex W. Peimer, Ph.D. candidate, Department of Geography and GIScience

1. PROBLEM AND RESEARCH OBJECTIVES

Statement of Critical State Water Problem: Illinois faces historically and geographically differentiated water quality impacts. Urbanization threatens water quality in the greater-Chicago region (Wilson and Weng 2011), widespread, intensive agriculture and tile drainage in East-Central Illinois has dramatically altered water quality as far away as the Gulf of Mexico (David et al. 2010), and coal mining poses unique challenges to water quality protection in southern Illinois (Kravits and Crelling 1981). Additionally, widespread channelization and ditching of agricultural streams is associated with conversion of wetland and prairie to farmland (Hergert 1978; McCorvie and Lant 1993), and these impacts are irreversible by natural processes alone (Urban and Rhoads 2003). While in 1820 there were 22 million acres of prairie in Illinois, this total plunged to a mere 2,300 acres by 1978 (IDNR). Thus, significant historical and contemporary land use dynamics in Illinois have degraded water quality.

Compensatory stream mitigation represents a potential means to overcome these historical and contemporary threats to water quality. The 2008 Compensatory Mitigation Rule, developed under Clean Water Act Section 404, requires that permitted unavoidable impacts to surface water are off-set by purchasing mitigation credits (Hough and Robertson 2009). Mitigation credits are produced at a mitigation bank; a segment of a stream that is restored, enhanced, or conserved to provide ecological benefit according to crediting criteria (Lave et al. 2008). Credits represent commensurable ecological value between the site of impact and site of mitigation; the goal is to achieve No Net Loss of ecological function nationally (Hough and Robertson 2009). All mitigation projects are subject to review by individual Corps[1] districts, and each of the four Corps districts in Illinois has independent crediting authority (Doyle et al. 2013). This has led to inconsistencies in crediting and credit pricing among Corps districts. Thus Corps districts in Illinois are developing a single statewide crediting guideline. The current protocol, the Illinois Stream Mitigation Method (ISMM), was published in 2010. The St. Louis Corps has organized a 24-member working group of state and federal regulators and scientists to improve the ISMM's ability to off-set losses.

The problem that Illinois faces is to come up with a way to measure "stream credits" to mitigate adverse stream impacts. The problem is twofold: 1) regulators must develop a protocol for measuring stream credits, and 2) off-sets must be ecologically comparable to impact sites (Lave et al. 2008). Addressing this problem requires attention to both social and biophysical theories. Socially, the problem is to develop a new system of measure by articulating different knowledge domains (i.e. law, economics, and science) (Espeland and Stevens 1998; Robertson 2006). Biophysically, the problem is to use ecological and stream restoration techniques at the reach-scale to provide a comparable amount of ecosystem function to that lost elsewhere (McDonald et al. 2004; Palmer 2009; Doyle and Shields 2012). It is therefore important to

[1] Corps of Engineers

determine a) if mitigation off-sets losses, and b) whether constraints to successful mitigation are ecological, political-economic, or both.

Statement of Expected Results and Benefits: There are two expected results from this study. First, this study will be the first of its kind to research the decision making process that occurs in developing stream mitigation credit criteria. Previous research that has traced market development in wetlands (Robertson 2004), greenhouse gases (MacKenzie 2009), and carbon crediting (McAfee and Shapiro 2010) shows the importance of this type of work. It is in the creation of the crediting protocol itself that environmental knowledge and values influence landscape outcomes. Second, this research will also be the first to directly compare the kinds of ecological functions lost at adverse impact sites with ecological functions supposedly provided by stream mitigation banks. The benefit of this study is that it will provide insight into the effectiveness of policy articulation: from the stage of policy interpretation through the stages of policy implementation and monitoring. Such a perspective will demonstrate the importance of conceptualizing environmental policy in a way that recognizes the simultaneity and inter-play, of and between, social and biophysical processes (Lave et al. 2014).

Nature, scope and objectives of the project: This project combines social and biophysical research. The scope of this project is the *process of compensatory stream mitigation banking in Illinois.* This research will follow the development of the crediting protocol, implementation of this protocol to assign stream credit values, and analyze the building and outcome of a stream mitigation bank. The objectives of this project are to 1) explain how adverse impacts to a stream in one location are commensurated with off-sets to a stream elsewhere, and 2) to assess, through direct biophysical comparison, if mitigation off-sets losses. The overall research question that this project addresses therefore is: *What is the translational process by which Section 404 impacts are deemed commensurate with Section 404 mitigation activities?* To answer the overall research question I will answer four sub-questions by drawing upon qualitative and quantitative methods in both the social and biophysical sciences:

1) How are (and what types of) ecological and geomorphic science included into the ISMM?
2) How do mitigation bankers decide on the location, size, and type of bank that they build?
3) How do regulators decide the number of stream credits lost or gained while using the ISMM?
4) Are the ecological functions lost at adverse impact sites off-set by mitigation at a stream mitigation bank? If so, over what temporal and spatial scales? If not, why not?

2. METHODOLOGY

Social data, methods and analysis: Questions 1, 2, and 3 will be answered using a mixed-methods approach (Ho 2009). The student researcher has IRB approval and has been granted permission by the St. Louis Corps to participate in field application of ISMM to assess the value of sites in terms of stream credits. The student researcher originally planned to also participate in discussions regarding the development of the Illinois Stream Mitigation Method. However, since the Illinois Stream Team has not met recently, the student researcher relied on secondary documents that recorded meeting procedures and discussions as well as interviews with participants of discussions. Additionally, the student researcher includes interviews with the Missouri stream assessment team members and review of the Missouri mitigation method for two reasons. First, the Illinois stream assessment team borrows the Missouri method, and therefore it

is necessary to understand what decisions went into making the Missouri method to more fully capture the ecological and geomorphic science that is included in the Illinois method. Second, the student researcher includes the Missouri team to increase the sample size and to verify references that are made to the Missouri method by Illinois team members.

Question 1) How are (and what types of) ecological and geomorphic science included into the ISMM?

This question is answered using three methods: Semi-structured open-ended interviews, reviews of notes and correspondence during method development, and review of drafts to successive versions of the Illinois and Missouri stream mitigation methods. Semi-structured open-ended interviewing was used to question individuals involved in creating the crediting protocol about major assumptions of the protocol, the strengths and weaknesses of the protocol, what they would change about the protocol, and if they believe the protocol enables the off-setting of adverse impacts to streams. These data provide insight into individual differences of opinion and determine who has authority and ability to influence what kind of information is included in the crediting protocol. Interviews are supplemented with a review of notes taken during group meetings during method development and reviews of successive changes made to the Illinois and Missouri mitigation methods. By comparing changes made to the mitigation methods with details of discussions and debates during method creation it will be possible to further understand what constrains and enables the inclusion of best-available ecological and geomorphic science into the mitigation methods. Furthermore, reviews of successive drafts of the Illinois and Missouri methods provides evidence for the types of scientific information and data that are considered relevant when developing the Illinois and Missouri stream mitigation methods.

Question 2) How do mitigation bankers decide on the location, size, and type of bank that they build?

This question will be answered using semi-structured open-ended interviews with mitigation bankers (two in Illinois that sell stream credits). The student researcher will meet with mitigation bankers and ask questions pertaining to site selection and development. Meetings will be held on location at mitigation banking sites.

Question 3) How do regulators decide the number of stream credits lost or gained while using the ISMM?

This question is answered using a combination of three methods: Semi-structured open-ended interviews with regulators, participant observation of the use of the Illinois stream mitigation method and negotiation with Section 404 applicants during the mitigation phase of impact projects, and participant observation with mitigation practitioners while monitoring a mitigation banking site. First, the student researcher will meet and interview Corps project managers to understand how project managers interpret federal and regional guidelines and policies when implementing Section 404 compensatory mitigation regulation. Second, the student researcher will also utilize participant observation during the discussion with an applicant over what mitigation is necessary to off-set their Section 404 impacts. This participant observation includes a site visit and evaluation using the Illinois stream mitigation method. Finally, the student researcher will participate with a mitigation banker during bank monitoring and assessment.

Question 4) Are the ecological functions lost at adverse impact sites off-set by mitigation at a stream mitigation bank? If so, over what temporal and spatial scales? If not, why not?

Question 4 will be answered using biophysical science and methods to characterize the physical, chemical, and biological characteristics of impacted and mitigated Section 404 stream sites. The dominant biophysical factors are a combination of physical, chemical and biological processes. Utilizing a watershed approach, geomorphic characterization, and measurement of riparian corridor loss, the student researcher will characterize the physical, chemical, and biological condition of a mitigation banking site and the impacted sites that it supposedly compensates.

A widely held assumption in stream ecology is that geomorphic variability is positively correlated with biological diversity (Bartley and Rutherford 2005; Laub et al. 2012). While there are debates over the generalizability of this principle (e.g. Palmer et al. 2010), the assumption that geomorphic variability leads to diverse and positively functioning stream ecosystems is well-entrenched in the classifications used in the ISMM. For example, high "functional" value is given to streams with "natural meanders" and pool-riffle systems, while low value is given for straightened streams without visible pool-riffle systems. As such, this study assesses the overall exchange of geomorphic variability between impacted sites and the mitigation site.

Analyses include: i) channel dimension analysis, ii) channel sediment-size distribution analysis, iii) space-for-time substitution water quality analysis of impact and mitigation sites (temperature, pH, and conductivity), iv) riparian corridor and channel length change over time (before and after permit issuance) at impact and mitigation sites, v) watershed area delineation, vi) water level variation at mitigation bank.

GEOMORPHIC CHARACTERISTICS

i) **Channel Dimension Analysis:** *Longitudinal Profile (i.e. thalweg) and Cross-Sectional Profile:* The longitudinal profile (i.e. thalweg) and cross-sectional profile will be measured using total station topographic survey instruments. Thalweg measurements will consist of measurements of the deepest point in the channel ~2 meters through the extent of the study reach. The line that connects the depth point measurements will constitute the thalweg, and the vertical variation of this line is the longitudinal variability. Measurement of eight to ten bankfull cross-sectional profiles ensures statistical robustness of data analysis (Bartley and Rutherford 2005). The bankfull level will be identified using appropriate indicators (minimum width-depth ratio, abrupt transition from channel to floodplain, vegetation changes). The cross-sectional profile will consist of measurements of both bankfull width and elevation data. The cross-sectional profile elevation data will be collected at all major changes in slope across the channel complemented by a regular spacing of measurement locations consistent with the channel size. Width and depth variation between sequential cross-sections constitutes cross-sectional variation.

ii) **Channel Sediment Size Analysis:** Channel sediment will be collected from the bed of the channel upstream and downstream of impacts in both pools and riffles. Pools, or deep and gradually sloped portions, collect the finest range of sediment in a stream. Riffles, or shallow and steeper portions, collect the largest range of

sediment in a stream. Together, sampling the pools and riffles will capture the probable range of sediment in each water body. The two dominant impact activities being questioned are channel culverting and channel bank vegetation clearance. In the case of culverts, sediment will be collected upstream and downstream of culverts. In the case of vegetation clearance, sediment will be collected upstream of vegetation clearance, through the reach of cleared vegetation, and downstream of the cleared vegetation. Samples will be collected using bottom sampling grabbers. Samples will be dried, split, sieved, and weighed in the Geomorphology Soils Lab of University of Illinois, Champaign-Urbana campus to determine the particle size distribution.

HYDROLOGICAL CHARACTERISTICS

iii) **Watershed delineation:** Upstream watershed area from the downstream point of impact sites and the mitigation site were calculated using 10 meter digital elevation models (DEMs) in ArcGIS™. DEM sinks were identified and filled prior to flow direction mapping. Watershed area is a proxy for stream discharge. Comparison of watershed areas serves as a comparison for relative discharge. Watershed area is also correlated with the variability and duration of flooding events (Pociask and Matthews 2013). Watershed area therefore also serves as a proxy for the relative frequency and duration of flooding events.

iv) **Mitigation bank water level variation:** Water level variability in the mitigation site will be measured using a HOBO continuous-recording water level recorder. The water level recorder will capture hydrologic variability at 15-minute intervals. Data will be downloaded from the water-level recorder to produce flow a flow variability and duration curve. This data is important for understanding the connectivity between the channel and riparian corridor of the mitigation banking site.

WATER QUALITY CHARACTERISTICS

v) **Water quality analysis:** Water quality measurements will be taken at each reach using a YSI Professional ProPlus meter and hydro probes. Probes were calibrating according to YSI specificities. Measurements of temperature (℃), pH, and (specific) conductivity (µS/cm) will provide information on chemical and thermal hydrologic properties. These measurements, in turn, will be used to interpret the overall biological quality and function of the stream reaches. Data will be compared against water quality standards and historical measurements taken by the Illinois EPA.

RIPARIAN VEGETATION

vi) **Riparian vegetation loss:** Total area of riparian corridor vegetation documented in Section 404 permit documents will be compared against the total area of riparian vegetation loss at each impact site measured using Google Earth ™.

STATISTICAL ANALYSIS

vii) **Statistical Analysis:** There are a variety of statistical methods available for the analysis of variability (Bartley and Rutherford 2005; Laub et al. 2012). Bartley and Rutherford (2005) and Laub et al. (2012) each analyzed multiple metrics of geomorphic vulnerability and associated statistical analyses of variability. **Thalweg variability** will be analyzed using the "degree of wiggliness" factor (w), or the degree of vertical variation of channel depth from the mean elevation; where $w = \sqrt{n \sum(\Delta\phi_i)^2}$, and n= the number of points collected, and $\Delta\phi_i$ is the vertical deviation of each point from the mean (Bartley and Rutherford 2005). The coefficient of variation (CV) will be used to analyze the **variability in channel width and depth of the cross-section profiles** (Laub et al. 2012). CV is the ratio of the standard deviation and mean of a measurement. CV width and depth $= (\frac{\sigma}{\mu})$, where σ is the standard deviation of cross-sectional bankfull width and depth measures, and μ is the mean width and depth of the cross-section. **Sediment variability** will be analyzed using the measurement of sediment sorting (Bartley and Rutherford 2005). Phi sorting is a measure of the standard deviation of the sediment size distribution about the mean sediment size, where Sort $= (\phi 84 - \phi 16)/2$. $\phi 84$ is a grain size that 84 percent of the sample distribution is smaller than, and $\phi 16$ is a grain size that 16 percent of the sample distribution is smaller than. The phi (ϕ) system ranges from -12 to 14, where -12 phi sizes are boulders, and 14 correlates with very fine clays. **Planform variability** will be analyzed by calculating the sinuosity of all stream sites. A stream is considered "straight" if it has a sinuosity less than 1.2, and "meandering" if it has a sinuosity greater than 1.5 (Schumm 1963; Chang 1979).

3. PRINCIPLE FINDINGS AND SIGNIFICANCE

Principle findings to Question 1:

How are (and what types of) ecological and geomorphic science included into the ISMM?

The Illinois and Missouri stream mitigation methods were designed with similar overarching priorities and goals in mind. Both methods began with a template/pre-existing stream mitigation method (e.g. Missouri began with the 2002 Charleston, SC method; Illinois began with the 2007 Missouri method) and then modified and crafted these pre-existing methods to suit 'state-specific needs'. Neither the Illinois or Missouri team changed the overall format or calculation method of their template methods; instead changes and modifications were focused to within-document elements to encourage standard use (see Table 1 in Appendix).

The Illinois and Missouri stream mitigation method were designed to be used by non-experts. For example, in the words of one St. Louis Corps regulator: "every regulator, resource agency commenter, farmer, consultant, private citizen, developer and so on throughout the entire state that may become subject to Clean Water Act 404 regulation will need [to be capable of using the approved method]." Thus the methods in Illinois and Missouri are designed "to be done pretty

quickly, pretty much office-based, and actually…[Will Jones[2]], he was going to be the only person from the Corps working on this…It wasn't like an army of minions out doing assessments. He needed something he could do in half an hour. And he might have said that in specific" (Author interview, 05/26/2015). From this perspective, the ease of completion depended significantly on the work load of an individual Corps regulator.

Scientifically-based information was only included if it was deemed simple and was recognized by state and federal authorities (e.g. could a scientific requirement be legally required of a Section 404 or 401 water quality certificate applicant?). Thus, ecological and fluvial geomorphic science was included inasmuch as it was consistent with three overriding priorities: 1) Making the method useful in the regulatory setting of each state, 2) Working closer toward achieving "in-kind" ecological goals by encouraging more in-channel work and less riparian corridor work, and 3) Ensuring that impact and mitigation credits off-set to result in "no-net loss."

A shared approach by the Missouri and Illinois stream teams was to use "activity-based" classification systems in lieu of direct functional measurements to assess the overall ecological integrity of impacts and mitigation projects. "Activity based" means that each activity (e.g. an impact activity, such as clearing vegetation or installing a culvert) is given a credit value. These activities are ranked based on two parameters: the number of functions impacted, and the spatial scale/overall physical condition (see Figure 1 below). Rather than measuring the actual functional outcome of impact activities, the Stream Assessment Teams used secondary scientific reports to get an overall sense of "expected" outcomes from different activities. This approach is "useful" to Section 404 regulators because it enables an overall assessment of stream crediting to happen by anyone in a very short time period (e.g. less than an hour). Neither Illinois nor Missouri had a formal method for determining the "net adverse impact" or "net benefit" of activities.

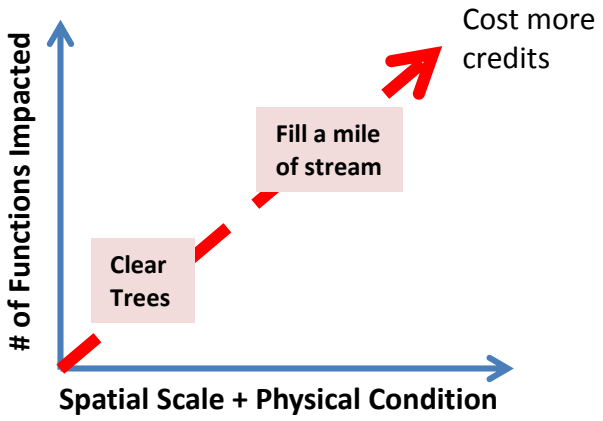

Figure 1. Schematic of the ranking of the "net degradation" caused by impact activities.

The principle challenge in making this method accepted statewide is that the measurement protocol needed to reflect the working priorities and conditions of each agency that shared in the methods creation (cf. Timmerman and Berg 1997). Thus, the predominant modifications made by the Missouri team (of the Charleston, SC stream assessment protocol) and the Illinois team (of the

[2] All research participants have been assigned pseudonyms to ensure anonymity

2007 Missouri stream assessment protocol) were to include state-recognized, legally-defensible classifications, examples of activities (impact and mitigation) that are common and accepted by state and federal agencies in each state, incorporate "user notes" and language modification to encourage more consistent and transparent use of the method, and to do so by making the method direct more desirable ecological outcomes (i.e. encourage "in-kind" work by decreasing the value of riparian buffers and increasing the credit value of in-channel restoration). Therefore, impacts and mitigation activities are considered "commensurate" by virtue of how well they meet the pre-existing working conditions of Section 404 regulatory agencies.

Therefore, ecological and geomorphic information is constrained because a) regulators resist requiring field measurements when assessing the impact and benefit of mitigation activities, b) regulators cannot require applicants to do something that exists beyond their legal authority, and c) regulators are not the only ones reviewing credit calculations. A reorganization of agency priorities is necessary to enable the inclusion of more scientific principles and methodologies that take more time, require more training, and are more site-specific.

In conclusion, at this point, the Illinois stream mitigation method is not a functional assessment protocol. Multiple things would need to occur to make this method "more functional." However, both the Illinois and Missouri methods are "living documents" and will undergo future changes. Changes will be made in response to the finalization of the Environmental Protection Agency's 2015 Waters Rule (which defines the legal scope of Section 404), as Corps districts progressively require more in-channel mitigation, and as the Illinois and Missouri stream assessment teams develop new consensuses over what types of activities are more or less commensurate with one another.

Principle findings to Question 2:

How do mitigation bankers decide on the location, size, and type of bank that they build?

There are two kinds of compensatory stream mitigation: in-channel work and riparian corridor tree plantings. While this report focuses on stream mitigation *banking* (which in Illinois consists 100% of riparian tree plantings), PRM stream work in Illinois consists of *both* in-channel work and riparian corridor tree plantings. Site selection, mitigation planning, and mitigation management and monitoring of stream mitigation banks in Illinois therefore resembles wetland mitigation rather than conventional stream mitigation projects.

Site Selection and Planning: Site selection and mitigation planning/goal setting are interrelated. Often mitigation practitioners have existing skills, ideals, or methods in mind when selecting a potential mitigation site. As one mitigation banker explained (who operates 2/3rd of the banks that sell stream credits in Illinois as of February 2016): "Typically I have three wetland types that I target…forested, emergent, and riparian corridor…Things that other people are doing are scrub-shrub habitat, or wet meadow, or wet prairie. But I don't do any of those" (Author interview, 05/28/2015). Because mitigation bankers utilize riparian corridor restoration and enhancement techniques (i.e. tree plantings), bank goals focus on hydrologic connectivity and the intended benefit to stream quality from converting farmland to a floodplain wetland. For example,

one mitigation bank selling stream credits has goals to "reduce nutrient loading and increase nutrient fixation" and "maintain and enhance hydrologic functions and values."

From the Corps' perspective, these are positive ecological restoration goals because these wetland types are types that have been historically lost in the Mississippi bottomland region and southern Illinois over the past century and a half. Joined with both the regulatory requirements and site selected, the banker and regulator formulate a site-specific plan. This plan culminates in the publication of a "Mitigation Banking Instrument." The banking instrument "is the administrative document which establishes ecological criteria for the [Corps] approval of bank credits, the financial sureties the banker must provide against site failure, the kind of ecological monitoring which is required, and other administrative details" (Robertson 2004, p. 363).

Riparian corridor stream mitigation bank sites are selected according to two overarching priorities: i) regulatory requirements and crediting values, and ii) mitigation practitioners' ecological goals and costs. Regulatory requirements vary district-to-district, but most requirements focus on site land use/land cover history, the presence/absence of native or non-native vegetation, and the existing tree/vegetation cover relative to the expected pre-disturbance "climax community." In the St. Louis Corps district portion of southern Illinois, mitigation bankers can only earn credits on sites that are "prior converted wetlands." Prior converted means that the land was "improved" (i.e. drained, cleared, etc.) prior to December 23, 1985 and continues to be used for agricultural purposes, among other criteria. For comparison, in Iowa (almost entirely within the Rock Island Corps district), in addition to being classified as prior converted, land must also have existing and maintained water management structures on site (e.g. tile drainage structures) to be eligible as a compensation site (Personal communication).

Regulators are not only concerned with land classifications, but also have ecological goals in mind. Therefore, when working with a mitigation banker during instrument development, they will insist or require that sites have appropriate site conditions. For riparian corridor plantings, this includes appropriate vegetation, soil, hydrology, and stream stability. Regulators first require that applicants have selected a site that is predominantly non-native vegetation. Without non-native vegetation (e.g. reed canary grass), sites are considered "already functioning" and therefore are not considered of low value to deserve crediting for improvements. If a banker selects a site that meets "Enhancement" (<50% planting) rather than "Creation" (>50% tree planting) criteria, they will need more land to increase their overall credit bank.

Mitigation bankers and regulators initially rely on soil maps when determining if a site is worth visiting to assess. However, because soil maps (e.g. county soil surveys) are at broader scale than is required for site-specific assessments, the predicted soil classification does not always match the observed soil cores. As one banker put it: "You gotta come to these sites, there's no way around it…I don't know how you just go off of the books…If you come out [ready to buy land or do work] and there isn't hydric soils [*sic*] then what do you do? You've gotta find [hydric soil]" (Author interview, 05/28/2015).

When interpreting soil hydrology, mitigation bankers do so with their overall priorities and goals in mind. Depending on the wetland type that bankers plant, their goal is to restore and jumpstart "old growth" forests with minimal ongoing mitigation management. To this end, for

one mitigation banker, the key interpretive factors are the presence of hydric soils, gently sloping land, and a stable stream with a degraded riparian corridor. Stream stability is determined by visually interpreting streambank features and considering stream sinuosity. A "stable" stream is desirable because it is an indication that the riparian tree plantings will last and reach mature heights. Furthermore, sites with minimal slopes and appropriate hydrology for their target plants will require less extensive ongoing maintenance and management.

The most significant hurdle to site selection is not necessarily identifying hydric conditions, but a parcel of land that meets these criteria and is also either for sale or willing to be sold or leased. Cost of land is an issue, but in many cases ideal property is owned by a landowner unwilling to part with agricultural land--even if it is not highly productive. In one instance a mitigation banker identified desirable land for mitigation along a river that sat between two parcels of a park preserve. This was an ideal scenario because the banker could potentially leave the mitigation bank to the park preserve to maintain and keep out of production in perpetuity. However, the banker was concerned that the landowner would not part with the land. The banker expressed intrigue into why this farmer continued to plant in what appeared to be wet "unproductive fields."

The size of mitigation banking sites is typically larger than PRM wetland and stream mitigation projects. This is because mitigation banks are designed with the expressed purpose of offsetting multiple future impact activities, rather than single projects. Bank size depends on a combination of: a) total land area acquired, b) the potential number of credits that may be needed in the future, c) the type of credits that a banker targets (e.g. emergent wetland versus bottomland hardwood forest), and d) administrative components (e.g. level of monitoring, level of site protection). The three mitigation banks that sell stream credits in Illinois are 82.75, 62.08, and 79.04 acres in total area (RIBITS).

Principle Findings to Question 3:

How do regulators decide the number of stream credits lost or gained while using the ISMM?

Impact Site Credit Determination: Section 404 permit applications are reviewed using a three-level mitigation hierarchy based on the 1978 National Environmental Policy Act: avoid, minimize, and compensate impacts (Hough and Robertson 2009). Avoidance means to not take proposed actions that result in degradation of surface water quality. Minimization means to implement best-management or design practices that reduce the overall degradation caused by a development activity. Compensation, the main focus of this research project, means to replace lost or damaged resources with a substitute aquatic resource (Hough and Robertson 2009). Not all Section 404 permits require compensation. However, when an activity is deemed to require compensation, it is only determined after first considering avoidance and minimization possibilities. While very few Section 404 permits are denied by the Corps or vetoed by the Environmental Protection Agency (<1% nationwide), many are rescinded during the application process because applicants may find avoidance, minimization, and compensation requirements to be too costly and/or time consuming (Personal communication).

A key constraint on Section 404 permit review is both time and resources (Power 1977; Womble and Doyle 2012). A way to mitigate this constraint is to meet directly with applicants

and clearly explain regulatory expectations and requirements. Prior to such meetings--called pre-application meetings--Corps regulators often do a "test run" of the total expected credits from what they know about a project. Corps managers typically use photographs and descriptions included in a pre-project wetland and stream delineation report, Google Earth ™, soil maps, and other data, to calculate an estimated total number of stream credits required for the proposed impact project with the ISMM. During the pre-application meeting the Corps regulator will then walk through the potential mitigation methods (e.g. channel reconstruction, riparian tree plantings, etc.) that will generate sufficient credits to meet compensation requirements. The purpose of this pre-application meeting and the pre-site credit estimation is to further streamline the permit process by walking applicants through their requirements and what flexibility is possible.

As findings to Question 1 describes above, the ISMM is designed to be a rapid-assessment protocol that does not require any background or technical experience in ecological or geomorphic sciences. However, while the ISMM is designed to be easily and consistently applied, there is no set method for determining its constituent parts. Rather than being a prescriptive method, it is mainly formal. This is most obvious in the determination of Stream Type and Existing Condition of a stream proposed to be impacted. For example, when determining the "adverse impact" of a Section 404 application, Corps regulators and/or applicants must determine the net impact in stream credits using the Adverse Impact Worksheet built into the ISMM. The Adverse Impact Worksheet contains six impact factors that, when accumulated, are intended to represent the total adverse functional impact of an adverse impact activity. Each regulator uses their best-professional judgment to determine each of the six adverse impact factors. These six are: i) Stream Type impacted, ii) Priority Water impacted, iii) Existing Condition, iv) Impact Duration, v) Activity, and vi) Cumulative Impact (a linear impact factor).

Determination of Stream Type Impacted: While designed to be an objectively interpreted classification, in practice, this classification is heavily determined by the best-professional judgement of each Corps regulator/applicant. Stream Type is broken into three classifications in the 2010 ISMM: a) Ephemeral/Intermittent (0.1 stream credits per impact reach), b) Intermittent with Seasonal Pools (0.4 credits), c) Perennial (0.8 credits). These classifications are defined along hydrological lines. Perennial streams are groundwater fed streams that, in a normal hydrological year, sustain base flow. Intermittent Streams with Seasonal Pools, by contrast, are only connected to groundwater in pools, and therefore may not have complete flow in a normal hydrological year. Ephemeral/Intermittent streams, by contrast, only have flow resulting from precipitation events, and therefore may be dry for most of the year or only have flowing water immediately following rain events. The implication is that, depending on the time of year, and if the Corps regulator/applicant only looks at the amount of water in the channel, they can come up with different conclusions over whether or not a stream is one classification or another.

This problem was abundantly clear during a site visit to assess the existing stream quality of a stream proposed to be partially filled and re-located. During this visit the Corps regulator, the applicant, and the engineering firm that was hired to conduct the PRM mitigation work and who also published a wetland and stream delineation assessment, collectively "assessed" an impact stream. The Corps regulator relied on the applicant and engineering firm to determine the potential boundaries of the proposed impact. Prior to this site visit, the Corps regulator had calculated a "draft" assessment of credits based on a site evaluation from the impact assessment included in

the Section 404 application material and desktop methods--such as Google Earth™ or USGS StreamStats. In the field, the Corps regulator was less certain of his initial calculations. The regulator considered the impact stream to be "Intermittent" based on the fact that this waterbody has a relatively small watershed area, and therefore based on surface water alone, has a low discharge.

Walking the length of the stream with the engineering firm, the Corps regulator relied predominantly on four pieces of evidence to determine the Stream Type: i) the amount of water in the stream given recent precipitation events, ii) the engineers report that during a "dry period" the stream still had flowing water, iii) identification of aquatic species, and iv) evidence of "high" flow events, such as bent vegetation or debris encapsulating vegetation. At the time of the visit, on June 25, 2015, the stream had multiple pools with fish and other aquatic species. The Corps regulator also looked at evidence of high-flows. Feeling comfortable that he had identified a well-defined "ordinary high water mark," he then began to question his initial "Intermittent" classification.

This new evidence, coupled with the engineers' remarks that the water body was also flowing in a "relatively dry" April, made the Corps regulator more willing to switch from an Intermittent to Perennial classification. In his own words out loud while walking the stream: "I would have a hard time not calling it perennial…but this is similar to what [the engineer] saw here in April…but when was the last rainfall?...if this site had water in April--and it hadn't rained--where is the water coming from?" (Author interview, 06/25/2015)

After leaving the site, one of the applicants informed the student researcher that there was a "natural groundwater spring" upstream of the impact reach. Once the student researcher informed the regulator that the applicant informed him of this fact the regulator was even more convinced that this stream is a Perennial waterbody. Evidence of a year-round groundwater source, by the hydrological definition of Stream Types, would be enough to tip the Corp regulators' opinion that this stream was Perennial and therefore was worth 0.8 Stream Type credits. <u>The definition of a Stream Type therefore can be a serendipitous decision that depends on what questions and evidence the regulator requests, the time of year and condition of the site during the assessment, and what evidence is put forward by others involved in permitting the activity</u>.

<u>*Determination of Priority Water Impacted:*</u> Priority Water determination is much more straightforward than Stream Type determination. Priority Water is classified into Primary, Secondary, and Tertiary; ranked from more to less biological significance. Each classification is based on pre-existing ecological, water quality, and habitat rating systems and databases of relevant resource agencies involved in Section 404 permitting. For example, if a waterbody is listed on the Illinois EPA 303 (d) Impaired Water List for 'aquatic life use of indigenous aquatic life use' it is considered a Secondary Water (0.4 stream credits per reach). By contrast, Primary waters are those that are ranked as "Biologically Significant Streams" (IDNR), "Significant Mussel Beds," or other state and national biological rating lists. Tertiary waters "include all other freshwater systems not ranked as primary or secondary" (ISMM 2010, p. 5).

<u>*Determination of Existing Condition of an Impacted Waterway:*</u> Other than Stream Type, Existing Condition is perhaps the most interpretive and loosely applied adverse impact category.

Existing Condition is separated into three classifications: "Fully Functional" (1.2 credits), "Moderately Functional" (0.6 credits) and "Functionally Impaired" (0.2 credits). According to the developers of the Missouri stream mitigation method, this impact factor is designed such that all streams should be assumed to be "Moderately Functional" unless it can be otherwise demonstrated with evidence supporting "Fully" or "Functionally Impaired" classification. In practice, not all assessors start from this assumption. Only in later versions (approved 2013 Missouri method; draft and in-development 2013 Illinois method) is this assumption made clearer in the document directions with the addition of "User Notes."

The Existing Condition factor is the most direct example of the way in which the Illinois (and Missouri) stream mitigation methods are rooted in physically-based assumptions of aquatic integrity and overall ecological function. Furthermore, this factor is rooted in the assumption that streams that have no direct sign of human modification (e.g. have not been channelized) are more functional than streams that do have human modifications. For example, a stream reach is "Fully Functional" if:

> it has all of the following characteristics: Has not been channelized, levied, impounded, or artificially constricted. Is not listed on the Illinois Section 303 (d) Impaired Waters List. Has no stream impact (see Activities for a list of impacts) within 0.5 mile upstream or downstream of the proposed stream impact or mitigation site. And has one of the following characteristics: Scores A or B for either Diversity or Integrity (Illinois Biological Stream Rating System). Has riparian buffer of deep-rooted native vegetation that is greater than 50 feet wide on both sides of the stream (ISMM 2010, pp. 5-6).

Corps regulators/credit assessors must therefore confidently identify whether or not the current stream condition exhibits historical evidence of human modification. Determination of Existing Condition is based primarily in physical-condition clues (e.g. are there culverts nearby? Is there visible bank erosion and sedimentation?) that are not necessarily representative of overall ecological or geomorphic function. Implicit in this assessment is the notion that an actively eroding and depositing stream is "improperly functioning."

Thus, in practice, determination of Existing Condition is based on visual, physical, and aesthetic clues (e.g. any evidence of human modification or human activities in the stream channel?). In this case, prior to the site visit, the Corps regulator had considered this stream to possibly be "moderately" or "poorly" [functionally impaired] functioning. This was based on the assumption that there was no direct evidence of channelization (i.e. the stream has likely not directly been modified), but at the same time the stream reach is surrounded by human impacts. This particular stream reach sits in a narrow valley between a railroad embankment on one side and a coal ash fill to the other. The regulator therefore considered that, while the stream channel itself was not *directly* modified or manipulated in recent history, the construction of embankments and slopes likely alter the local hydrology and runoff in a way that introduces "external" instability into the stream system.

When the Corps regulator walked the stream, he was met with paradoxes and internal contradictions. While the stream channel itself was not manipulated, there were rock and concrete deposits that were only likely sourced from some upstream human modification. At the same time however, this waterbody was not listed as "Impaired" on any Illinois EPA Section 303 (d) database, had visual evidence of biological functionality (e.g. identification of multiple fish

species), and therefore the regulator felt this may be even be a fully functional waterbody. In the end, while simultaneously re-adjusting his assessment of Stream Type, the regulator indicated that: "If I did change anything I may change it to poorly functioning [functionally impaired]…but to be honest it's got pools and riffles and it's probably functioning…I need to read the [ISMM] again" (Author interview, 06/25/2015).

Determination of Impact Duration, Activity, and Cumulative Impact of Activity: Impact Duration, Impact Activity, and Cumulative Impact are relatively straightforward determinations in the ISMM. Impact Duration is simply the period of time in which impact activities occur. Temporary impacts (0.05) occur in less than 180 days, Short term impacts (0.1) remain evident after 180 days and will not exist after two years, and Permanent impacts (0.3) will be greater than two years. There are nine Impact Activities: Clearing vegetation (0.05), Utility crossing/bridge footing (0.15), Below grade culvert (0.3), Armor (0.5), Detention (0.75), Morphological disturbance (1.5), Impoundment (2.0), Pipe (2.2), and Fill (2.5). The Missouri team found that in some instances applicants were incorrectly identifying activities, and therefore have added clarifying user notes to the 2013 Missouri stream mitigation method. Cumulative impact is the product of the total linear footage of stream impact per reach (as measured through the channel center line) and a cumulative impact factor of 0.0003.

Riparian Corridor Mitigation Credit Determination: Once a riparian corridor has been monitored, it is eligible to earn credits. For riparian corridor there are two methods in existence--the former way of doing it (area and length based) and the new way (riparian corridor crediting protocol). Prior to the 2008 Rule, the primary metric used to commensurate impact and mitigation activities were either area or length measurements. For example, one mitigation banker in southern Illinois uses 200 feet x 100 feet (20,000 ft^2) blocks as a "riparian credit" for two of their mitigation banking sites. Thus, if a developer impacts 40,000 ft^2 of riparian corridor, and they purchase stream credits from this bank, they would be purchasing 2 credits. Riparian credits are inter-changeable with "stream credits." Likewise, if a developer impacted 10,000 ft^2 of channel area, they could offset this by purchasing 0.5 riparian credits. This number can also be increased by adding a multiplier for being "out of kind." Hence, developers may be required to purchase as many as 1 credit (2:1 mitigation ratio) or possibly 1.5 credits (3:1 mitigation ratio) to offset their in-channel impact with riparian corridor credits purchased from this mitigation bank. Credit price is determined by the mitigation banker, and the Corps cannot request or require higher or lower credit prices.

More recently there has been a turn toward standardizing credit determination using the ISMM. Riparian credit determination in the ISMM is based on more than only total area planted and the removal of non-native species. Looking at the Riparian Corridor Worksheet (see Figure 2 in Appendix), there are three classifications of riparian corridor plantings: Creation (51-100% planting), Enhancement (10-50% planting), and Preservation (<10% planting). Creation generates the most credits per area of buffer width, with fewer credits generated for Enhancement and Preservation, respectively.

In addition to area and plant-survival-based crediting, riparian credits are also generated based on the type of waterbody that is chosen (0.05, 0.2, or 0.4 credits), whether or not buffers are created on both sides of the stream, the type of monitoring selected (0.1, 0.2, and 0.25

credits), the kind of property control that a site is placed under in perpetuity (e.g. deed restriction (0.1 credits) versus conservation easement (0.4 credits), and whether or not the mitigation work was implemented prior to, concurrent, or after impact activities. Therefore, from this new approach, riparian credits are determined on a case-by-case basis using formal requirements (the ISMM) that provide a framework/formula for calculating the total number of credits generated for riparian compensatory mitigation work.

Principle findings to Question 4:

Are the ecological functions lost at adverse impact sites off-set by mitigation at a stream mitigation bank? If so, over what temporal and spatial scales? If not, why not?

This study compares the geomorphic, hydrologic, water quality, and riparian vegetation characteristic of a mitigation banking site and the impact sites that it is intended to replace. The two primary impact activities covered by this study are 1) clearing of riparian corridor vegetation (see figure 3 in appendix for example), and 2) installation of in-channel culverts for access roads (see figure 4 in appendix for example). The mitigation activity is the enhancement (10-50% planting) and creation (51-100% planting) of floodplain forest. Impact activities occurred in and around August 2009. Riparian corridor credits at the mitigation banking site were approved for release (i.e. sale) by October 2008.

Because the impacts included in-channel impacts (i.e. culverts) and the mitigation only consisted of riparian corridor tree plantings, **the mitigation bank does not replace the ecological functions lost or damaged from impact activities**. In addition to not replacing in-channel damages, the mitigation work is conducted on a stream with much higher discharge. This study uses drainage area as a proxy for discharge. Geomorphologists have long studied the relationship between channel discharge and upstream drainage area (Knighton 1998). By analyzing data collected globally, geomorphologists and hydrologists show that as drainage area increases by orders of magnitude, so does channel discharge (Knighton 1998). Table 2 summarizes the upstream drainage area of the impact sites and the mitigation site. The mitigation site has a drainage area that is at least an order of magnitude larger than the drainage area of the impact sites. Thus, the mitigation site stream discharge is at least an order of magnitude greater than the discharge of the impact site streams.

Site	Impact/Compensation Activity	Drainage Area (km^2)
Impact 1	Vegetation clearance	14.245
Impact 2	Vegetation clearance	0.129
Impact 3	Vegetation clearance and culvert for access road	0.733
Impact 4	Vegetation clearance and culvert for access road	1.158
Mitigation bank	Riparian corridor planting	450.66

Table 2. Impact site upstream drainage areas (km^2).

Channel discharge is a "master variable" for stream ecology (cf. Doyle et al. 2005). Channels with discharge differences over many orders of magnitude perform markedly different ecological functions (cf. Poole 2002; Doyle et al. 2005). **Thus, in addition to the fact that the mitigation bank does not provide in-channel work, the stream itself probably provides stream functions differently than the impact sites.** However, there is a chance that the mitigation work provides unintended benefits to the in-channel area. The findings presented below are interpreted with this question in mind.

Unintended benefits?

In total, the permitted Section 404 activity that was offset by the purchase of credits from the mitigation banking site impacted a total of 48 ephemeral, intermittent and perennial streams and rivers, as well as ephemeral water features. Of these 48, 13 stream impacts required compensation in the form of mitigation. None of these 13 are classified as perennial by the permit documentation. This study focuses on four of these streams. The impacted streams surveyed in this study were largely relatively narrow, headwater channels that varied in sediment composition. Figures 3 and 4 in the appendix are photograph examples of both impact activities. Although the impact and mitigation site likely perform different stream functions, and the mitigation site does not replace these functions, there is a potential that the mitigation site provides unintended benefits. To assess this, it was necessary to compare the sites across many biophysical characteristics.

All Sites: Overall Geology, Soils, Climate, and Land Use

The impact sites and mitigation banking site have differences in climate, geology, soils, and surrounding land use (Table 3). The impact sites occur in two different eco-regions: the Karstic Northern Ozarkian River Bluffs eco-region (impact site 1) and the Southern Illinoian Till Plain eco-region (impact sites 2-4). The Karstic Northern eco-region receives 101.6-114.3 centimeters of rain on average annually. The average annual January low temperature is -6.1°C and the average annual July high temperature is 32.8°C (Woods et al. 2000). While similar, the Southern Illinoian region has a larger precipitation range (99.06-114.3 centimeters), with slightly warmer winters (-8.3°C average annual January low) and slightly cooler summers (31.1°C average annual July high) than the Karstic Northern region. The mitigation banking site is also in the Southern Illinoian region, and hence has similar temperature and precipitation ranges as impact sites 2-4.

The impact sites occur on steeper slopes than the mitigation bank, but all sites have similar soil textures according to the Web Soil Survey. Only one impact site (#1) sits in a low valley. All others are in steep headwater locations. All impact sites except #1 are less than 1 km streamwise from the headwater tip of their respective stream channel. The mitigation banking site sits on a flat till plain and is surrounded by wetland soil, oak-hickory forest, and farmland. It also is located much lower in a much larger watershed than the impact sites. Thus, the impact sites and the mitigation bank site have different slopes and drainage areas, but similar surrounding land uses and soil textures.

Site	Eco-Region	Bedrock?	Soil	Slope	Land Use
Impact Site 1	Karstic Northern Ozarkian River Bluffs	Mixed alluvial-bedrock stream. Mississippian limestone, sandstone, and siltstone	Alfisols, inceptisols, entisols and mollisols (Sonsac flaggy silt loam, Tice silty clay loam, Wakeland silt loam)	18-35% North/West; 0-5% East/South	Oak-Hickory forest (N/W); Corn and Soy (E/S)
Impact Site 2	Karstic Northern Ozarkian River Bluffs eco-region and boundary of the So. Illinoian Till Plain eco-region	None at surface.	Alfisols on both sides of the stream (Ruma-Ursa silt loams)	18-35% both sides of stream.	Oak and hickory cleared for the impact. Upstream is an actively farmed wheat field.
Impact Site 3	Southern Illinoian Till Plain eco-region	None at surface.	Entisol on both sides of the stream (Wakeland silt loam)	5-18% both sides of stream.	Oak-Hickory mixed forest upstream. Surrounded by corn and soy.
Impact Site 4	Southern Illinoian Till Plain eco-region	None at surface.	Entisol (Wakeland silt loam) and Alfisols (Bunkum, Marine, and Homen silt loam soils)	5-18% both sides of stream.	Cow pasture immediately bounds the stream. Corn and soy on both sides of the pasture.
Mitigation Bank	Southern Illinoian Till Plain eco-region	None at surface.	Inceptisol (Belknap silt loam), and alfisol (Hurst silt loam, Colp silt loam)	0-5% both sides of stream.	Bounded on the west by a mixed Oak-Hickory and the east by active corn and soy farm.

Table 3. Overall comparison of impact and mitigation bank site geology and climate. Eco-region data collected source: Woods et al. (2000). Soil and slope data from Web Soil Survey (http://websoilsurvey.sc.egov.usda.gov/App/HomePage.htm; Last accessed June 2, 2016). Bedrock and land use data from personal site visits and speaking with landowners.

All Sites: Geomorphology, Water Quality, and Riparian Corridor Areas

The impact sites and mitigation banking site have considerably different cross-sectional shapes and variability. On the whole, the mitigation banking site is wider and deeper than the impact sites, and has less variability in bankfull width measures. The impact sites have similar variability in bankfull width and average channel depth variability (see table 4). These findings indicate that the impact sites and mitigation banking site perform different physical stream functions.

The average bankfull width of impact sites varied from 2.3 m (Site 2) to 6.2 m (Site 1). The coefficient of variability (CV) of bankfull width, a metric of variance, ranged from 0.22 (Site 3) to 0.50 (Site 2). The average depth across impact sites varied from 0.48 m (Site 2) to 0.88 m (Site 3). The average of the CV of depth of all cross-sections varied from 0.18 (Site 3) to 0.40 (Site 1). Based on the CV of cross-sectional dimensions, Site 1 has the greatest cross-sectional channel depth variability, while Site 2 has the greatest cross-sectional bankfull width variability. Site 1 is the widest channel, Site 2 is the narrowest and shallowest, and Site 3 is the deepest.

The banking site has a mean bankfull width of 18.3 m and an average channel depth of 2.6 m. Thus the banking site almost three times as wide as the widest impact site, and more than nine times the bankfull width of the narrowest impact site. The banking site is also almost three times as deep as the deepest impact site. Unlike the impact sites, the banking site has limited bankfull width variability (0.096) and limited average depth variability (0.086).

Site	**No. of cross sections**	**Mean Bankfull Width (m)**	**Bankfull Width CV**	**Average Mean Depth (m)**	**Average Mean Depth CV**
Impact 1	8	6.183	0.255643	0.400	0.403992
Impact 2	9	2.321	0.499827	0.300	0.325176
Impact 3	7	5.072	0.220863	0.880	0.177727
Impact 4	7	5.267	0.24869	0.569	0.225992
Bank	4	18.345	0.09572	2.590	0.086293

Table 4. Summary of cross-sectional measurements for all sites.

Longitudinal variability (i.e. ‘wiggliness’) and planform (sinuosity) measurements were taken at all sites. The impact sites have considerably different planform characteristics than the mitigation banking site. On the whole, the impact sites have greater longitudinal variability, but less planform variability. See figures 5-9 in the appendix for thalweg data.

All four impact sites have a variable thalweg. The wiggliness values from 17.9 (Site 4) to 31.2 (Site 1). Despite that Site 2 has more than double the channel gradient than Site 3, the two have similar longitudinal variability (20.7 and 20.9, respectively). Impact site channel gradient ranges from 2.5 % (Site 2) to 0.6 % (Site 1). Impact site sinuosity varies from 1.10 (Site 3) to 1.39

(Site 4). Based on these measurements, impact site 1 has the greatest thalweg variability, but impact site 4 has the greatest planform variability (sinuosity) of the four impact sites.

The mitigation banking site has much lower thalweg variability than all of the impact sites. The mitigation banking site also has a much lower channel gradient than most impact sites. Compared with the steepest impact site (#2), the mitigation banking site has approximately $\frac{1}{15}$ the channel gradient. While the mitigation banking site lacks downstream depth variability, it has the most varied channel planform. The mitigation banking site has a sinuosity of 1.5, while the highest impact site sinuosity is 1.39 (Site 4).

Site	Thalweg Wiggliness	No. of samples	Distance Sampled (m)	Channel Gradient (%)	Reach Sinuosity
Impact 1	31.2303381	97	238.3	0.610	1.22
Impact 2	20.65481213	35	67.6	2.507	1.11
Impact 3	20.91432064	67	71.4	1.154	1.10
Impact 4	17.94311383	79	98.6	1.191	1.39
Bank	2.264463649	15	82.5	0.172	1.5

Table 5. Summary of downstream depth measurements and site slope of all sites.

Channel bed sediment was collected at Sites 2, 3, 4, and the mitigation banking site. Both sediment size variability and phi sort were calculated. Although each site has silt loam soils, there is a wide variability in the relative proportions of gravel, sand, and silt/clay at each site (Table 6) Site 3 has the greatest sediment variability of the three impact sites sampled. Site 2 had an abundance of gravel, while sites 3 and 4 had more sand than any other size range.

Compared with the three impact sites measured, the mitigation banking site has less sediment variability. All impact site samples had gravel, sand, and silt/clay. No mitigation banking site sample contained gravel. Bed material at the mitigation banking site also has a narrower phi range than that at any impact site. The mitigation banking site phi range (0.75-0.95) reflects the dominance of silt/clay-sized particles in the mitigation banking site samples. By contrast, impact sites had phi ranges that varied by as much as 2 phi units (Site 3, 1.45-3.5), reflecting significant proportions of sand- and gravel-sized particles.

		Range			Average			
Impact Site	No. of samples	Percent sample Gravel	Percent sample Sand	Percent sample Silt/Clay	Percent sample Gravel	Percent sample Sand	Percent sample Silt/Clay	Phi Sort Range
2	6	32.5-63.3	34.2-58.2	2.3-9.3	51.65232	44.04901	4.298672	1.8-2.875
3	4	2.1-16.4	39.3-82.9	6.8-44.3	7.721798	66.67326	25.60494	1.45-3.5
5	6	7.0-62.6	36.1-76.4	1.0-30.7	36.15131	57.3752	6.473488	1.6-2.5

Table 6. Sediment variability among all sites. Gravel = 31.5 mm to 2.0 mm diameter; Sand = 1.4 mm to 630 micrometers; Silt/Clay = < 630 μm.

In a review of Illinois DOT wetland mitigation banking sites, Pociask and Matthews (2013) found that streams with smaller drainage areas had more frequent, but lower duration, over-bank flood events. Thus, in addition to differences in stream discharge, the impact sites and mitigation banking site most likely differ in the frequency and duration of overbank events. Because the connectivity of stream channels to the surrounding floodplain is critical for performing ecological functions (Ward et al. 1999; Freeman et al. 2007), differences in overbank events in turn has different impacts on ecological functions. The impact sites and mitigation banking site perform different ecological functions based on differences in stream hydrology and channel-riparian corridor connectivity.

The connectivity of the mitigation banking site and its floodplain was measured over a four-month period using a HOBO water level recorder (see figure 10). The mitigation banking site had one over-bank flow event between July 5 and November 5, 2015. This event lasted over 24 hours (approximately 28). June 2015 was one of the wettest months on record, and so it is likely that there were multiple other over-bank events in June too (http://mrcc.isws.illinois.edu/).

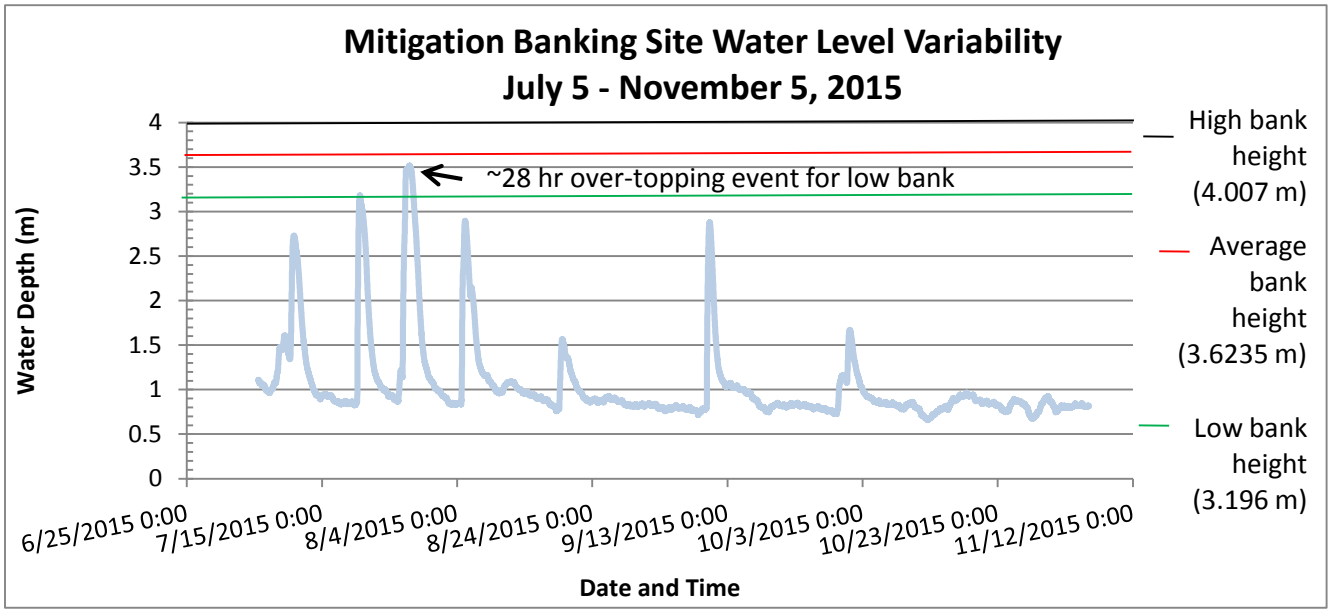

Figure 10. HOBO water level recorder data for stream mitigation banking site.

Water Quality Measurements

Water quality measurements are water-level dependent. Impact sites 2, 3, and 4 are ephemeral and intermittent streams that have limited water depth except during precipitation events. These sites had limited or insufficient water depth during multiple sampling periods. For these reasons, temperature, conductivity, and pH measurements were only taken at impact sites 1, 4, and the mitigation banking site (see table 7). Figures 11-19 in the appendix include graph representations of all measurements.

There are five main findings to emphasize. First, all pH measurements fall within the acceptable range established by the IEPA (IEPA 2004). Impact sites 1 and 4, and the mitigation

banking site, are not likely impaired for uses (e.g. recreation, aquatic life) by pH. Second, the impact sites tend to have a wider temperature range than the mitigation banking site. Impact site 1 had a temperature range of 1.3°C and 3.3°C during the two sampling periods. The temperature range at impact site 4 is 6.2°C. By contrast, the temperature range at the mitigation banking site was only 0.4°C and 1.4°C during the two sampling periods. The mitigation banking site thus has a more stable temperature than the impact sites. This difference likely reflects the differences in discharge because shallow water heats and cools faster than deep water. During sampling, the water depths at the impact sites was much less than the depth at the mitigation banking site.

Third, impact site 1 and the mitigation banking site have similar pH and specific conductivity variability. The pH of the two sites varied less than 0.5 pH units, while the specific conductivity varied less than 40 µS/cm. This finding can be explained by the fact that flowing surface waters generally will not vary much in pH and conductivity unless non-point or point sources of dissolved minerals alter background values.

Fourth, except for one measurement upstream of the mitigation banking site, the mitigation banking site stream had lower pH values than all measurements taken at the impact sites. These differences cannot be explained by temperature differences. In general, as temperature increases, pH decreases (Girard 2005). However, in this case, the mitigation banking site also has lower overall temperatures than the impact sites. Other possible explanations for differences in pH include the geology of a site (e.g. clay soils decrease pH), photosynthesis (e.g. increased photosynthesis from algal growth results in increase in pH), and acid mine drainage (Girard 2005).

The mitigation banking site stream has been listed as impaired by the IEPA for manganese, sulfates, nitrogen, pH, siltation, low dissolved oxygen, total dissolved solids, habitat alterations, and total suspended solids (IEPA 2004). The mitigation banking site watershed has a history of coal mining. As of 2004 there was only one permitted, active coal mine in the mitigation banking site watershed; but this mine is downstream of the reach surveyed herein (IEPA 2004). The lower pH levels in the mitigation banking site thus likely reflects a combination of algal growth, differences in soil pH with the impact sites, and discharge from surrounding land uses (e.g. even historic mine tailings).

Fifth, values of specific conductivity are similar at all sites, but impact site 4 had the highest specific conductivity. Conductivity is a measure of the concentration of charged atoms present in a water body and can be indicative of the salinity or concentration of total dissolved solids (e.g., toxic metal, H+ cations, etc.) (Girard 2005). Conductivity is also affected by temperature; warmer water has a higher conductivity (Girard 2005). Water bodies have a range of conductivity that reflects the overall concentration of total dissolved solids for a given water temperature and volume (Girard 2005).

For comparison to nearby streams with similar drainage areas, Rayse Creek near Waltonville, IL (227.9 km² drainage area; a disturbed watershed with agriculture), has a conductivity ranging from 200 to 1400 µS/cm. Lusk Creek near Eddyville, IL (111.1 km² drainage area; an undisturbed watershed with forests) has a conductivity ranging from 40 to 170 µS/cm (Groschen and King 2005). Both of these creeks were measured between 2001 and 2003 by the IEPA and the USGS (Groschen and King 2005). The difference in conductivity of these two waterbodies reflects the differences in land use in these two watersheds (Groschen and King 2005).

Undisturbed, forested watersheds in Illinois have lower conductivity values than disturbed, agricultural watersheds (Groschen and King 2005).

All measurements of specific conductivity (i.e. on both days) ranged between 508-555 µS/cm at site 1, 544-625 µS/cm at the mitigation banking site, and 459-839 µS/cm at site 4. Based on these findings, site 4 has a considerably higher concentration of total dissolved solids than site 1 and the mitigation banking site (e.g. 839 versus 553 µS/cm conductivity). Likewise, site 4 is likely more saline than site 1 and the mitigation banking site.

Site	**Air temp (°C)**	**Avg. water temp (° C)**	**Temp range (° C)**	**Avg. pH**	**pH range**	**Average Sp.Cond. (µS/cm)**	**Sp.Cond. range (µS/cm)**	**pH within IEPA standard?**
Site 1								
Day 1	29.4	21.08	20.8-22.1	8.149	8.103-8.191	539.79	508-544	Yes
Day 2	27.8	23.45	21.1-24.4	8.240	8.190-8.284	541.67	518-555	Yes
Site 4								
Day 1	26.7	25.53	23.2-29.4	8.060	7.624-8.639	717.5	459-839	Yes
Bank site								
Day 1	30.6	25.4	25.2-25.6	7.493	7.392-7.658	623.5	622-625	Yes
Day 2	23.9	20.53	19.7-21.1	7.386	7.333-7.406	563.43	544-583	Yes

Table 7. Summary of water quality measures across impact sites 1 and 4 and the mitigation banking site.

Riparian Vegetation Area

This study uses a Section 404 permit as its case. The Section 404 permit documents provide a record of the total impact to streams, wetlands, and riparian corridors from the permitted activity. The permit documents also describe the compensation that was required for the permitted impacts. In this case 8 acres of riparian corridor were counted as cleared and the applicant needed to offset their impacts by providing 7.91 acres of "functioning riparian corridor". Riparian corridor counts as all trees both within 25 feet of each stream bank as well as all trees within the 150 foot right of way corridor. Using Google Earth ™, the student researcher measured approximately 50 acres of forest cover--both riparian and non-riparian--that was cleared in total for this permitted activity. Therefore, the mitigation work did not replace the total acreage lost to the permitted activity. The Section 404 applicant was not required to compensate for more riparian corridor impacts because not all impacts occurred on a waterbody that was deemed jurisdictional under Section 404.

Summary: Unintended Benefits?

This study originally set out to determine whether or not the mitigation site off-set functions lost at impact sites. However, since the impact sites and mitigation banking site are out-of-kind, it should not be expected that mitigation results in no net loss of stream function. Therefore, this study instead focused on unintended benefits from out-of-kind mitigation. While stream functions were not measured, characteristics that derive from stream functions were. The primary conclusion that can be drawn is that the mitigation site stream does not necessarily provide unintended benefits that replace impacts caused at impact sites. Further research is needed to differentiate between the benefits derived from wetland mitigation, the benefits derived from riparian corridor mitigation, and the combined benefits from both on the mitigation banking site stream.

SUMMARY AND SUGGESTIONS

Main Findings:

1. *Impact Activities*

Overall, impact activities occurred in different watershed locations than where the mitigation activities were located. The average upstream watershed area of impacted streams was 3.47 km^2, while the upstream watershed area of the mitigation banking site is 450.76 km^2. Since watershed area is highly correlated with stream discharge, the impact and mitigation site have significantly different discharge volumes and variability. This has ecological implications. Flow variability--including duration and frequency--are some of the most important factors in ecological effectiveness and function of stream systems (Doyle et al. 2005). Therefore, the impact activities and the mitigation site likely perform different ecological functions.

2. *Net Loss of Functionality*

The impact sites and mitigation site serve different functions. This is primarily because a) the impact sites include in-channel impacts while the mitigation site does not, b) impacts and mitigation are in different watershed positions, and also c) impacts and mitigation streams have considerably different geomorphic characteristics and variability. There is therefore a net less in functionality by these impact activities.

3. *Impact Sites Are Geomorphically Diverse*

A primary assumption of the newly designed mitigation method is that credits are more valuable for diverse physical forms. However, as this study shows, the impacted reaches are more geomorphically varied than the mitigation site. Impact sites have more diverse channel forms (width, depth, and sediment).

4. *Impacts May Be Ongoing*

While the permit documents describe the impact activities (i.e. tree clearance and culvert placement for access roads) as temporary, the results from these activities may still continue to this day. Impact site 1 is a poignant example; just as recently as between March and June 2015 the stream undercut tree roots and the tree fell into the stream. The functional impacts of vegetation clearance may therefore be ongoing. The burden of managing stream changes rests with the landowners and not the applicant. Therefore, it is important to understand the temporal extent of Section 404 impacts to remove the responsibility of stream management from landowners.

Suggested Modifications/Changes to Regulation Practices

i) Continue to emphasize Avoidance and Minimization.
ii) Encourage more in-channel compensatory mitigation work
iii) Standardize impact site calculation and assessment: Rather than only requiring that a classification be met, guidance should suggest a specific methodology through which method users will systematically assess impact site stream type and existing condition. A possible solution would be to develop a flow chart-style methodology that directs users, step by step, to sequential data sources when making assessment decisions using the Illinois and Missouri stream mitigation methods.
iv) Incorporate more site-specific data to assess the actual function of the impact and mitigation site: Regulators should establish priority goals--short term and long term--and progressively incorporate more complex and robust analysis techniques. For example, four short term metrics that could be incorporated immediately are watershed area, channel slope, channel sinuosity, and sediment type. Using USGS StreamStats, regulators can require applicants to assess the drainage area and therefore relative discharge of the impact/mitigation site. Additionally, regulators can use Google Earth ™, Soil Survey data, and stream delineation reports to gain a cursory sense of the streams slope, sinuosity, and sediment type. All of this information will be necessary when beginning to make more process-based decisions regarding stream mitigation. Long-term metrics, by contrast, would be site-specific analysis of stream power--or the ability of the stream to transport, erode, and deposit different sized sediment and material, and channel change over time.
v) Impact duration is not simply a question of construction work: The Illinois and Missouri stream mitigation methods need to more fully acknowledge and assess the long-term impacts of development activities. Unless this is done in some way, the methods will continue to fail to replace lost aquatic functions.

Next Steps in Research

The following steps are necessary to continue this study in order to fully address the degree to which impacted and mitigated streams perform different functions.

1) Track the use and development of the Illinois and Missouri stream mitigation methods to further evaluate when and how methods can be made more standard and more ecologically robust.

2) Track the vegetation condition of the mitigation banking site beyond the monitoring period.
3) Conduct repeat channel geomorphology surveys to assess change over time.
4) Improve the spatial and temporal resolution of water quality measurements, including additional measurements of dissolved oxygen and turbidity.
5) Measure velocity to estimate discharge at all impact and mitigation sites to develop process-based data that can inform the overall stability of each stream.
6) Install water level recorders at impact sites to assess frequency and duration of overbank flow events.

4. STUDENT WORKERS

Alex W. Peimer, *PhD student (Dept. of Geography and GIScience)*--conducted all interviews, analysis, and field work with assistance from:

Courtney Reents, *MS student (Dept. of Geography and GIScience)*--assisted in channel surveys, water quality monitoring, water level recorder installation, and sediment collection
Bailey Morrison, *PhD student (Program in Ecology, Evolution and Conservation Biology)*--assisted in water level recorder installation
Dan Meyer, *PhD student (Dept. of Philosophy)*--assisted in channel surveys
Marisa Monier, *MSW student (Dept. of Social Work)--assisted in channel surveys*
Dora Cohen, *PhD student (Program in Ecology, Evolution and Conservation Biology)*--assisted in channel surveys and sediment collection
Sandy Wong, *PhD student (Dept. of Geography and GIScience)*--assisted in channel surveys and sediment collection
Rebecca Shakespeare, *PhD student (Dept. of Geography and GIScience)*--assisted in channel surveys and sediment collection

Work that will be published based on this funding:

1) Alex W. Peimer's Ph.D. dissertation: "Banking on Offsets: A Political Ecological and Eco-Geomorphic Analysis of Section 404 Compensatory Stream Mitigation Banking in Illinois, U.S.A."
2) Yet to be determined journal articles.

5. APPENDIX

Types of Changes	MO 06[2] to MO 07[1]	MO 07[1] to MO 13[1]	MO 07[1] to IL 09[2]	IL 09[2] to IL 10[1]	IL 10[1] to IL 13[2]
Add (e.g. add reference to a new rule)	11	52	32	15	43
Remove (e.g. remove example)	1	36	12	9	16
Modify Language (e.g. changing category names)	10	15	14	9	25
Group (e.g. grouping all cumulative impacts into one scale factor)	0	2	2	1	1
Ungroup (e.g. pulling out a specific morphologic change as its own category)	0	0	2	0	0
Change number (e.g. minimum buffer distances)	0	14	20	3	***
Total	22	119	82	37	102***

Table 1. Summary of changes made to successive versions of the Illinois and Missouri stream mitigation methods. ***Crediting worksheet numbers were changed between the 2010 ISMM and the draft 2013 ISMM. These changes consisted of direct copies of portions of the Riparian Corridor and In-Stream Work Worksheets from the 2013 MSMM.

A.3. RIPARIAN WORKSHEET

Priority Waters	Tertiary 0.05	Secondary 0.2	Primary 0.4	
Net Benefit (for each side of stream	Riparian Creation, Enhancement, Restoration, and Preservation Factors (select values from Table 1) (MBW = Minimum Buffer Width = 50')			
Supplemental Buffer Credit	Condition : MBW restored or protected on both streambanks To calculate:(Buffer Credit Stream Side A + Buffer Credit Stream Side B) / 2			
Monitoring	Level I 0.10	Level II 0.20	Level III 0.25	
Site Protection	Deed Restriction 0.1		Conservation Easement / Title Transfer 0.4	
Mitigation Construction Timing	Schedule 1 0		Schedule 2 0.1	Schedule 3 0.3
Temporal Lag (Years)	Over 20 -0.3	10 to 20 -0.2	5 to 10 -0.1	0 to 5 0
Mitigation Factor	In HUC 12 watershed or bank service Area: 1.0 Out of kind, HUC 12 watershed, or bank service Area: 0.5			

Factors		Stream Reach 1	Stream Reach 2	Stream Reach 3	Stream Reach 4	Stream Reach 5
Priority Area						
Buffer credit	Stream Side A					
	Stream Side B					
Supplemental Buffer Credit Met (Buffer on both sides)						
Monitoring						
Site Protection						
Mitigation Construction Timing						
Temporal Lag						
Sum Factors (M)=						
Linear Feet of Stream Buffer (LF)= (don't count each bank separately)						
Credits (C) =M X LF						
Mitigation Factor (MF) x (C)						
Total Credits Generated						

Total Riparian Restoration Credits Generated = _____

Figure 2. Riparian corridor credit worksheet (ISMM 2010).

Figure 3. Trees cleared at Site 1. Looking downstream (Photo by Alex W. Peimer).

Figure 4. Vegetation cleared and in-channel culvert installed at Site 3. Looking downstream (Photo by Alex W. Peimer).

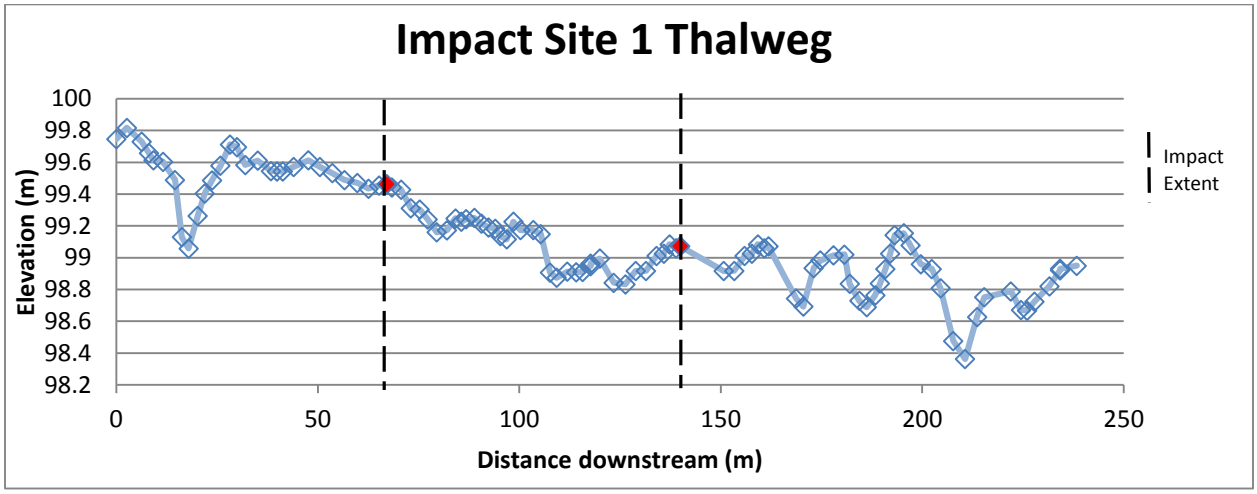

Figure 5. Impact site 1 thalweg.

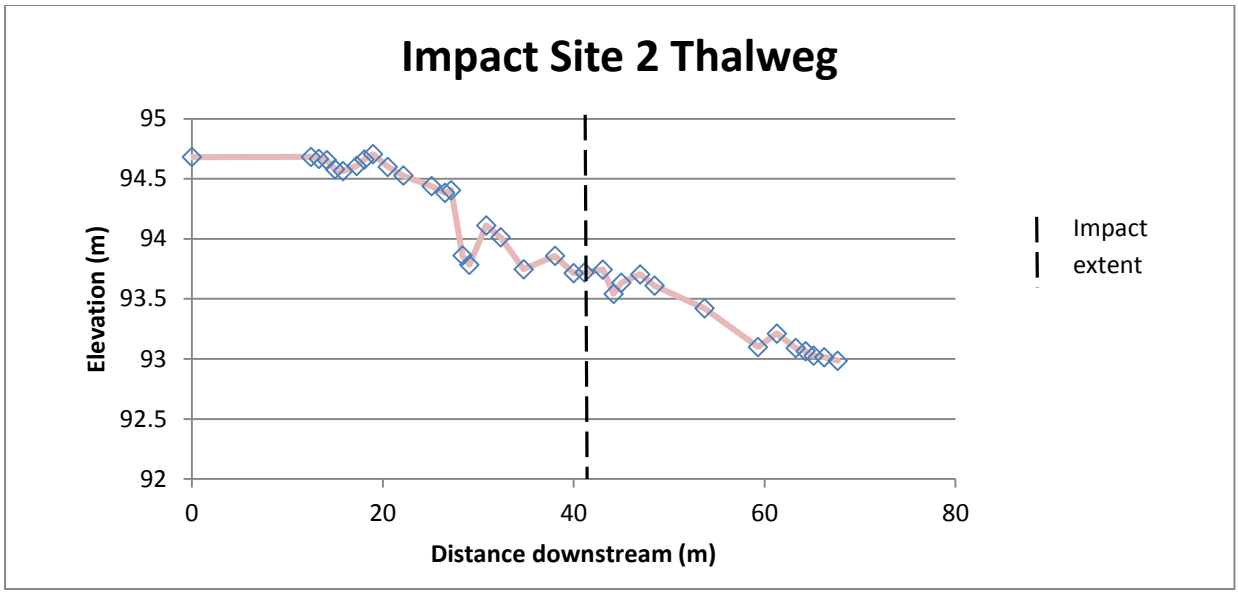

Figure 6. Impact site 2 thalweg.

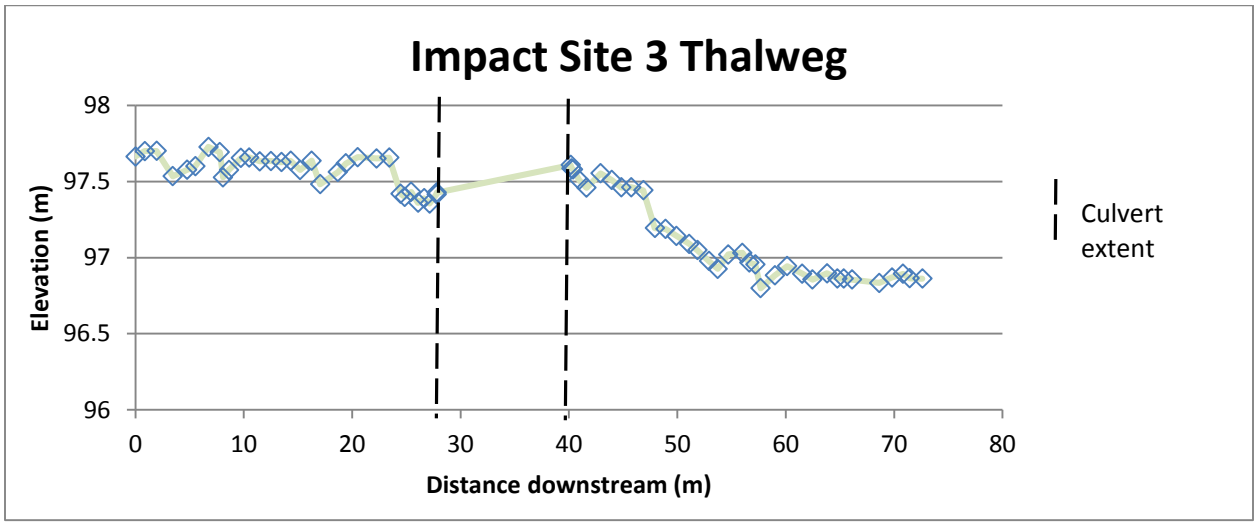

Figure 7. Impact site 3 thalweg.

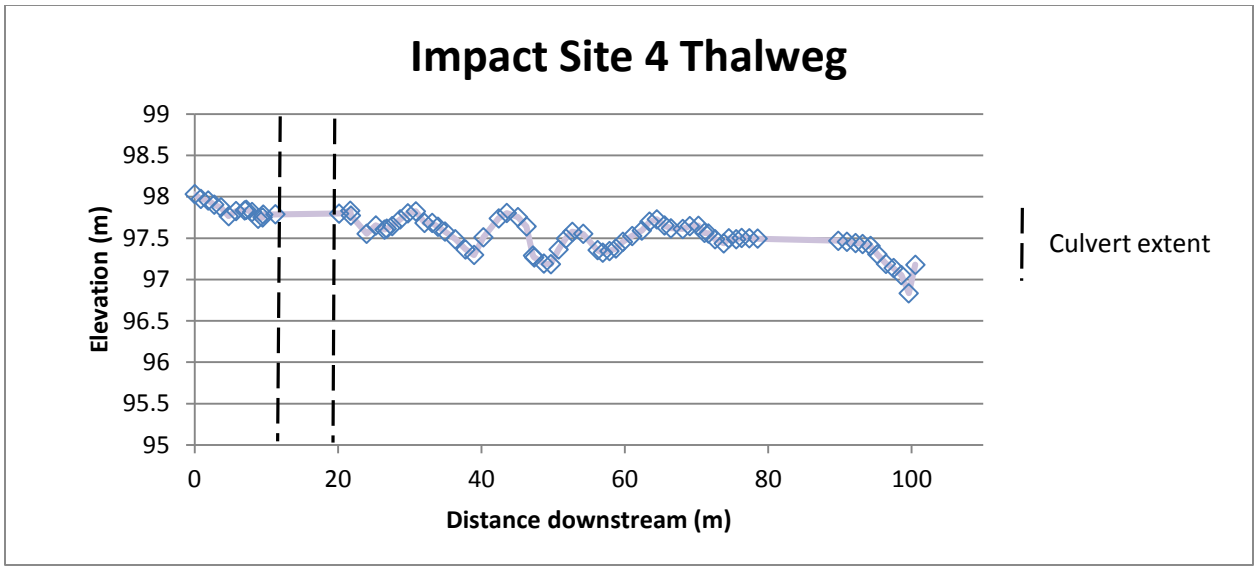

Figure 8. Impact site 4 thalweg.

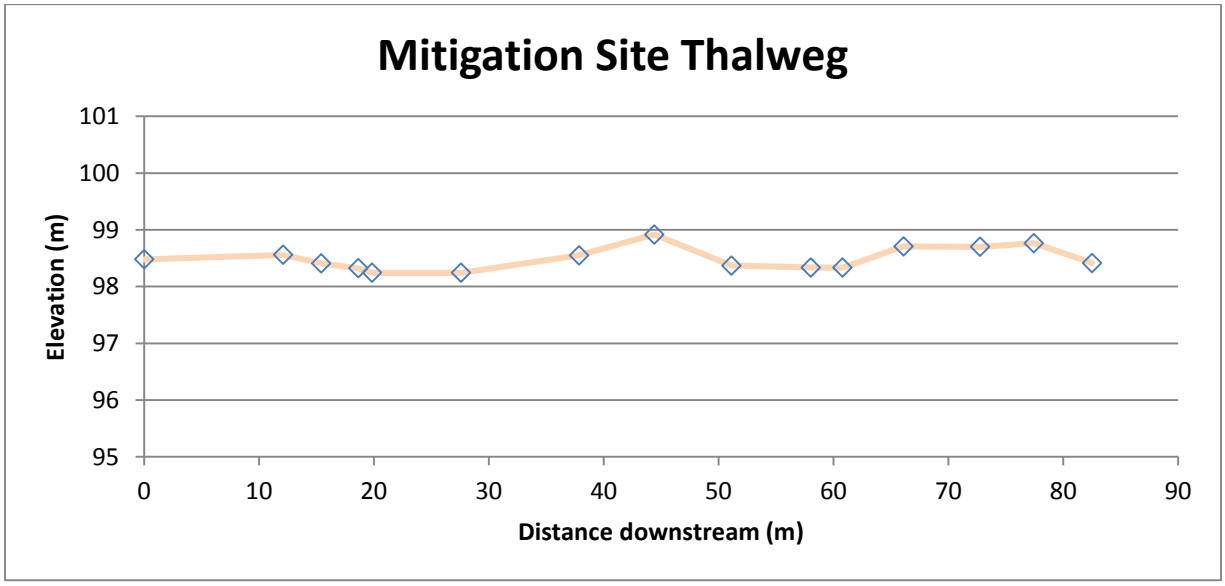

Figure 9. Mitigation site thalweg.

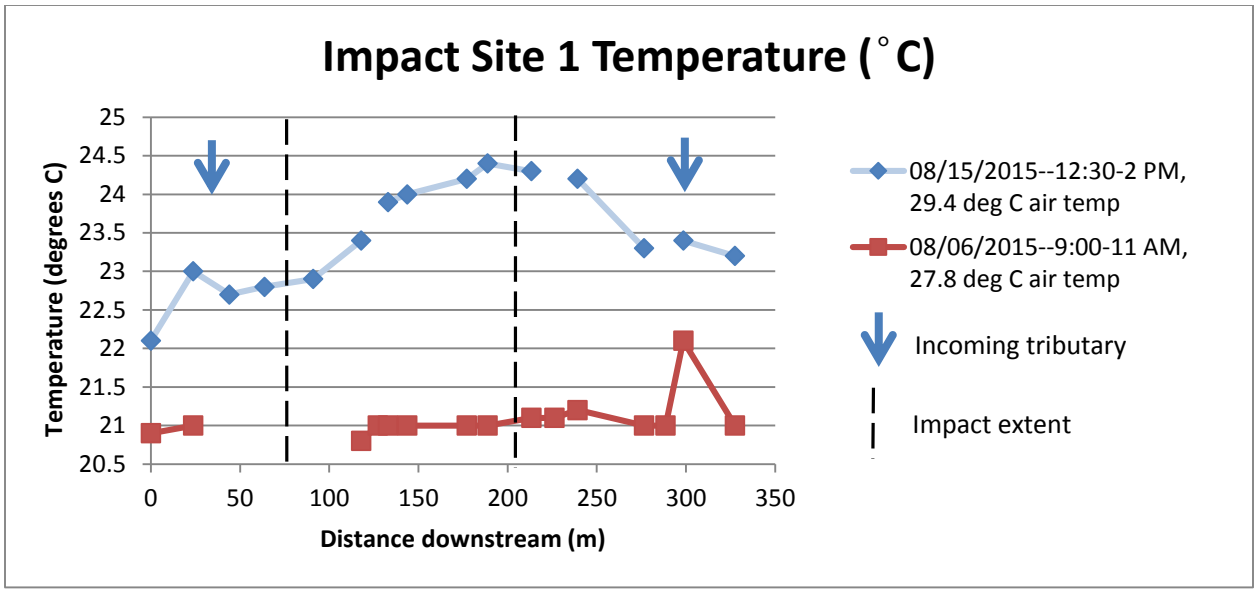

Figure 11. Impact site 1 temperature measurements.

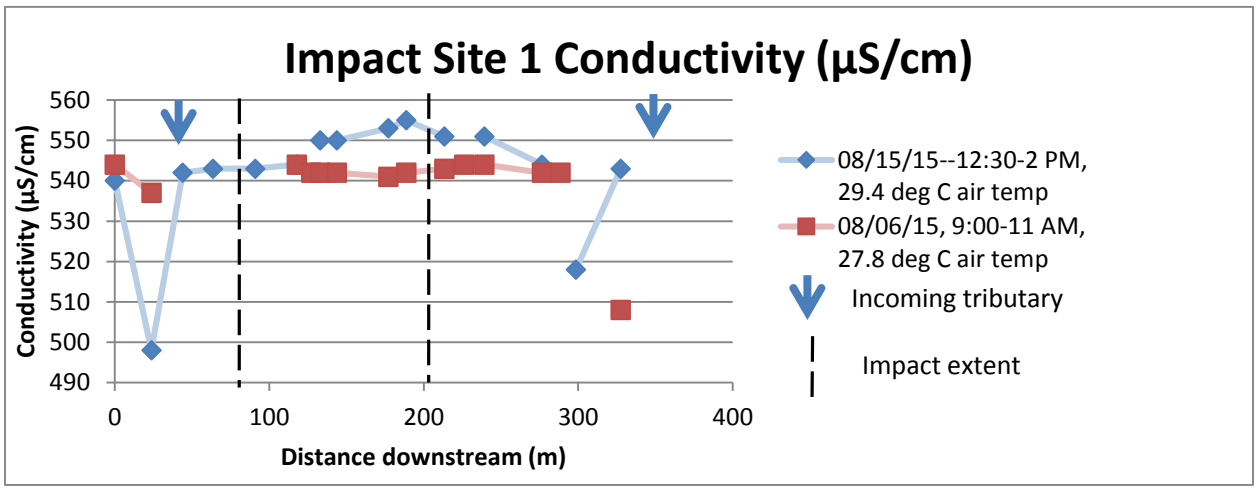

Figure 12. Impact site 1 conductivity measurements.

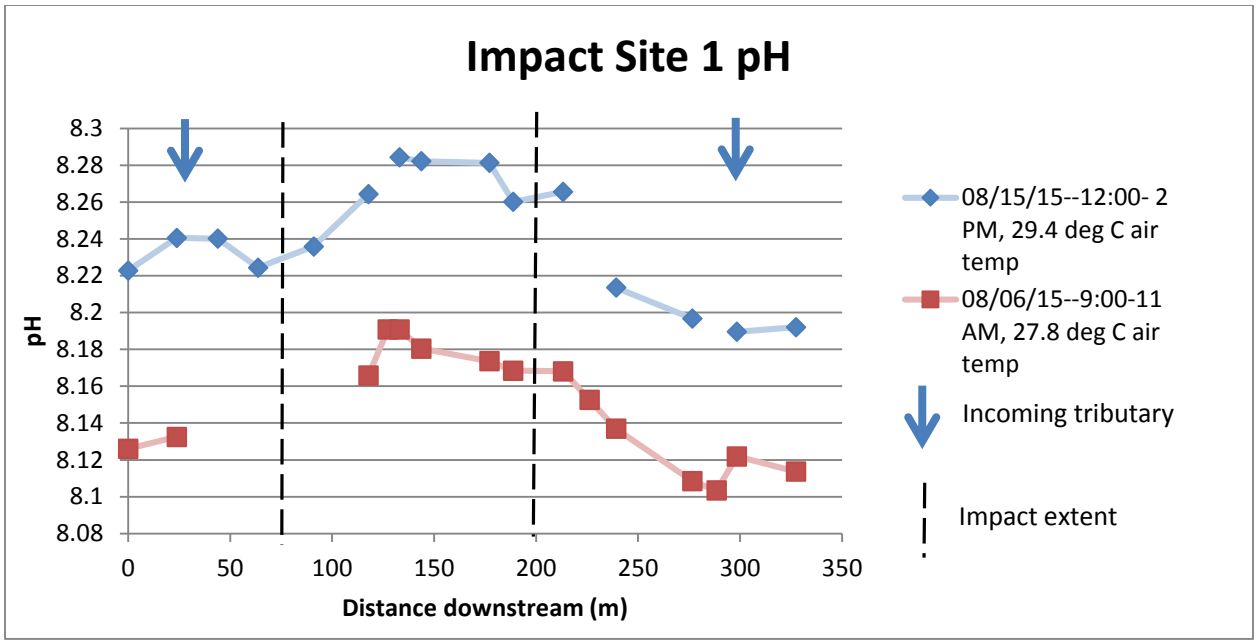

Figure 13. Impact site 1 pH measurements.

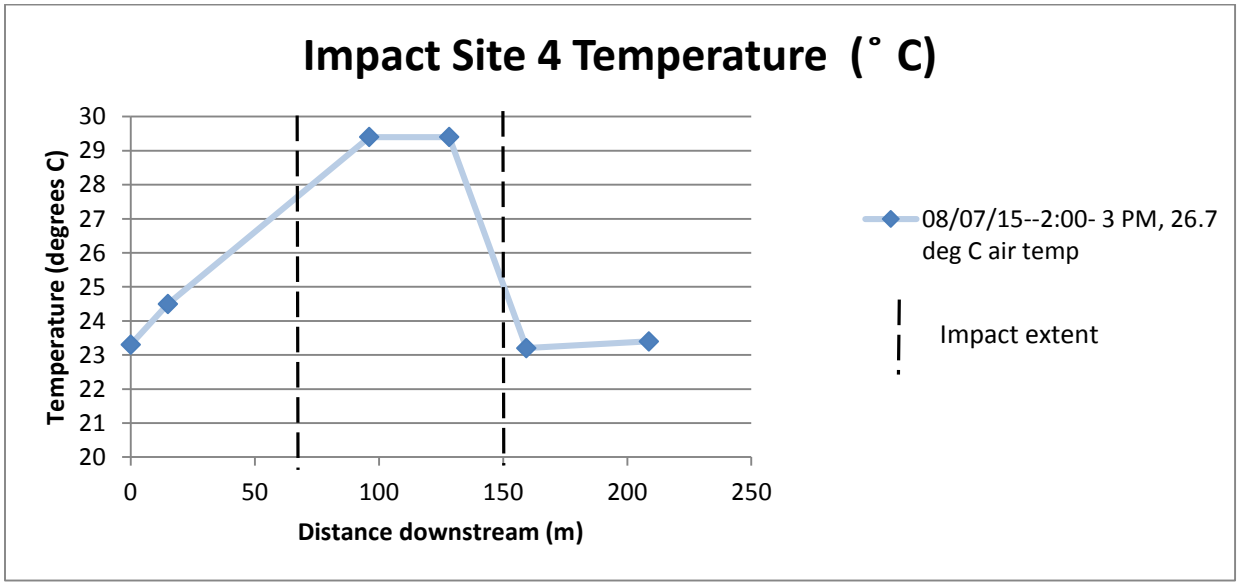

Figure 14. Impact site 4 temperature measurements.

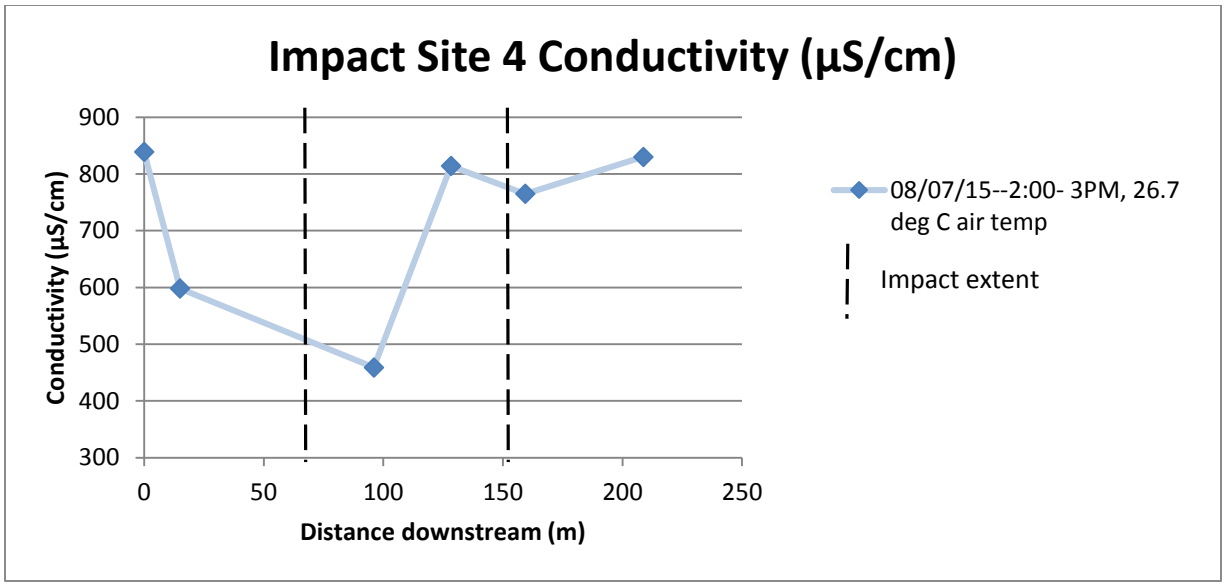

Figure 15. Impact site 4 conductivity measurements.

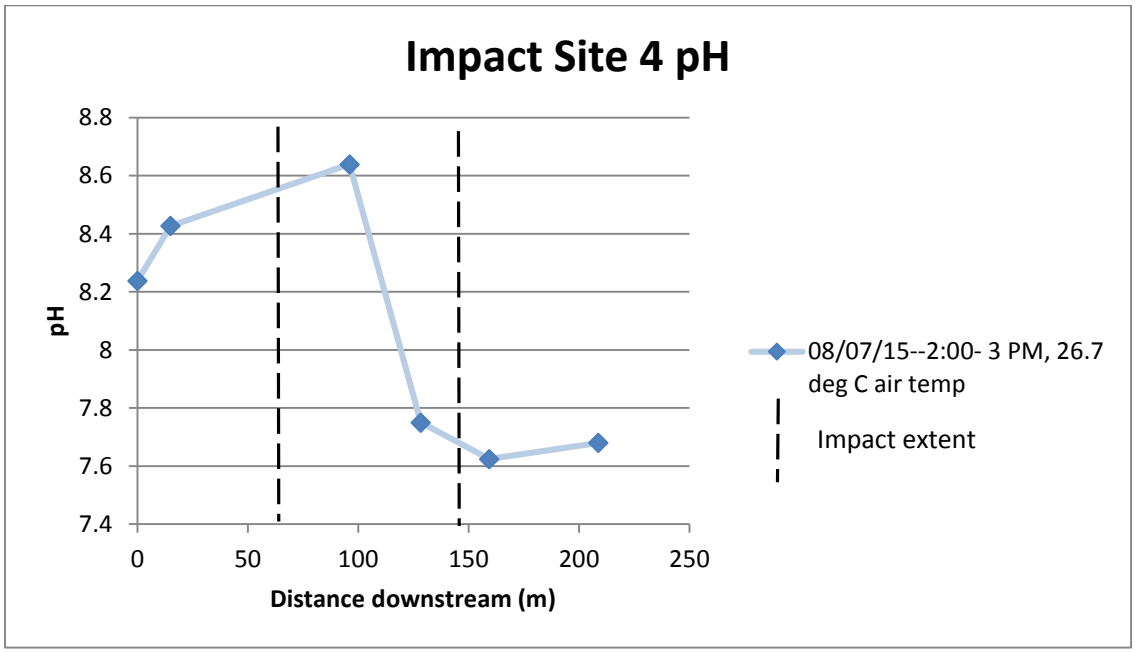

Figure 16. Impact site 4 pH measurements.

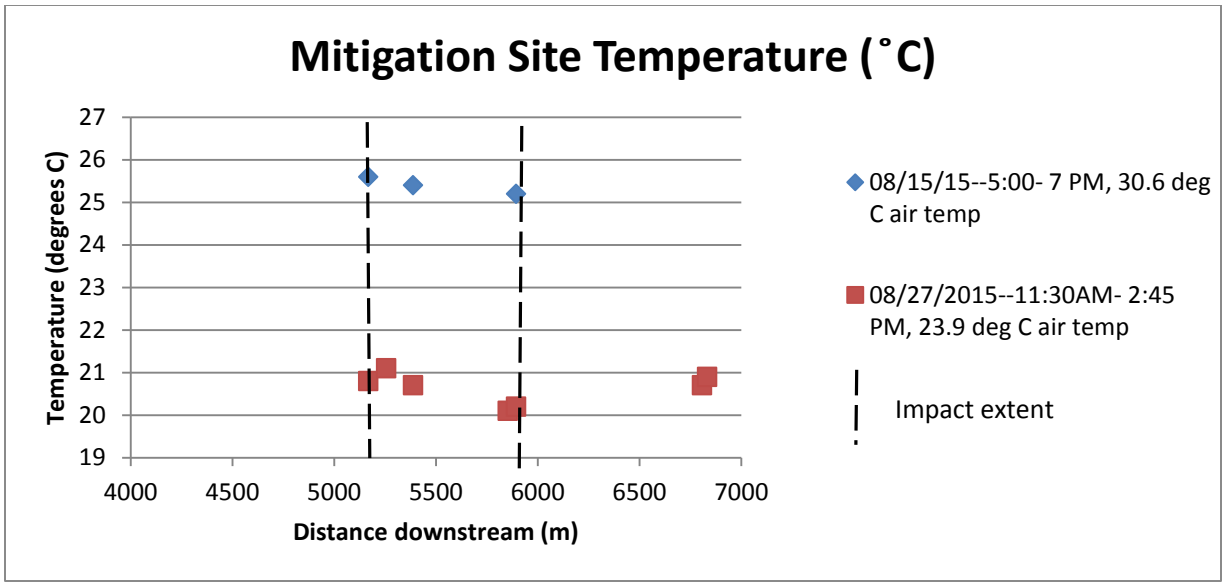

Figure 17. Mitigation site temperature measurements.

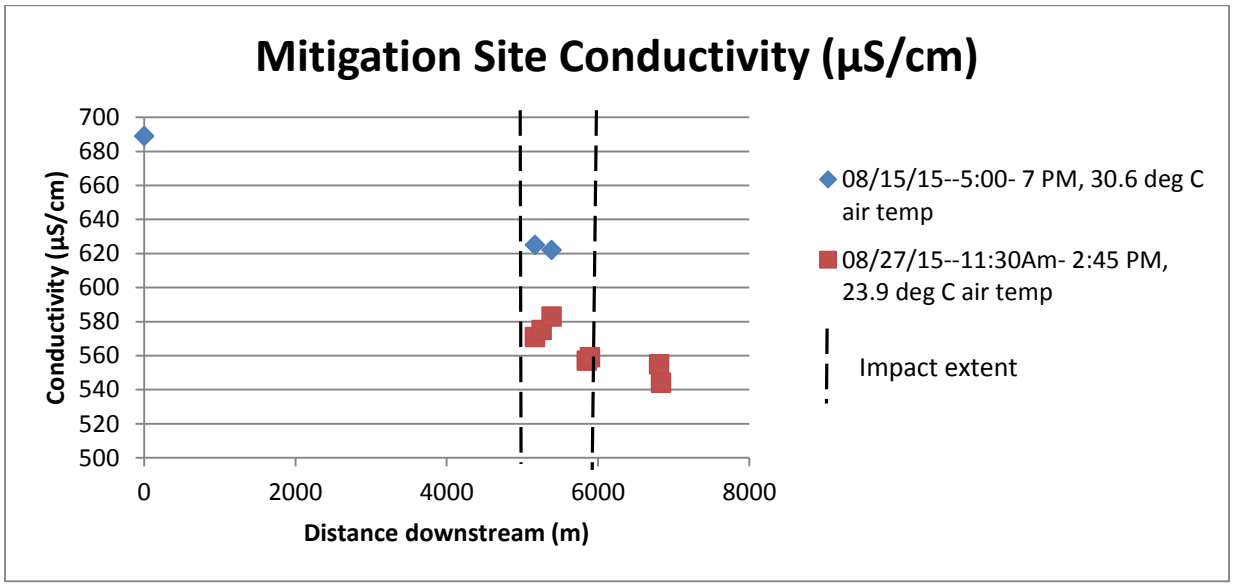

Figure 18. Mitigation site conductivity measurements.

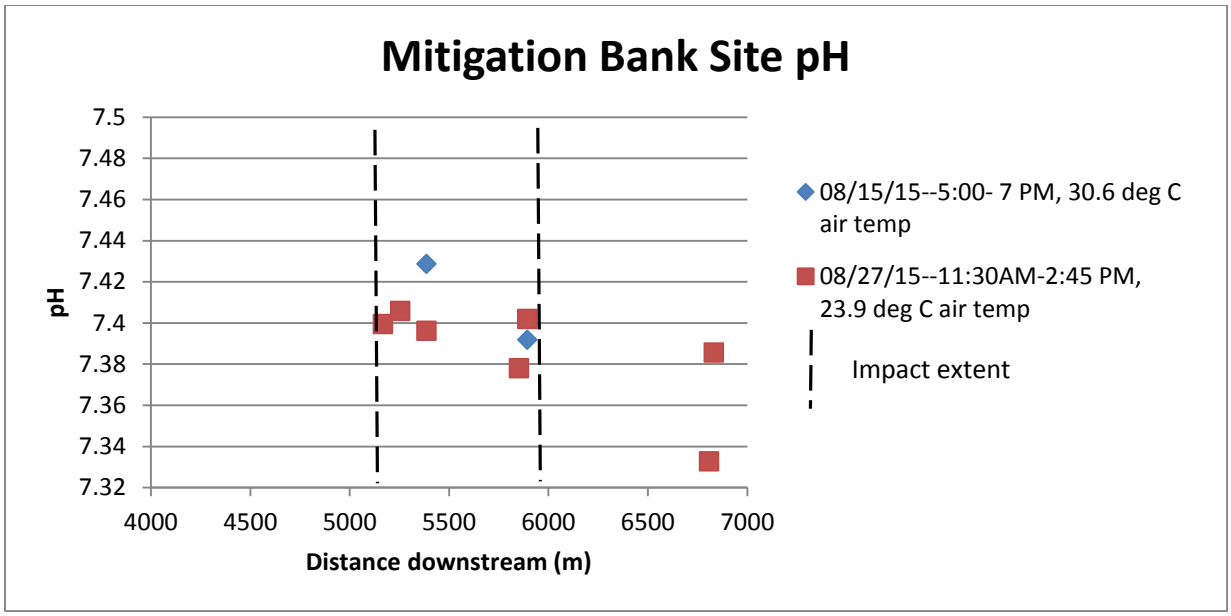

Figure 19. Mitigation site pH measurements

6. REFERENCES

Bartley, R. and Rutherford, I. (2005). Measuring the reach-scale geomorphic diversity of streams: application to a stream disturbed by a sediment slug. *River Research and Applications*, 21: 39-59.

BenDor, Todd, Sholtes, J., & Doyle, M.W. (2009). Landscape characteristics of a stream and wetland mitigation banking program. *Ecological Applications* 19.8: 2078-2092.

David, Mark B., Drinkwater, L.E., & McIsaac, G.F. (2010) Sources of nitrate yields in the Mississippi River Basin. *Journal of Environmental Quality* 39.5: 1657-1667.

Doyle, M. W., Stanley, E.H., Strayer, D.L., Jacobson, R. B., & Schmidt, J.C. (2005). Effective discharge analysis of ecological processes in streams, *Water Resour. Res., 41*, W11411.

Doyle, Martin W., & Yates A.J. (2010). Stream ecosystem service markets under no-net-loss regulation. *Ecological Economics* 69.4: 820-827.

Doyle, Martin W., & Shields F.D. (2012). Compensatory Mitigation for Streams Under the Clean Water Act: Reassessing Science and Redirecting Policy1. *Journal of the American Water Resources Association*: 494-509.

Doyle, Martin W., et al. (2013) River Federalism. *Annals of the Association of American Geographers* 103.2: 290-298.

Espeland, Wendy Nelson, & Stevens M.L. (1998). Commensuration as a social process. *Annual review of sociology*: 313-343.

Freeman, Mary C., Pringle, C.M., & Jackson, C.R. (2007). Hydrologic Connectivity and the Contribution of Stream Headwaters to Ecological Integrity at Regional Scales. *Journal of the American Water Resources Association (JAWRA) 43*(1), 5-14.

Girard, J. E. (2005). Principles of environmental chemistry (p. 320). *US: Jones and Barlett*.

Groschen, G. E., & King, R. B. (2005). *Evaluation of Measurements Collected with Multi Parameter Continuous Water-Quality Monitors in Selected Illinois Streams, 2001-03* (No. 2005-5060). Geological Survey (US).

Herget, James E. (1978). Taming the environment: the drainage district in Illinois. *Journal of the Illinois State Historical Society (1908-1984)*: 107-118.

Ho, Karen. (2009). *Liquidated: an ethnography of Wall Street*. Duke University Press.

Hough, Palmer, and Morgan Robertson. (2009). Mitigation under Section 404 of the Clean

Water Act: where it comes from, what it means. *Wetlands Ecology and Management* 17.1: 15-33.

IDNR. http://dnr.state.il.us/education/podcasts/textfiles/prairies%20podcast.htm Last accessed September 3, 2014.

Illinois Environmental Protection Agency (IEPA) (2004). Little Muddy River TMDL Report. Bureau of Water, Springfield, Illinois. *IEPA/BOW/04-016*.

Knighton, D. (1998). Fluvial forms and processes: London. *Edward Arnold*.

Kravits, Chris M., & Crelling J.C. (1981). Effects of overbank deposition on the quality and maceral composition of the Herrin (No. 6) coal (Pennsylvanian) of southern Illinois. *International Journal of Coal Geology* 1.3: 195-212.

Lave, Rebecca, et al. (2014). Intervention: Critical physical geography. *The Canadian Geographer/Le Géographe canadien* 58.1: 1-10.

_____, Robertson, M.M., & Doyle, M.W. (2008). Why you should pay attention to stream mitigation banking. *Ecological Restoration* 26.4: 287-289.

Laub, B. G., Baker, D. W., Bledsoe, B. P., & Palmer, M. A. (2012). Range of variability of channel complexity in urban, restored and forested reference streams. *Freshwater Biology 57*(5): 1076-1095.

MacKenzie, Donald. (2009). Making things the same: Gases, emission rights and the politics of carbon markets. *Accounting, Organizations and Society* 34.3: 440-455.

McAfee, Kathleen, & Shapiro E.N. (2010). Payments for ecosystem services in Mexico: nature, neoliberalism, social movements, and the state. *Annals of the Association of American Geographers* 100.3: 579-599.

McCorvie, Mary R., & Lant, C.L. (1993). Drainage district formation and the loss of Midwestern wetlands, 1850-1930. *Agricultural History*: 13-39.

McDonald, Adrian, et al. (2004). Rivers of dreams: on the gulf between theoretical and practical aspects of an upland river restoration. *Transactions of the Institute of British Geographers* 29.3: 257-281.

Midwest Regional Climate Center. July 5, 2015. http://mrcc.isws.illinois.edu/multimedia/releases/2015/20150702_RecordJuneRainfallAdFlooding.pdf. Last accessed March 23, 2016.

Palmer, Margaret A. (2009). Reforming watershed restoration: science in need of application and applications in need of science. *Estuaries and Coasts* 32.1 (2009): 1-17.

Palmer, M. A., Menninger, H. L., & Bernhardt, E. (2010). River restoration, habitat heterogeneity and biodiversity: a failure of theory or practice?. *Freshwater biology 55*(s1): 205-222.

Pociask, Geoffrey E., & Matthews, J.W. (2013). Restoration Progress and Flood Disturbance at IDOT Wetland Mitigation Sites. *FHWA-ICT-13-016*.

Poole, G. C. (2002). Fluvial landscape ecology: addressing uniqueness within the river discontinuum. *Freshwater Biology*, *47*(4), 641-660.

Robertson, Morgan M. (2004). The neoliberalization of ecosystem services: wetland mitigation banking and problems in environmental governance. *Geoforum* 35.3: 361-373.

_____. (2006). The nature that capital can see: science, state, and market in the commodification of ecosystem services. *Environment and Planning D* 24.3: 367.

Roni, Philip, and Ed Quimby, eds. (2005). *Monitoring stream and watershed restoration*. CABI.

Timmermans, S., & Berg, M. (1997). Standardization in action: achieving local universality through medical protocols. *Social studies of science 27*(2): 273-305.

Urban, Michael A., & Rhoads, B.L. (2003). Catastrophic human-induced change in stream-channel planform and geometry in an agricultural watershed, Illinois, USA. *Annals of the Association of American Geographers* 93.4: 783-796.

United States Geological Survey. (2007). Technical Supplement 13A: Guidelines for Sampling Bed Material. *Part 654 National Engineering Handbook*.

Ward, J. V., Tockner, K., & Schiemer, F. (1999). Biodiversity of floodplain river ecosystems: ecotones and connectivity. *Regulated Rivers: Research & Management*, *15*(1), 125-139.

Wilson, Cyril O., & Weng, Q. (2011). Simulating the impacts of future land use and climate changes on surface water quality in the Des Plaines River watershed, Chicago Metropolitan Statistical Area, Illinois. *Science of the Total Environment* 409.20: 4387-4405.

Woods, Allan J., Omernik, J.M, & Moran, B.C. (2000). *Illinois Level III and Level IV Ecoregions*.

Modeling and prediction of watershed-scale dynamics of consumptive water reuse for power plant cooling

Basic Information

Title:	Modeling and prediction of watershed-scale dynamics of consumptive water reuse for power plant cooling
Project Number:	2015IL296B
Start Date:	3/1/2015
End Date:	2/28/2016
Funding Source:	104B
Congressional District:	IL-15
Research Category:	Engineering
Focus Category:	Hydrology, Management and Planning, Wastewater
Descriptors:	None
Principal Investigators:	Ashlynn S. Stillwell, Zachary Barker

Publication

1. Barker, Zachary A.; Ashlynn S. Stillwell, 2016, Implications of Transitioning from De Facto to Engineered Water Reuse for Power Plant Cooling, Environmental Science and Technology, 50(10), 5379-5388.

Modeling and Prediction of Watershed-Scale Dynamics of Consumptive Water Reuse for Power Plant Cooling

Research category: Engineering

Student category: Graduate

Keywords: hydrology, power plants, streamflow, watershed management

Principal Investigator:
Ashlynn S. Stillwell, Ph.D.
Assistant Professor
University of Illinois at Urbana-Champaign
ashlynn@illinois.edu
(217) 244-6507

Co-Principal Investigator:
Zachary A. Barker, E.I.T.
Graduate Research Assistant
University of Illinois at Urbana-Champaign
zbarker2@illinois.edu

Congressional district: 13th Congressional district of Illinois

Final Report: Modeling and Prediction of Watershed-Scale Dynamics of Consumptive Water Reuse for Power Plant Cooling

SUMMARY OF PROBLEM AND RESEARCH OBJECTIVES

The energy-water nexus – the relationship between energy and water resources – is an area of emerging concern among resource managers, policy makers, and academics [1-6]. Of particular interest in Illinois is the overlap between thermoelectric power plants, which require cooling to condense process steam, and water resources. In Illinois, thermoelectric power plants (using primarily coal and nuclear fuels) account for over 85% of freshwater withdrawals [7]. Since many of those facilities use open-loop (or once-through) cooling with lower consumptive demands, they only consume an estimated 2% of the water withdrawn [8]; however, nationwide water consumption data have not been reported since 1995.

As water resources endure strain from additional demands and changing climate, researchers and resource managers have considered use of alternative water supplies, such as reclaimed water from municipal wastewater treatment plants (WWTPs) [9-11]. Reclaimed water can be a drought-resistant, non-potable water source for power plants, decreasing water demand conflicts with other users and reducing thermal loading on major rivers, such as the Illinois River with several power plants in series. However, since reclaimed water use typically requires cooling towers instead of open-loop cooling, water reuse for power plants could increase water consumption via evaporation along with additional capital cost for infrastructure.

Our work modeled water reuse at select thermoelectric power plants in Illinois, and estimated the watershed-scale dynamics of additional water consumption. While water reuse for power plants can be a beneficial water management approach locally, the additional water consumption might have significant negative impacts downstream for other water users, including navigation. To model and quantify these conditions, we completed the following research objectives in the study area shown in Figure 1 and described in Table 1:

1. Evaluate the degree of de facto water reuse at power plants in the study area, based on the incidental presence of wastewater effluent in the natural water source.
2. Determine the geographic and technologic feasibility of using reclaimed water to cool existing power plants in the study area.
3. Create a hydrologic model of the study area watersheds to simulate the dynamic downstream impacts of retrofitting reclaimed water to cool power plants.

Table 1. The study area power plants have varying characteristics and costs to retrofit. Results have been rounded.

				Water Withdrawals		Retrofit to Cooling Towers		
Name	Capacity (MW)	Fuel	Existing cooling system	Open loop (MGD)	Closed loop (MGD)	Capital Cost (10^6 US$)	Annual Treatment Cost[b] (10^6 US$)	Total Annual Cost (10^6 US$)
Will County	898	Coal	Open-loop	607	7.5	US$81	US$4.29	US$9.57
Joliet 9	360	Coal	Open-loop	263	2.1	US$33	US$0.76	US$2.91
Joliet 29	1,320	Coal	Open-loop[a]	956	12.0	--	US$2.71	US$2.71
Braidwood	2,450	Nuclear	Open-loop	1,850	87.6	US$1,770	US$24.8	US$140
Dresden	2,020	Nuclear	Open-loop[a]	1,440	68.9	--	US$31.5	US$31.5
Kendall County	1,260	Natural Gas	Closed-loop	--	0.2	--	US$0.09	US$0.09

4. [a] Has facilities to operate as closed-loop but primarily utilizes open-loop cooling.
5. [b] Estimated as $984 per million gallons [12].

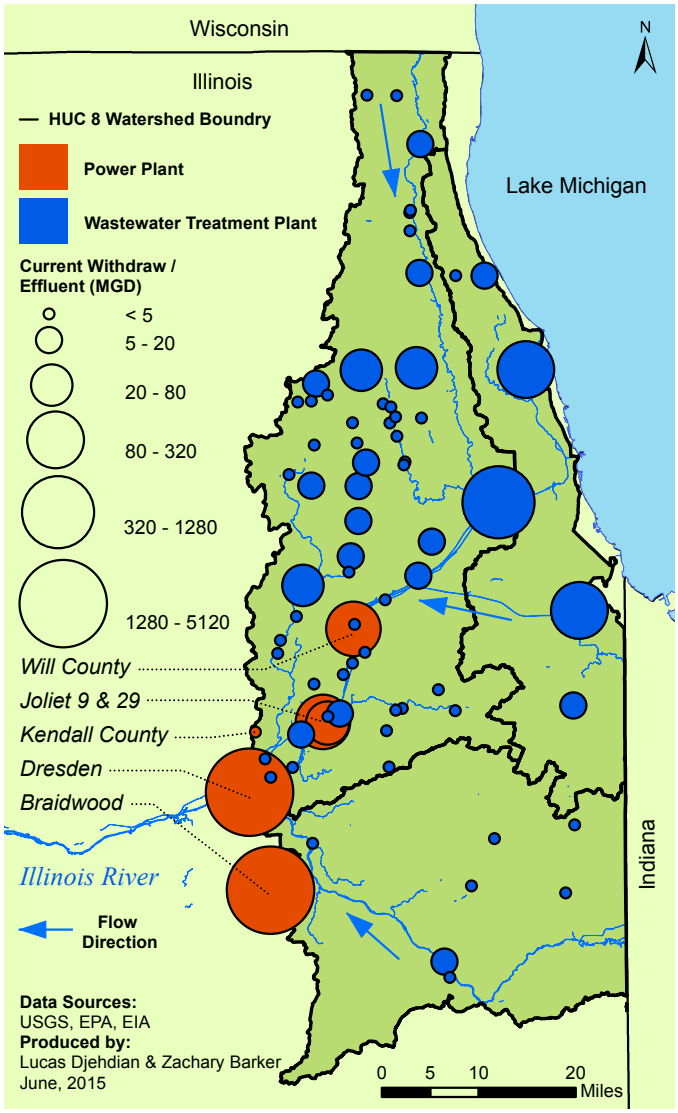

Figure 1. The Greater Chicago Area includes 72 wastewater treatment plants and 6 power plants. Of the power plants, 5 operate primarily by open-loop cooling which cumulatively withdraw more water than the wastewater produced and are located on the downstream side of the study.

SUMMARY OF METHODOLOGY

We used the following high-level methodology to address the project's research objectives:

1. Evaluation of de facto water reuse at power plants.

Using historic streamflow levels for the Des Plaines and Kankakee Rivers, serving as the current sources of cooling water for power plants in the study area, we quantified the current level of de facto water reuse at existing thermoelectric power plants. De facto water reuse is typically evaluated as a ratio of cumulative upstream discharge from WWTPs to instream flow, as demonstrated by Rice et al. for different percentiles of streamflow, which vary throughout the year [13]. We used the quantified de facto water reuse as the baseline current conditions representing power plant cooling operations.

2. Determination of feasibility of reclaimed water use at power plants.
Considering the de facto water reuse baseline, we then determined the geographic and technologic feasibility of retrofitting power plants in the study area to use reclaimed water in closed-loop cooling towers. This feasibility analysis used a GIS-based hydroeconomic model [11] combining land use [14] and elevation raster data [15] with power plant [16,17] and WWTP [18] data to determine the least cost path of a pipeline to deliver reclaimed water to a power plant from surrounding WWTP(s). The least cost path represents the best pipeline route that minimizes capital costs, and was selected with a genetic algorithm to simulate possible pipeline routes between facilities. Output from the GIS-based hydroeconomic model indicates the least cost feasible sources of reclaimed water for a given power plant.

3. Development of a hydrologic model to simulate downstream impacts of water reuse.
Using reclaimed water to cool power plants can help mitigate the impacts of water disruptions (such as droughts and heat waves); however, consumptive use of water that was previously returned to a waterway can have negative downstream impacts on streamflow, especially when supporting navigation. To understand the dynamic impacts of consumptive water reuse, we developed a hydrologic model of streamflow in the study area and in the Illinois River downstream. This statistics-based mass conservation model synthesized historical streamflow records with estimated changes in WWTP discharge and power plant withdrawal and consumption to predict streamflow at various gauge points downstream. Downstream flow was estimated based on historical data from the U.S. Geological Survey (USGS) with different water reuse consumption scenarios. We performed statistical hypothesis testing of output from the downstream impacts model to reveal any statistically significant changes in streamflow as a result of upstream consumptive water reuse.

MAJOR FINDINGS

De facto water reuse at power plants
Using flow data from USGS gauging stations in the study area and wastewater effluent averages, we calculated the median de facto reuse at each power plant. Although a straightforward calculation, the spatial aspects of the data are important. For our small urban watersheds, quantifying de facto reuse requires consideration of any discharges, withdrawals, or engineered operations of the waterways. In a few instances, discharges or withdrawals exist between the stream gauge and power plant. Figure 2 illustrates one of these instances (panel (B)) where a wastewater treatment plant might discharge downstream from a stream gauge. Under this condition, we include the wastewater effluent in the numerator and denominator of the de facto calculation (using Equation 1) since the upstream gauge does not account for its flow.

$$\%\, de\ facto\ reuse = \frac{\sum_{all\ i} q_{w,i}}{q_s} \qquad (1)$$

where q_w is the wastewater effluent from an upstream wastewater treatment plant i and q_s is streamflow at the point of withdrawal, both in similar units. We use similar mass balance logic for instances where two streams merge or the nearest gauge is downstream from the power plant.

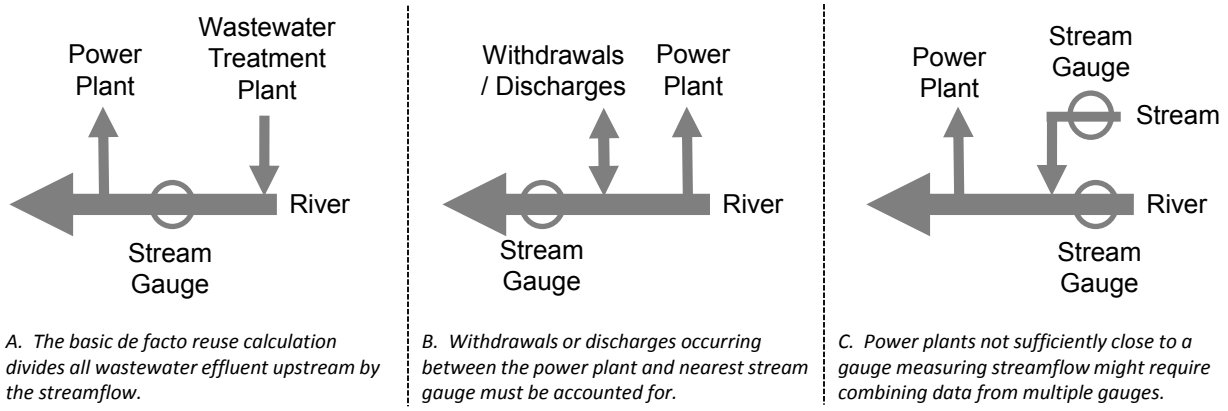

A. The basic de facto reuse calculation divides all wastewater effluent upstream by the streamflow.

B. Withdrawals or discharges occurring between the power plant and nearest stream gauge must be accounted for.

C. Power plants not sufficiently close to a gauge measuring streamflow might require combining data from multiple gauges.

Figure 2. This hypothetical diagram illustrates the need to account for withdrawals and discharges that occur after the stream gauge and before the power plant in both the numerator and denominator of the de facto reuse calculation.

In the City of Chicago, as well as many older cities, the storm and sanitary sewers are combined, which is an important consideration in calculating de facto reuse. During large storm events, stormwater combined with sanitary wastewater can overwhelm wastewater treatment infrastructure, causing a combined sewer overflow (CSO). Since wastewater bypasses the treatment plant (and, therefore, measurement), we did not have sufficient data to calculate de facto reuse during a CSO event; in response, we removed data associated with CSOs.

We used the medians of the remaining data to calculate the de facto reuse at each power plant. The Will County power plant has the largest median de facto reuse at 65% while the two Joliet and Kendall County power plants are at 55% and 25%, respectively. (The two Joliet power plants are adjacent and therefore have the same de facto calculation.) The two nuclear power plants, Dresden and Braidwood, have de facto reuse less than 0.5%, due to withdrawals from the Kankakee River, a primarily agricultural basin that does not include large quantities of wastewater discharge. We can explain these results as a function of proximity to the large Metropolitan Water Reclamation District of Greater Chicago (MWRD) wastewater treatment plants. Following the waterway downstream, the de facto reuse percentage decreases because the catchment area contributes more streamflow while discharges from smaller wastewater treatment plants have minor effects.

We analyzed daily wastewater effluent and streamflow data from the MWRD and the USGS, respectively, between the years 2007 and 2014. Daily data for the remaining wastewater treatment plants were unavailable; therefore, we approximated daily effluent flow from reported annual averages. In our study area, MWRD effluent comprises 85% of the total wastewater produced such that sufficient daily variation is captured.

Upon first analysis, a large number of days yield a de facto reuse greater than 100%, which is inconsistent with the physical representation in Equation 1. This finding reveals that on some days USGS stream gauges report less flow downstream than is reported being discharged from the wastewater treatment plants upstream. Our study area scale was sufficiently small to avoid time lag challenges; similarly, infiltration, evaporation, or unaccounted withdrawals do not appear to be of concern. We explain this result by the highly engineered and complex system of dams controlling the waterways and employ a one-week moving average to the data before calculating the de facto reuse. We represented the de facto reuse visually by depicting wastewater effluent (numerator in Equation 1) against streamflow (denominator in Equation 1), shown in Figure 3. Although the one-week moving average smoothing did not eliminate all the

points greater than 100%, it reduced their number and magnitude. The remaining percentages greater than 100, left of the dotted line in Figure 3, were within our margin of error.

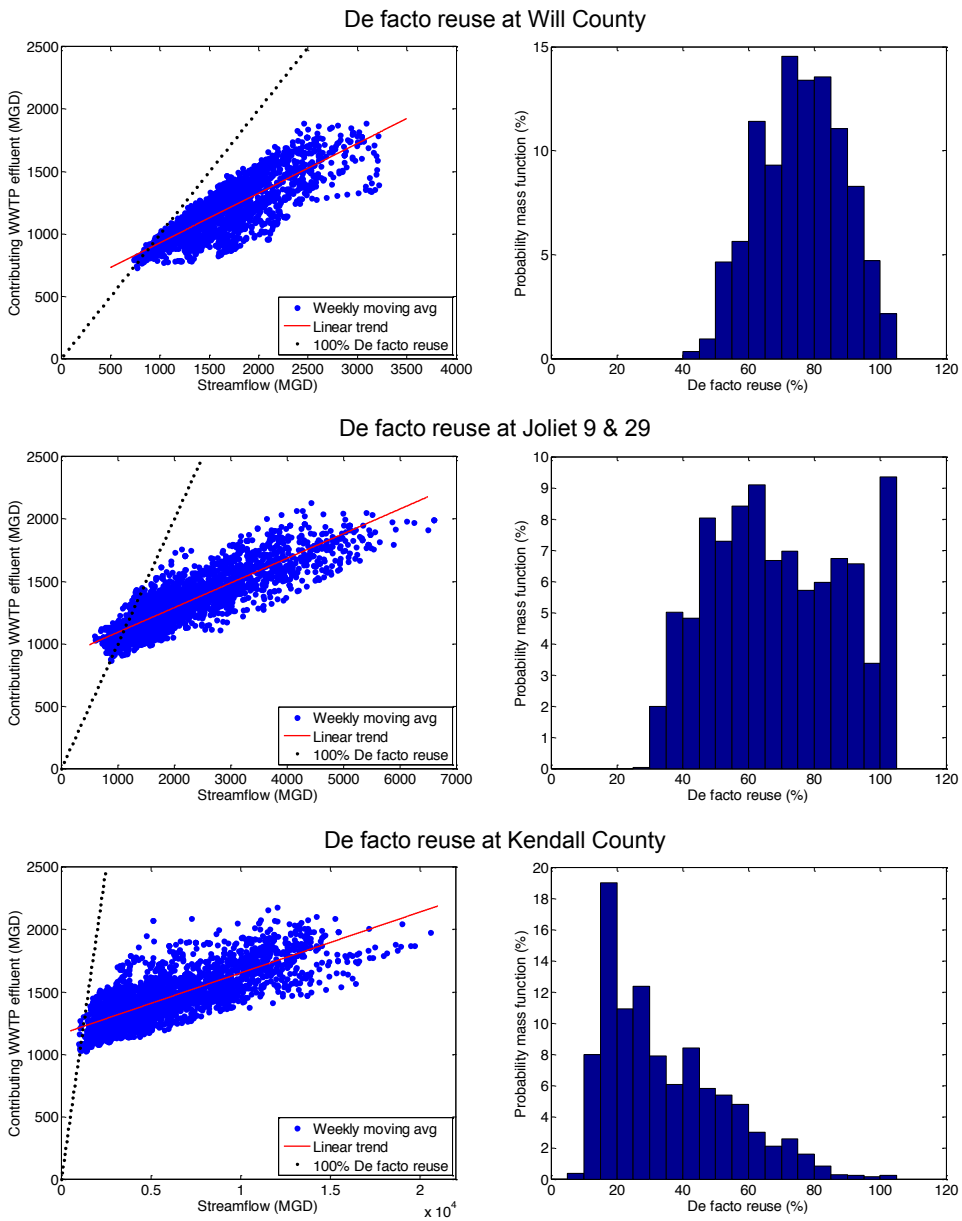

Figure 3. Conditioning to remove data that occurred on days with recorded combined sewer overflows, correlation exists between streamflow and wastewater effluent in the highly urban watershed of Chicago.

The regression plots in the left column of Figure 3 demonstrate that wastewater effluent and streamflow are in fact correlated due to the linear trend. Will County is the power plant nearest to the large wastewater treatment plants, which is reflected by the high slope of the trend line. The trend lines become flatter with increasing downstream distance, indicating the location-specific nature of de facto reuse. These findings reveal that the assumption made by Rice et al.

[13], that wastewater effluent is independent of streamflow is acceptable in most basins, but that assumption breaks down in highly urban environments, such as in the Chicago area.

Representing the de facto reuse as a probability mass function in the right column of Figure 3, we found that de facto reuse varies substantially. As with the median de facto calculation, these probability mass functions reflect the proximity to the large MWRD wastewater treatment plants. The de facto reuse at Will County is wastewater dominated while Kendall County is runoff dominated. At Joliet 9 and 29 the de facto reuse is more distributed.

Due to limited data availability for wastewater treatment plants in the Kankakee basin, no higher resolution analysis was performed. Since the two nuclear plants in this basin have such low preliminary de facto reuse percentages, a more precise analysis would likely reveal consistently low levels of de facto reuse.

Engineered reuse with reclaimed water at power plants

To compare the de facto reuse scenario to an engineered reuse scenario, we formulated an optimal system to supply reclaimed water to power plants. Combining a digital elevation model and land use rasters from the USGS, we created a cost scaling raster for the greater Chicago area. We expanded the cost scaling raster beyond the watershed boundary to allow the paths to traverse the least expensive route. Topography in the study area is relatively flat, such that the cost scaling raster reflects differences in urban density.

We simulated retrofitting power plants to use reclaimed water in recirculating cooling towers. Of the 6 power plants in the study area, only one (Kendall County) uses cooling towers; the remaining facilities operate open-loop systems, although Dresden and Joliet 29 have the necessary cooling towers on site. To determine the water withdrawal and consumption rates associated with retrofitting recirculating cooling, we used empirical and literature values specific to power generation in Illinois [17]. Under this assumption of cooling system retrofits, the Stickney, North Side (O'Brian), and Calumet WWTPs each have enough effluent to supply all power plant demands in the study area.

We found the least cost path between the wastewater treatment plants and power plants using the cost scaling raster with geographic information systems software (ArcMap by ESRI), displayed as the thin black lines in Figure 4. The genetic algorithm examines possible reclaimed water pipelines and selects the optimal solution, displayed as the thicker black line in Figure 4, representing piping reclaimed water from Stickney WWTP to each of the power plants.

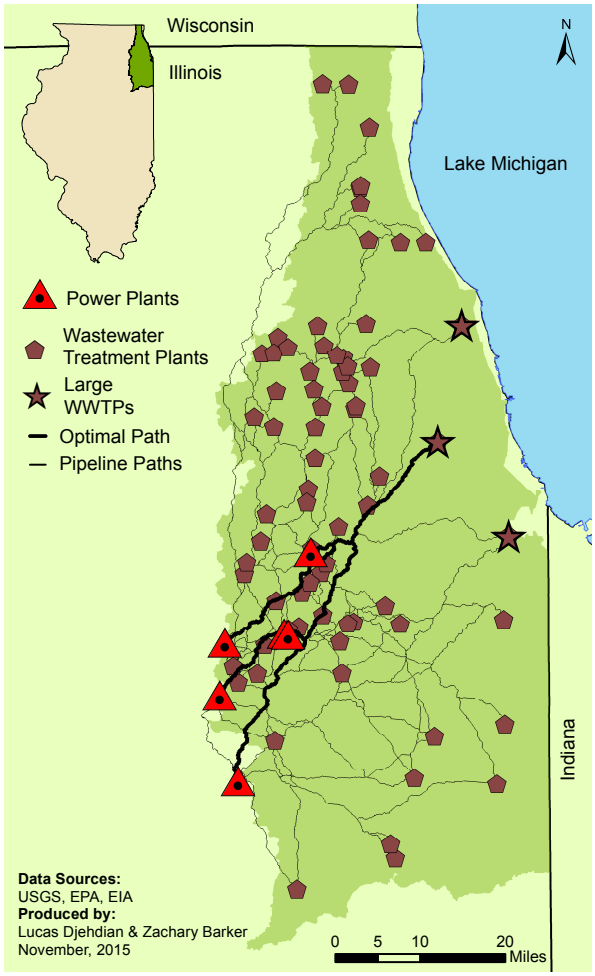

Figure 4. The least cost engineered reuse solution is a pipeline connecting the nearest treatment plant capable of providing all cooling demands.

Cost

To approximate the cost of retrofitting power plants to use reclaimed water (engineered reuse), we used the average of the low and high estimates from literature for each power plant in our study area, listed in Table 1. Due to the lack of data on the cost of cooling towers at nuclear power plants, there is high uncertainty in the retrofit cost estimate. The estimated pipeline construction cost is $356 million, or $23 million/yr using a 30-year amortization period and interest rate of 5%. The total length of pipe is estimated to be 93 miles long with diameters ranging from 0.5 to >6 ft. Similar feasible (yet sub-optimal) solutions for complete sourcing from the Calumet or Northside (O'Brian) WWTPs reveal estimated costs of $423 million and $615 million, respectively.

Combined, the total capital costs for the engineered reuse scenario is approximately $2.24 billion, with cooling tower costs representing 84% of the sum. This result is important when considering that the closed-loop cooling with de facto reuse scenario comprises the bulk of the capital costs required for engineered reuse. Naturally, de facto reuse with current cooling technologies, representing the baseline natural conditions, does not require any additional expense. These cost estimates represent a first-order approximation in motivating future in-depth studies.

Listed in Table 1, operation and maintenance costs for recirculating cooling, utilizing engineered reuse, are non-negligible. These costs comprise about one third of the total annual cost. This proportion is high due to the fouling and treatment costs associated with cooling with reclaimed water. We assume the operation and maintenance costs associated with open-loop cooling to be the baseline for comparison and, therefore, are zero. Due to lack of quality data, we cannot estimate treatment costs associated recirculating cooling utilizing de facto reuse. However, due to the high presence of wastewater, we expect the costs to be closer to the engineered reuse than zero.

Reliability

To calculate reliability, we quantitatively evaluated the likelihood of a power generation "failure" via a thermal variance event. We collected and organized documentation from the Illinois Environmental Protection Agency (IEPA) of thermal variances from 2003 to 2014 [19]. During this time period, 76 thermal variance days were recorded in the Chicago area out of 4,015 total days. Defining thermal variances as failures, we found that the system of power plants in our study area is 98% reliable under de facto reuse conditions; however, this computation does not consider future climate shifts. We account for anticipated increases in streamflow temperatures (likely leading to additional thermal variance days) by conditioning the data on the 80th percentile of seasonal ambient air temperatures, leading to a simulated power generation reliability of 91%. We conditioned on the 80th percentile because it correlates to a modest 2.5 °F increase in the Chicago area average air temperature [20].

We further grouped the variances into seasons for comparison to a seasonal climate metric, represented as the deviation from the seasonal average air temperature, illustrated in Figure 5. Most thermal variances occurred during the drought of 2012; however, Dresden nuclear plant also had variances during 2005. Unlike the current de facto reuse conditions used to calculate reliability, reliance on engineered reuse introduces negligible power generation reliability concerns due to the relatively consistent quality and temperature of reclaimed water. The tradeoff with a reclaimed water system is the reliance on critical pipeline infrastructure that is also at risk for failure, but leaving the existing cooling water intake structures as a backup can mitigate that risk.

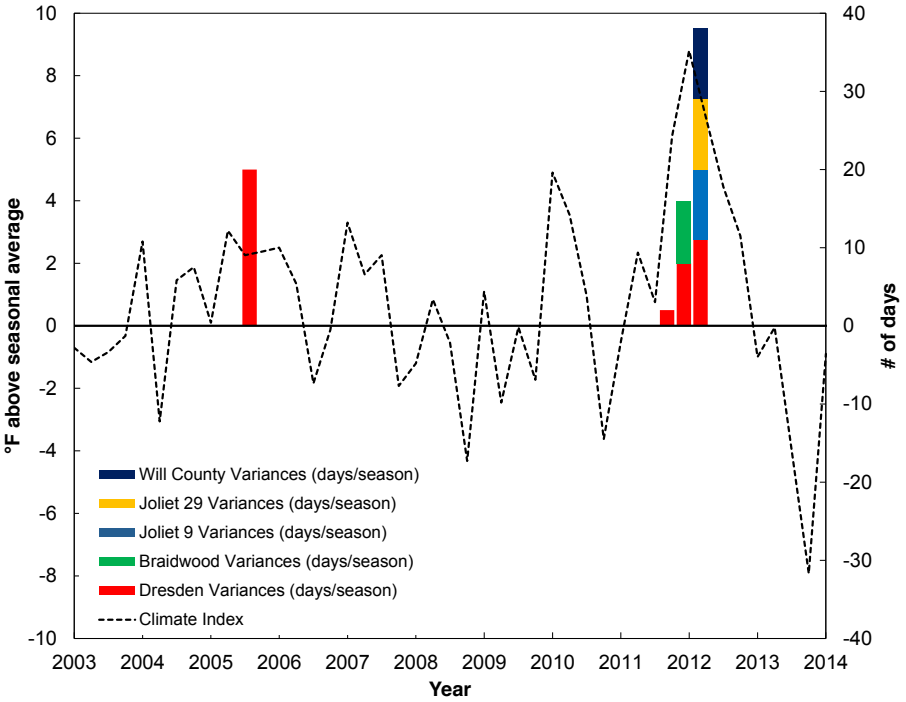

Figure 5. Without power plant operational data, we use thermal variances as a proxy for failure. Warmer seasons produce more thermal variances that have negative ramifications for the power plant and environment.

Performance

To assess the power plants' operational performance under the de facto and engineered reuse scenarios, we modeled the capacity loss due to warmer cooling water and power consumed during reclaimed water pumping. Using reported average monthly intake temperatures from the Energy Information Administration for the years 2010 through 2013, we applied a capacity loss model for each of the power plants. Since we did not have detailed operational information on these power plants, we used estimates from literature for the threshold at which the intake temperature begins to affect capacity [21]. Shown in Figure 6, the modeled capacity loss at each power plant is compiled (illustrated as stacked bars) to represent the total generation capacity loss for our study area. A peak capacity loss of 250 MW occurs for our de facto reuse scenario compared to a peak capacity loss of 400 MW for the engineered reuse scenario. The capacity loss under the de facto reuse scenario is due to the increased temperatures along the river, ranging from 26 to 29 °C. The maximum temperature of wastewater effluent, as reported by MWRD, is 23 °C, which is equal to the modeled threshold for efficiency loss in power plant cooling. Capacity loss in the engineered reuse scenario is the result of additional power demands for cooling tower operations.

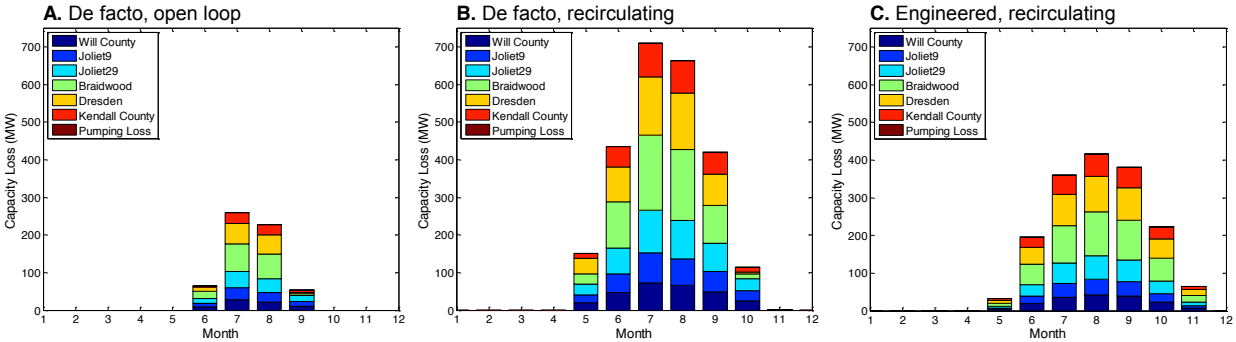

Figure 6. Capacity loss is greatest during the summer months due to the intake of warm cooling water. While recirculating cooling with cooling towers (B,C) introduces additional capacity loss compared to open-loop cooling (A), the impact is less pronounced in the engineered reuse case (C).

Although the engineered reuse scenario causes less capacity loss from elevated cooling water temperatures than the de facto scenario with recirculating cooling towers, we accounted for the pumping and distribution of reclaimed water from the wastewater treatment plant. We found the power associated with pumping reclaimed water to the power plants to be less than 1 MW. In comparing de facto reuse conditions with recirculating cooling (Figure 6(B)) and the engineered reuse scenario (Figure 6(C)), reclaimed water for power plant cooling is preferable due to substantially lower capacity losses due to consistency of water temperature, even when accounting for reclaimed water pumping. Notably, the capacity gains using reclaimed water, observed during summer months with peak electricity demand, are on the same scale as a small power plant. Using an electricity price of $0.08 per kWh [22] and assuming the study area power plants would be operating at full capacity, we calculated a first order approximation of revenue loss of about $62 million/year due to cooling inefficiencies under engineered reuse compared to current de facto conditions. However, compared to de facto reuse with cooling towers, there is a net savings of $47 million/year, which exceeds the initial cost estimate for reclaimed water pipeline construction. That is, when retrofitting to use cooling towers, engineered reuse with reclaimed water provides economic advantages via improved performance.

Overall, our results indicate that use of reclaimed water for power plant cooling has strategic advantages and tradeoffs. The engineered reuse with recirculating cooling scenario reveals advantages compared to de facto baseline conditions in terms of reliability. These reliability gains are due to the predictable temperature of reclaimed water and its use in recirculating cooling towers, mitigating the need for thermal variances. When comparing recirculating cooling scenarios, engineered reuse with reclaimed water has lower capacity loss (that is, better performance) than recirculating cooling under de facto reuse conditions. These improvements in reliability and performance, however, come at the tradeoff of increased infrastructure cost, yet estimated revenue loss from power plant derating is comparable to these investment costs. Consequently, use of reclaimed water for power plant cooling might be a strategic infrastructure investment to benefit both energy and water resources.

Downstream impacts of consumptive water reuse

To quantify the dynamic downstream flow impacts of consumptive water reuse, we created a model extending beyond the original study area to include the downstream Illinois River, shown in Figure 7. The Illinois River, a tributary of the Mississippi River, provides a navigable waterway to Chicago and Lake Michigan via the Des Plaines River and the Chicago Sanitary & Shipping Canal. Along the route, there are eight locks and dams operated by the U.S. Army Corps of Engineers. While drastically reducing cooling water withdrawals, retrofitting power plants in the

area to use reclaimed water in cooling towers would increase total water consumption by an estimated 200 million gallons per day (MGD). Fortunately, the supply of wastewater effluent in the study area is very large due to high population densities and combined sewer infrastructure, with the total amount of treated effluent typically exceeding 1,800 MGD.

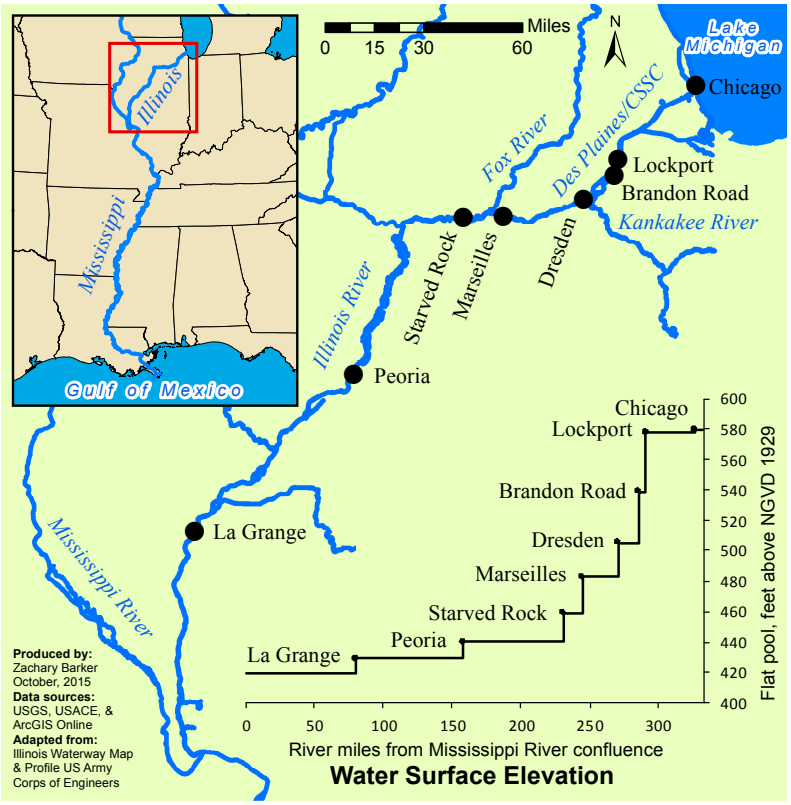

Figure 7. The Illinois River connects Lake Michigan with the Mississippi River and is downstream from the proposed consumptive use of reclaimed water.

Defining what uses of water are important downstream is critical for understanding the impacts of water reuse. For the Illinois River, the most critical downstream stakeholder is barge traffic. The Illinois River does not sustain large fishing operations or support a large amount of water withdrawals. A small number of power plants downstream from the original study area currently rely on the Illinois River for cooling water; however, these facilities are not considered in this analysis because their operations would not be affected by the simulated changes in the flow regime. Barges are important to the region for cost-effective transportation of coal, petroleum, agricultural products, and other raw materials. Since barge traffic relies on a channel deep enough to float, we focused our analysis on this critical stakeholder. Unique to this system is the source of water during dry periods. Lake Michigan diversions are already used to act as make-up water during low flows and could not be increased due to international treaties.

Scenario analysis

To quantitatively assess the downstream impacts of reclaimed water consumption, we employed scenario analysis, comparing the proposed scenario to the current baseline (de facto) conditions. We were primarily interested in the effects of consuming 200 MGD of reclaimed water for cooling power plants; however, many other water reuse applications are possible and could be evaluated with this methodology. To explore these possibilities, we examined how the system changes due to the entire range of possible reclaimed water consumption levels. The

minimum of this range is defined by zero consumption, or no change, and the maximum is defined as the total consumption of the 1,800 MGD of wastewater produced in the Chicago region. For this analysis, we assumed a uniform demand of reclaimed water on a daily and seasonal timescale. Since our main application is cooling baseload thermoelectric power plants, this assumption is reasonable because these power generators typically have fairly constant water demands.

We used streamflow and stage data from the USGS and the U.S. Army Corps of Engineers. The data at the locks and dams represent the tailwater side of the infrastructure and include 25 years of daily data. The data reported at these sites represent our baseline (de facto) scenario and a selection of these data are displayed as flow duration curves in Figure 8. We simulated our engineered water reuse scenarios by subtracting the quantity of water consumption from all data points to shift the flow duration curves. The 200 MGD consumption scenario, representing cooling study area power plants with reclaimed water, is illustrated in Figure 8.

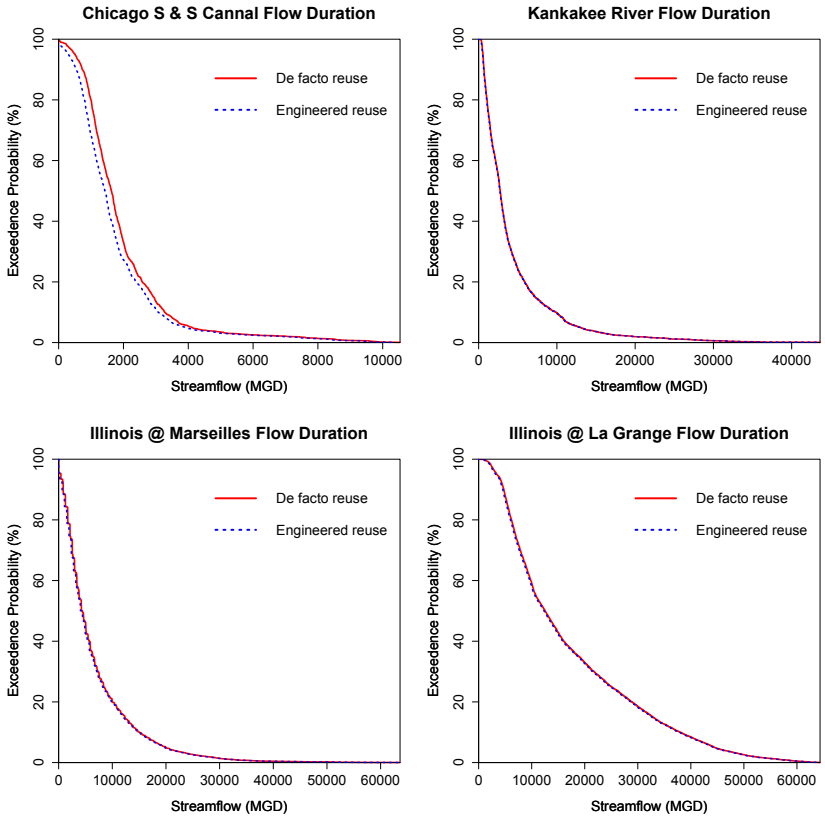

Figure 8. Consuming reclaimed water upstream shifts the flow duration curves downstream.

At all of the streamflow gauges shown in Figure 7, excluding the Kankakee River, the flow duration curve shift is to the left, illustrating lower streamflow. The flow duration curve for the Kankakee River, however, shifts to the right signifying more streamflow in the engineered reuse scenario than in the de facto scenario. In the engineered reuse scenario, two power plants that currently withdraw water from the Kankakee River instead consume reclaimed water that is produced on the Des Plaines branch of the Illinois River headwaters. While all of the flow duration curves in Figure 8 depict the same 200 MGD reduction in streamflow, gauges further downstream have larger drainage areas, and, therefore, the flow regime shift appears smaller.

Statistical significance

To quantify the difference between flow regimes illustrated in Figure 8, we used statistical techniques to estimate the difference between means between the baseline (de facto) scenario and each engineered water reuse scenario. We calculated *t*-statistics to quantify the statistical significance of the difference between streamflow means for each gauge. A significance level of 0.05 was used for α, which correlates to a *t*-statistic threshold of approximately 2. Test statistic results greater than this threshold were considered statistically significant; that is, a statistically significant difference exists between the mean baseline (de facto) streamflow and streamflow with upstream consumptive water reuse at *t*-statistic values greater than 2.

Using a step size of 10 MGD for the range of reclaimed water consumption (0 to 1800 MGD), we evaluated the maximum level of water reuse (consumption) possible without observing a statistically significant simulated downstream impact. Although the entire range of consumption scenarios were calculated, scenarios up to 500 MGD reclaimed water consumption are displayed in Figure 9. From these results, the 200 MGD scenario for power plant cooling has a significant impact on streamflow at the first two gauges downstream from the wastewater treatment plant. These impacts of reclaimed water consumption diminish with distance downstream, becoming insignificant by 50 river miles downstream.

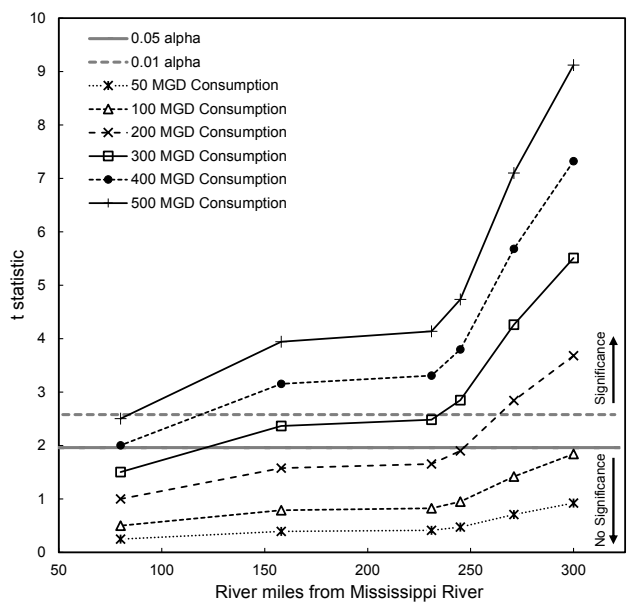

Figure 9. Reclaimed water consumption above 100 million gallons per day (MGD) would lead to statistically significant changes in downstream flow, with impacts varying with distance. The right hand side of the figure represents the Chicago area (300 river miles from the Mississippi River) and the left hand side is near the confluence.

Reclaimed water consumption could approach 100 MGD in this simulation and not have a statistically significant impact on downstream flow. While this amount of water reuse would not provide cooling water to all six power plants in the study area, a few could be cooled without ramifications of any significant downstream impacts. Also shown in Figure 9 is the level of significance threshold for α of 0.01, representing a more relaxed threshold for significant downstream impacts. Increasing this threshold (by decreasing the value of α) allows the maximum reclaimed water consumption to increase to 150 MGD. Since the *t*-test for 200 MGD reclaimed water consumption returns a statistically significant difference in means for

streamflow gauges directly downstream, we further investigated the negative economic impacts that reclaimed water consumption might have on downstream barge transit.

Probability of failure

Defining barge transportation as the most at risk downstream stakeholder, we focused on river stage instead of streamflow directly. The U.S. Army Corps of Engineers aims to maintain a minimum depth of 9 feet along the Illinois River. Using the reported stage and streamflow data immediately downstream from each lock and dam, we found the current probability that the minimum stage is not met. All five gauges have some low but non-zero probability of failure in the baseline (de facto) scenario.

Since we have defined our threshold as a stage, we converted the reclaimed water consumption from a reduction in streamflow to a reduction in stage. Ideally, rating curves would define this relationship; however, these curves were not available or accurate for low flows at the study gauges. To establish a relationship between streamflow and stage, we used linear regression. Nonlinear relationships could also be used; however, for the highly engineered operation of the Illinois River, nonlinear models did not produce more accurate results. Since our focus is on low flows that put downstream users at risk, we used only the lower 50th percentile of streamflow in developing the rating curve. Figure 10 depicts this process for one of the gauges and is representative of the method for each location. Also illustrated in Figure 10 is the linear model result from using the entire data set for the regression. The full data linear regression does not accurately represent the range of low flows of interest. Further, the lower slope would underrepresent the reduction in stage from upstream reclaimed water consumption. Using the slope from the rating curve, we shifted the stage using Equation 2:

$$l_t' = l_t - mr_t \tag{2}$$

where l_t' is the stage given reclaimed water consumption, l_t is the reported stage, m is the slope of the rating curve, and r_t is the amount of reclaimed water consumption; all for the same time t. By shifting the stage, similar to the shifting of the flow duration curve, we assessed the number of data points that fell below the threshold of 9 feet at each gauge. We then calculated the probability of failure to find the expected failure rate for each downstream gauge at varying levels of reclaimed water consumption.

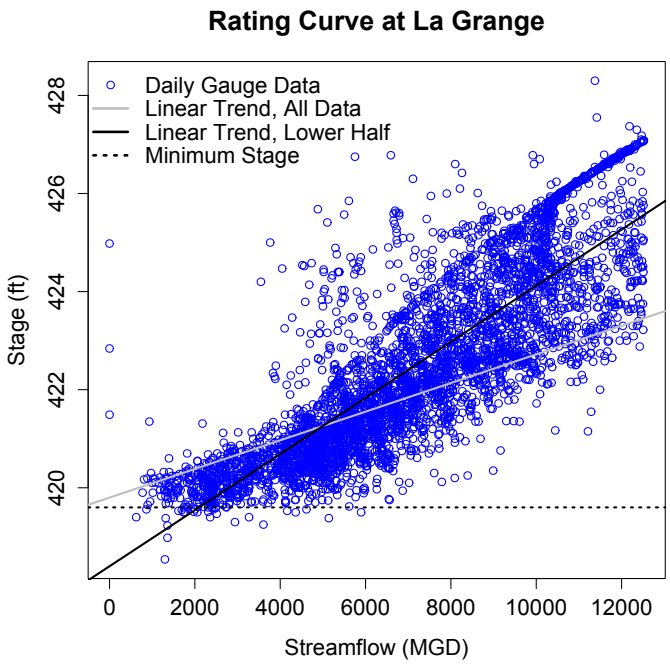

Figure 10. In the absence of accurate rating curves, we used linear regression to estimate the relationship between streamflow and stage.

Figure 11 displays the probability of failure results for each gauge on the Illinois River. The 200 MGD consumption scenario representing water reuse for power plant cooling reveals minor increases in probability of failure with all gauges less than 1%. At Peoria, the most extreme change, the probability of failure increases from 0.39% to 0.99%. In the scenario with consumption of all of the reclaimed water produced in the Chicago area (1800 MGD), the probability of failure would increase to a maximum of 15% at Peoria. While illustrating the potential downstream impacts of water reuse on an annual basis, this approach does not capture the seasonality of precipitation. In Illinois, precipitation is higher during the first half of the year than the second. To account for these seasonal precipitation patterns, we conditioned the probability of failure on the time of year, repeating the same analysis with two datasets: 1) data from January through June (spring), and 2) data from July through December (fall). The results show similar findings comparing gauges to each other; however, the magnitudes are significantly different. During the spring, the wet season, failure probabilities are less than 4% even for total reclaimed water consumption at 1800 MGD. During the fall, the dry season, probabilities of failure approach 25% for total reclaimed water consumption; however, the 200 MGD scenario (representing water reuse for power plant cooling) is still below 2%.

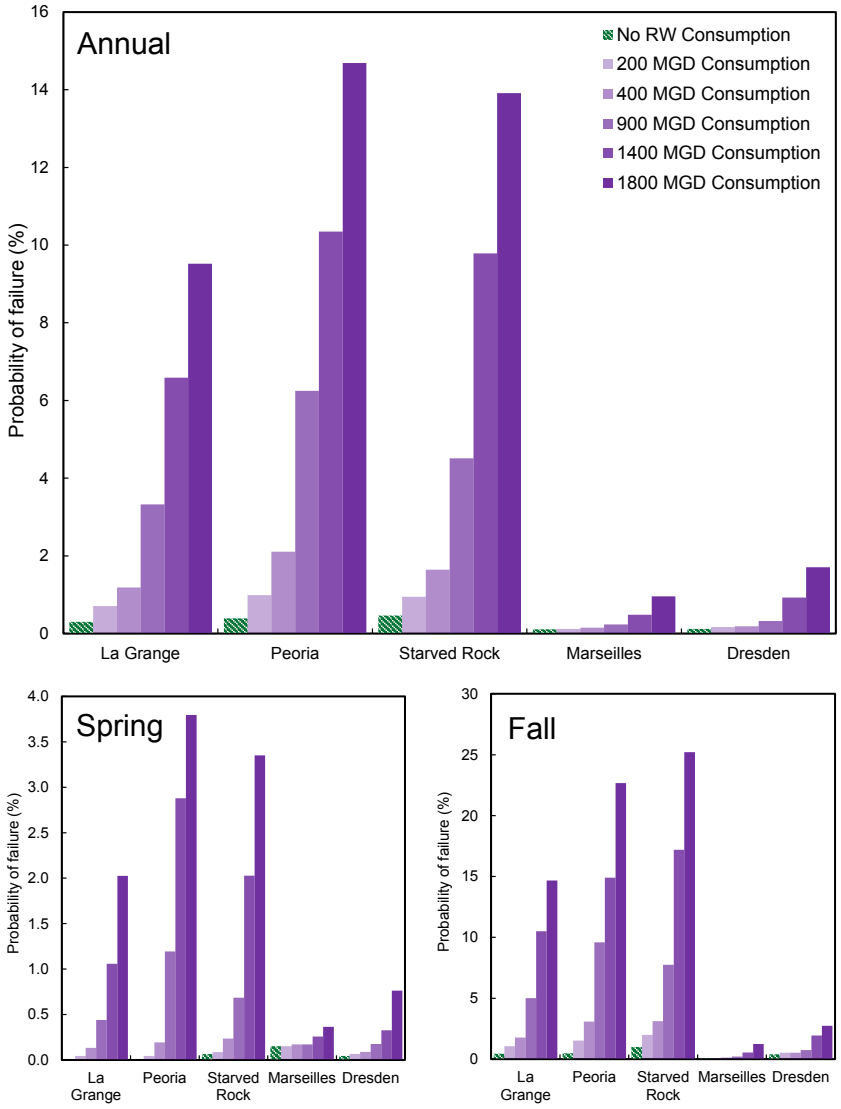

Figure 11. The probability that the stage at each gauge falls below the 9-ft minimum channel depth is small under current conditions (no reclaimed water [RW] consumption) and increases marginally under the proposed consumption scenario of 200 million gallons per day (MGD).

Value

To quantify the effect of decreased navigability of the Illinois River in an economic perspective, we calculated the relative value of barge transportation. The U.S. Army Corps of Engineers reports the tonnage and type of each commodity that passes through each lock [23]. Using these data for the years 1999 through 2014, we assessed the amount of commodities passing through each lock via barge. The average, shown in Figure 12, is representative of the larger trends in movement of commodities along the waterway. Most importantly, the data reveal that areas further downstream see more barge traffic, with the difference associated mainly with food and farm products. On average, the most upstream gauge, Lockport, sees roughly half of the tonnage of the most downstream gauge, La Grange. This increase in commodity movements downstream is favorable for cooling Chicago area power plants with reclaimed water since the consumptive affects diminish with downstream distance.

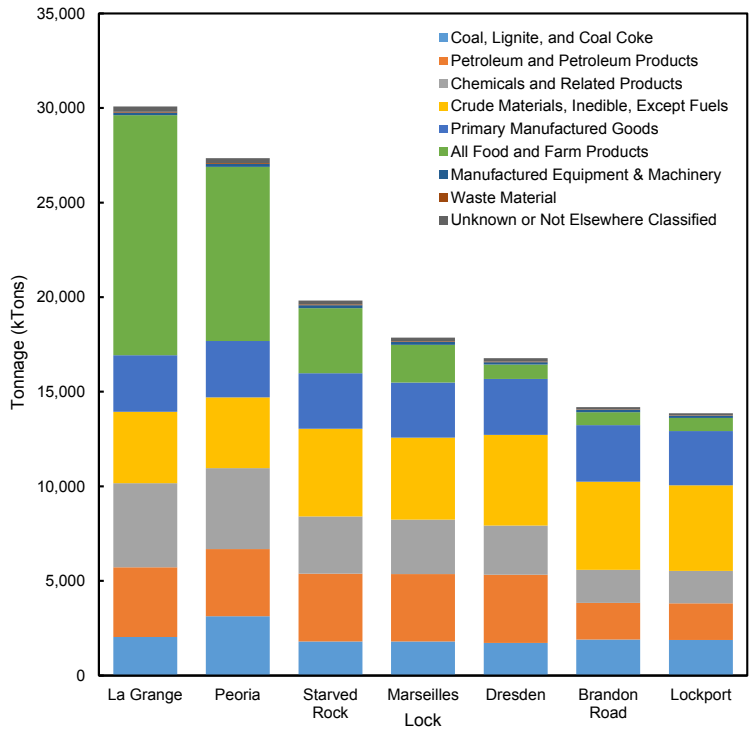

Figure 12. The average tonnage recorded passing through the locks on the Illinois River increases with proximity to the confluence with the Mississippi River. (La Grange is the gauge furthest downstream and Lockport is the furthest upstream in the study area.)

In order to assign value to barge traffic, we used the Commodity Flow Survey and the associated Freight Analysis Framework (FAF^3) [24], which tabulate commodity flows by mode of transportation and origin/destination. Combining all flows to and from Illinois gives a snapshot of the total transportation portfolio. Although these numbers represent a single year of commodity flows, we assumed the percentage of tonnage distributed by mode and commodity stays relatively constant. From these data, we directly calculated the waterborne market share of transportation; however, these values might include other waterways not downstream of the proposed consumptive water reuse. To account for these spatial considerations, we estimated the unit value of each commodity given by Equation 3:

$$Unit\ Cost = \frac{V}{T} \tag{3}$$

where V is the value and T is the tonnage. Multiplying the unit cost by the tonnages reported at each downstream gauge yields not only a value associated with barge traffic but also reflects the spatial variability between different sections of a waterway.

From the FAF^3, waterborne transportation accounts for 5% of the total tonnage of commodities transported in Illinois. Trucks, by comparison, account for about 70% of the total tonnage. Comparing the waterborne tonnage reported by the FAF^3 and the U.S. Army Corps of Engineers data for the locks, we found that barges on the Illinois River account for about one-third of the total waterborne tonnage. Comparing the total value of commodity flows through, to, or from the state of Illinois, barge traffic on the Illinois River accounts for about 1% of the total. This fraction varies annually; however, barge traffic on the Illinois River represents a small subset of overall transportation in the state.

Based on our results, we demonstrated that water reuse for power plants – using reclaimed water from wastewater treatment plants to cool thermoelectric power generators – can be a sustainable energy and water management approach both locally and regionally. Electric power generators can benefit from increased reliability when using reclaimed water for cooling. The downstream flow impacts from additional upstream consumption become statistically insignificant within 50 river miles downstream, illustrating the negligible change to downstream flow regimes. Water reuse can be beneficial at local and regional levels.

PROJECT TEAM

The project team included PI Ashlynn Stillwell, Assistant Professor, and co-PI Zachary Barker, M.S. student and Graduate Research Assistant, both in the Department of Civil and Environmental Engineering at the University of Illinois at Urbana-Champaign. Additional research support came from Undergraduate Research Assistant Lucas Djehdian, who was funded by the CEE Research Experiences for Undergraduates program.

PUBLICATIONS

Details of the results were published in Zachary Barker's thesis, *Local and downstream impacts of water reuse at power plants*, available at https://www.ideals.illinois.edu/handle/2142/88999. Results of the first two objectives (quantifying de facto water reuse and engineered reuse with reclaimed water) appeared in a manuscript that is under consideration with *Environmental Science & Technology* (initial reviews were favorable, and the revised manuscript has been resubmitted). Results of the third objective (simulating downstream impacts) are in preparation for submission to a peer-reviewed journal during the spring 2016 semester. Excerpts of these manuscripts are included here.

REFERENCES

[1] Goldstein, R. and W. Smith. (2002). *Water & Sustainability (Volume 3): U.S. Water Consumption for Power Production – The Next Half Century*. Electric Power Research Institute, 1006786.

[2] Feeley III, Thomas J., Timothy J. Skone, Gary J. Stiegel Jr., Andrea McNemar, Michael Nemeth, Brian Schimmoller, James T. Murphy, and Lynn Manfredo. (2008). "Water: a critical resource in the thermoelectric power industry." *Energy*. 33(1), 1-11.

[3] Sovacool, Benjamin K. and Kelly E. Sovacool. (2009). "Identifying future electricity-water tradeoffs in the United States." *Energy Policy*. 37(7), 2763-2773.

[4] Stillwell, Ashlynn S., Carey W. King, Michael E. Webber, Ian J. Duncan, and Amy Hardberger. (2011). "The Energy-Water Nexus in Texas." *Ecology and Society*. 16(1), 2.

[5] Macknick, J., R. Newmark, G. Heath, and K. C. Hallett. (2012). "Operational water consumption and withdrawal factors for electricity generating technologies: a review of existing literature." *Environmental Research Letters*. 7(4), 1-10.

[6] Badr, Lamya, Gregory Boardman, and John Bigger. (2012). "Review of Water Use in U.S. Thermoelectric Power Plants." *Journal of Energy Engineering*. 138(4), 246-257.

[7] Kenny, Joan F., Nancy L. Barber, Susan S. Hutson, Kristen S. Linsey, John K. Lovelace, and Molly A. Maupin. (2009). *Estimated Water Use in the United States in 2005*. United States Geological Survey, Circular 1344.

[8] Solley, Wayne B., Robert R. Pierce, and Howard A. Perlman. (1998). *Estimated Water Use in the United States in 1995*. United States Geological Survey, Circular 1200.

[9] Veil, John A. (2007). *Use of Reclaimed Water for Power Plant Cooling*. National Energy Technology Laboratory.

[10] Li, Heng, Shih-Hsiang Chien, Ming-Kai Hsieh, David A. Dzombak, and Radisav D. Vidic. (2011). "Escalating Water Demand for Energy Production and the Potential for Use of Treated Municipal Wastewater." *Environmental Science & Technology*. 45(10), 4195-4200.

[11] Stillwell, Ashlynn S. and Michael E. Webber. (2014). "Geographic, technologic, and economic analysis of using reclaimed water for power plant cooling." *Environmental Science & Technology*. 48(8), 4588-4595.

[12] Walker, M. E., R. B. Theregowda, I. Safari, J. Abbasian, H. Arastoopour, D. A. Dzombak, M. K. Hsieh, and D. C. Miller. (2013) "Utilization of municipal wastewater for cooling in thermoelectric power plants: Evaluation of the combined cost of makeup water treatment and increased condenser fouling." *Energy*. 60, 139–147.

[13] Rice, Jacelyn, Amber Wutich, and Paul Westerhoff. (2013). "Assessment of De Facto Wastewater Reuse across the U.S.: Trends between 1980 and 2008." *Environmental Science & Technology*. 47(19), 11099-11105.

[14] Multi-Resolution Land Characteristics Consortium. (2011). National Land Cover Database 2011. Available: http://www.mrlc.gov/nlcd2011.php.

[15] United States Geological Survey. (2014). National Elevation Dataset. Available: http://nationalmap.gov/viewer.html.

[16] Energy Information Administration. (2012). Forms 860 and 923. Available: http://www.eia.gov/electricity/data/eia860/ and http://www.eia.gov/electricity/data/eia923/.

[17] DeNooyer, Tyler A., Joshua M. Peschel, Zhenxing Zhang, and Ashlynn S. Stillwell. (2016). "Integrating water resources and power generation: The energy-water nexus in Illinois." *Applied Energy*. 162(1), 363-371.

[18] Environmental Protection Agency. (2008). Water: Clean Watershed Needs Survey 2008 Data. Available: http://water.epa.gov/scitech/datait/databases/cwns/2008reportdata.cfm.

[19] State of Illinois. Illinois Government News Network http://www.illinois.gov/news (accessed Jul 28, 2015).

[20] Chicago Metropolitan Agency for Planning. *Appendix A : Primary Impacts of Climate Change in the Chicago Region*; Chicago, 2013.

[21] Miara, A., and C. J. Vörösmarty. (2013). "A dynamic model to assess tradeoffs in power production and riverine ecosystem protection." *Environ. Sci. Process. Impacts*. 15(6), 1113–1126.

[22] U.S. Energy Information Administration. State Electricity Profiles. http://www.eia.gov/electricity/state/.

[23] U.S. Army Corps of Engineers. Navigation Data Center http://www.navigationdatacenter.us/lpms/lpms.htm (accessed Oct 27, 2015).

[24] U.S. Census Bureau. *2012 Commodity Flow Survey*; 2015.

Using bioavailability to assess pyrethroid insecticide toxicity in urban sediments

Basic Information

Title:	Using bioavailability to assess pyrethroid insecticide toxicity in urban sediments
Project Number:	2015IL298G
USGS Grant Number:	G15AS00019
Start Date:	9/1/2015
End Date:	8/31/2018
Funding Source:	104G
Congressional District:	IL012
Research Category:	Water Quality
Focus Category:	Models, Sediments, Toxic Substances
Descriptors:	None
Principal Investigators:	Michael j Lydy, Amanda D Harwood, Kara Elizabeth Huff Hartz, Samuel A Nutile

Publications

There are no publications.

Annual Report

NIWR/USGS: Using bioavailability to assess pyrethroid insecticide toxicity in urban sediments

September 2015-March 2016

The following report summarizes the activities conducted in the Lydy Research lab as part of the NIWR/USGS grant "Using bioavailability to assess pyrethroid insecticide toxicity in urban sediments." The project began September 15 2015 and this report discusses work conducted in Year 1 through Mar 31, 2016. Two tasks were scheduled for this time period: 1) to prepare for Tenax extractions and *Hyalella azteca* toxicity testing (scheduled to begin in September 2016) and 2) to help USGS collaborators select sampling locations.

To prepare for toxicity testing, we initiated five culturing tanks containing the *H. azteca* population that will be dedicated to the project. We altered our existing culturing protocols to match the culturing protocols used by USGS-Columbia Environmental Research Center (CERC), which should improve inter-laboratory agreement for the bioassays. These changes included altering our reconstituted water composition and increasing water changes and feeding in the tanks. In addition, the USGS protocol uses same-day age *H. azteca* for toxicity test, and thus we began adapting their grow-out protocols for our laboratory. Finally, our three existing flow-through systems were brought back online, and we repaired pumps and minor leaks and tested the performance of each system. Preparation for toxicity tests work is in progress, as we are now conducting 10-day toxicity tests using reference and positive control sediments to assess the accuracy of the bioassay with using CERC protocols.

To prepare for Tenax extractions, we obtained deuterated analogs of our target pyrethroids and adapted our existing analytical method to use the deuterated analogs as internal standards. We added the target and qualifier ions for the deuterated analogs to our analytical method, and tracked the ion ratio of the deuterated to the non-deuterated through multiple injections to assure system stability. This revised analytical method is currently in use in our laboratory, and preliminary data shows good agreement (<10% relative standard deviation) between our matrix spiked samples (n=4).

The year one objectives also included assisting our USGS collaborators with the selection of sampling locations slated for the 2016 Northeast Stream Quality Assessment (NESQA). Beginning in November 2015, we participated in monthly conference calls with the USGS collaborators. Although the site selection was essentially complete at the beginning of the funding period, we reviewed the proposed NESQA 2016 urban sites for suitability and found that the selected sites will be good targets assessing pyrethroid contamination.

During the conference calls, the USGS collaborators noted that one unknown variable that has persisted through National Water-Quality Assessment program is the holding time of the sediment samples. While effort has been made to conduct bioassays between one to two months after sampling, it is not known if this holding time is adequate or (even necessary) for pyrethroids-contaminated sediment. To address this problem, we proposed a holding time study, in which we will assess the stability of the bioavailable concentration of pyrethroids in sediment samples using Tenax extractions. The research plan for this study was developed, that included the extraction of pyrethroid from sediment samples shortly after sampling (<48 hours), and after two weeks, one month, two months, four months and six months after sampling, and determine if changes in pyrethroid concentrations occur during storage. If the pyrethroid concentrations as a function of time are stable, then it may be possible to conduct sediment testing over a longer time

period after sampling. Alternatively, if changes in concentrations are observed, then we can provide a recommendation to USGS for an effective holding time. Due to the need to find a variety of pyrethroids in sufficient concentrations to observe a change, we opted to sample sediment from known contaminated sites in California. We coordinated with Patrick Moran and Lisa Nowell for the holding time study. P. Moran provided in-kind funding for the bulk analysis of the sediment samples (organic carbon and particle size, the latter was performed in Hue-Hwa Hwang's lab at the Illinois State Geological Survey). L. Nowell led the site selection effort, with the assistance from our research group and an outside collaborator, Don Weston (University of California Berkeley). L. Nowell also led the field crews for the California sample collection. The sediment samples were collected on April 6, 2016. Extractions for the holding time assessment are currently in progress in our laboratory.

In summary, we have met the objectives described by the proposal, and due to the work conducted in year one, we expect to be ready to analyze sediment samples when received in August 2016. In addition, we have shifted resources to conduct a sediment holding time study, which while not required by the funded activities, will answer an important question regarding the effect of storage of sediment on the quality of bioassay results.

Information Transfer Program Introduction

None.

Transfering Water Resources Information to the People of Illinois

Basic Information

Title:	Transfering Water Resources Information to the People of Illinois
Project Number:	2015IL297B
Start Date:	3/15/2015
End Date:	2/28/2016
Funding Source:	104B
Congressional District:	IL-15
Research Category:	Not Applicable
Focus Category:	None, None, None
Descriptors:	None
Principal Investigators:	Lisa Merrifield, Eliana Brown

Publications

There are no publications.

Illinois Water Resources Center

Technology Transfer Report

Impacts

Illinois plan will reduce nutrient pollution in the Gulf of Mexico

Relevance
By most estimates, Illinois is the largest contributor of nutrients to the Gulf of Mexico hypoxia. More than 400 million pounds of nitrate-nitrogen and 38 million pounds of phosphorus from Illinois farm fields, city streets, and wastewater treatment plants are carried to the Gulf each year by the Mississippi River system. Every summer, these nutrients spur algal blooms that leave an area roughly the size of Connecticut all but devoid of oxygen and marine life.

Response
IWRC partnered with scientists, government agencies, non-profit groups, agriculture groups, and wastewater treatment professionals to develop and begin to implement a plan for reducing nutrient pollution from point and non-point sources in priority watersheds.

Results
The Illinois Nutrient Loss Reduction Strategy, released in July of 2015, outlines a series of best management practices that are expected to ultimately reduce the amount of nitrogen and phosphorus reaching Illinois waterways by 45 percent. The strategy marks the most comprehensive and integrated approach to nutrient loss reduction in the state's history. Implementation, including the creation of monitoring plans to document reductions and water quality improvements, is actively underway with nearly 25 working group meetings facilitated by IWRC in 2015 alone. A team of scientists is also working to develop numeric nutrient criteria for all state waterways.

Outreach programs safeguard water quality in rural communities nationwide

Relevance
Government officials and residents of rural areas face unique challenges to securing safe drinking water and treating sewage. More than 15 million U.S. households rely on private wells and are solely responsible for safeguarding water quality. Public water systems in small, rural communities are also confronted with financial, staffing, technical knowledge, and infrastructure limitations that make it difficult to comply with federal and state standards.

Response
IWRC, in cooperation with the Illinois State Water Survey and Rural Community Assistance Partnership and with funding from the U.S. Environmental Protection Agency, manages two national community outreach programs focused on providing the information and tools needed to protect drinking and source water quality in rural areas. The web-based Private Well Class

offers groundwater science education and technical assistance for well owners, realtors, and others interested in well care best practices. WaterOperator.org is a mobile-friendly web portal with free, comprehensive resources tailored for small community and tribal water and wastewater operators.

Results
Since 2012, more than 4,500 homeowners and environmental health professionals in all 50 states, the District of Columbia, Puerto Rico, and Guam, including more than 900 in Illinois, have received free online training to improve understanding of proper well care and ensure their private water source remains safe to drink. The Private Well Class has also been adopted by public health agencies across the country as their primary public education tool for private well owners. Roughly 37,000 users have accessed online education resources at WaterOperator.org since 2009 to provide safe, compliant drinking water and sustainably operate their public water systems. This includes individuals from more than 400 Illinois communities.

Great Lakes Monitoring enhances its data resources

Relevance
U.S. EPA Great Lakes National Program Office (GLNPO) monitoring programs collect data, but this data is not being used by managers and scientists around the Great Lakes.

Response
Kristin TePas and Paris Collingsworth with GLNPO and Illinois-Indiana Sea Grant have continued to partner with the National Center for Supercomputing Applications to build upon greatlakesmonitoring.org with financial support from IWRC. Launched in 2014, this state-of-the-art data access portal displays environmental monitoring data from GLNPO and USGS as well as other state, federal, and academic monitoring groups. The website was designed to allow data views at multiple spatial and temporal scales and to allow user to customize data downloading to fit their own specific needs. During this reporting period, a new video was produced that describes the functionality of each webpage and how the integration of the pages will benefit the Great Lakes science community.

Results
The website has had nearly 900 users. Plus, new partners are coming onboard. Greatlakesmonitoring.org and the USGS-developed website Science in the Great Lakes (SiGL) will be linked to provide a comprehensive data management program for the Great Lakes basin. Working under the directive of the Lake Superior Environmental Collaborative, greatlakesmonitoring.org and SiGL.gov will provide Great Lakes scientists, managers, and citizens with an online repository for monitoring data and metadata, respectively.

Dead zone data helps resource managers protect Lake Erie fisheries

Relevance
In recent years, Lake Erie saw a reemergence of algal blooms and the growth of the hypoxic zone. Hypoxia influences the distribution of fish populations, which, in turn, can dramatically alter catch rates for commercial fisheries. As such, understanding large scale fluctuations in the

spatial extent of the hypoxic zone throughout the summer and early fall is of utmost importance in Lake Erie.

Response

Working with USGS and state and federal fisheries managers, professionals with the U.S. EPA Great Lakes Program Office and Illinois-Indiana Sea Grant used funding for IWRC and others to help obtain and deploy an array of dissolved oxygen sensors in Lake Erie. This three-year investigation of dissolved oxygen levels suggests that dead zones can spring up across the lake and disappear just as quickly.

Results

The Ohio Department of Natural Resources and USGS have made changes to their annual surveys based on study recommendations. Field researchers now plan to monitor dissolved oxygen levels more extensively throughout the survey to determine whether a nearby dead zone is triggering unusually high or low catch results. An interim policy has been agreed upon whereby bottom trawls that occur in waters with dissolved oxygen less than or equal to 2 mg/L will be excluded from analyses that calculate lake-wide year class strength of forage fish. In addition, the results from this survey have been distributed to interested scientists and are currently being used to validate a model of upwelling dynamics and to help explain the spatial distribution of benthic organisms in central Lake Erie.

Accomplishments

IWRC stormwater specialist grows rain garden experts
Eliana Brown, IWRC's outreach specialist, organized and participated in numerous events designed to help Master Naturalists, Master Gardeners, and others learn more about stormwater management, green infrastructure, and rain gardens in particular. A lecture and walking tour in Urbana, Illinois in July provided an opportunity for participants to learn about the engineering and design practices behind successful rain gardens. Students enrolled in the East Central Illinois Master Naturalist program were also given the chance to play "stormwater detective" and design plans for reducing runoff from properties. Together, these and other efforts reached roughly 200 people in 2015.

Over 200 attend the 2015 Illinois River Conference
In 2015, over 200 professionals attended the Illinois River Conference in Peoria. Researchers presented papers or posters on their work. Sessions dealt with water supply planning, water quality monitoring, nutrient loss, and other timely issues. IWRC has co-sponsored the Illinois River Conference since the mid-1990s, chairing sessions, designing programs, and organizing workshops at each conference. IWRC became a co-chair for the conference in 2014 and was integral in the planning and organization of the 2015 event.

IWRC website gets a new look
Ilwaterresources.org was released at the beginning of February 2016. The new site features more navigable content, eye-catching images, a broader range of initiatives, a news page, and educational videos. In its first month alone, the mobile-friendly website was viewed 832 times by more than 200 users. Before the end of the year, the site will also include a searchable database of IWRC-funded project reports and publications.

Illinois Water magazine tells story of IWRC impacts
The new year saw the first edition of Illinois Water, a yearly publication highlighting research and outreach projects supported by IWRC. The inaugural issue includes a feature story on the Illinois Nutrient Loss Reduction Strategy and IWRC's role in its development and implementation. Additional stories discuss new findings related to cancer-causing chemicals in coal tar sealcoat, why mowing stormwater detention basins may increase the risk of West Nile virus, and how one PhD student was able to turn an IWRC seed grant into a large, multi-stakeholder research project and outreach organization. The magazine also includes a guest story from a former NIWR-USGS intern who now works as a hydrologist for the USGS Illinois Water Science Center.

Photo contest attracts youth, amateur, and professional photographers
The "Water Is" photo contest asks Illinois residents to show what water means to them, their communities, and the state. Youth, amateur, and professional photographers participated in the first annual contest in 2015, for a total of roughly 70 submissions. The winning image was featured on the cover of the Illinois Nutrient Loss Reduction Strategy. Winners in each category were also announced on social media, shared in the Illinois Water magazine, and featured on IWRC's website.

USGS Summer Intern Program

None.

Student Support					
Category	**Section 104 Base Grant**	**Section 104 NCGP Award**	**NIWR-USGS Internship**	**Supplemental Awards**	**Total**
Undergraduate	16	0	0	0	16
Masters	5	0	0	0	5
Ph.D.	2	2	0	0	4
Post-Doc.	0	0	0	0	0
Total	23	2	0	0	25

Notable Awards and Achievements

IWRC funded five research projects that revealed gaps in stream mitigation protocols, the value economic and environmental value of water reuse for power generation, and the role stream restoration has on the makeup of fish communities. Additional projects demonstrated that PAHs from coal tar sealcoat are less bioavailable than previously believed and that low-head dams do hinder fish dispersal enough to create genetic isolation. (See research introduction for additional information.)

IWRC facilitated the completion and initial implementation of the Illinois Nutrient Loss Reduction Strategy. (See Information Transfer for details.)

Since 2012, more than 4,500 homeowners and environmental health professionals in all 50 states, the District of Columbia, Puerto Rico, and Guam, including more than 900 in Illinois, have received free online training through an IWRC and partner effort, allowing them to improve their understanding of proper well care and ensure their water remains safe to drink.

Roughly 37,000 users have accessed online education resources at WaterOperator.org, a web portal co-managed by IWRC, since 2009 to provide safe, compliant drinking water and sustainably operate their public water systems. This includes individuals from more than 400 Illinois communities.

The Ohio Department of Natural Resources and USGS made changes to their annual Lake Erie surveys based on the results of a three-year hypoxia study funded in part by IWRC.

IWRC, along with University of Illinois researchers and Extension specialists, received the 2016 Team Award for Excellence from the university's College of Agricultural, Consumer and Environmental Science.

Publications from Prior Years

1. 2014IL290B ("Influence of water quality and stormwater management on the ecology of mosquito-borne disease") - Articles in Refereed Scientific Journals - Mackay, Andrew J.; Ephantus J. Muturi; Michael P. Ward; Brian F. Allan, 2016, Cascade of ecological consequences for West Nile virus transmission when aquatic macrophytes invade stormwater habitats, Ecological Applications, 26(1), 219-232.